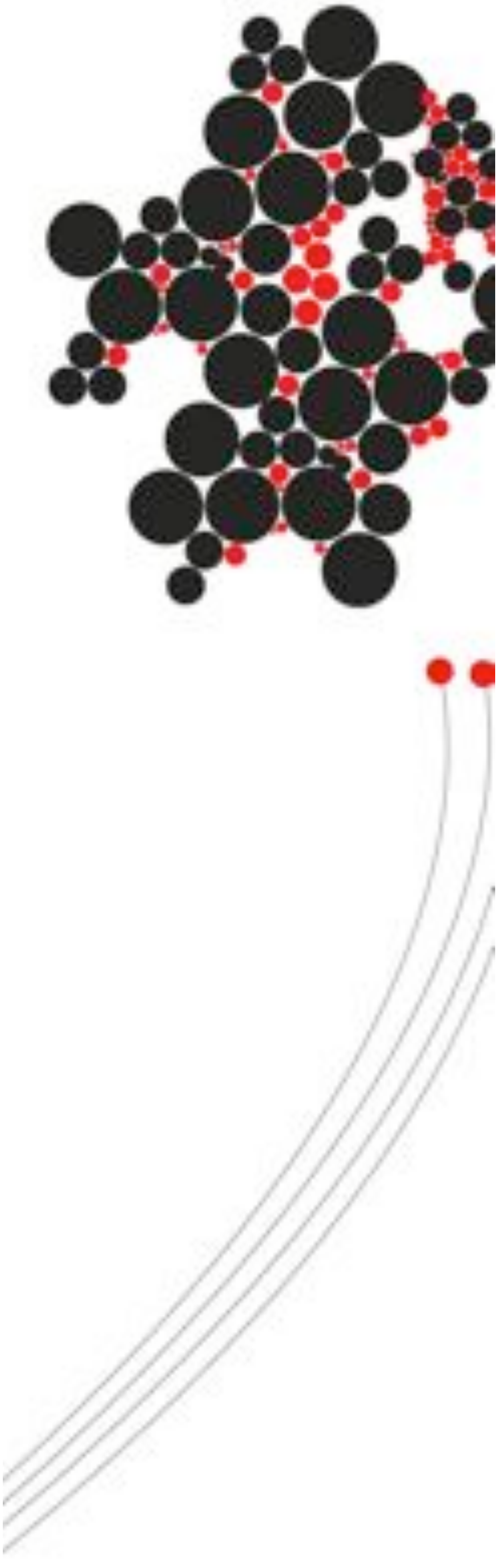

THE INFLUENCE OF WATER VAPOUR ON THE PHOTOCATALYTIC OXIDATION OF CYCLOHEXANE IN AN INTERNALLY ILLUMINATED MONOLITH REACTOR

Vic van Dijk

FACULTY OF SCIENCE AND TECHNOLOGY (TNW)
— THE PHOTOCATALYTIC SYNTHESIS GROUP (PCS)

Prof. dr. G. Mul
Dr. ir. D.W.F. Brilman
Prof. dr. ir. R.G.H. Lammertink

UNIVERSITY OF TWENTE.

23 SEPTEMBER 2011

Key words and phrases. photocatalysis, titania, TiO_2, anatase, cyclohexane, cyclohexanone, cyclohexanol, humidity, monolith, internally illuminated monolith reactor, IIMR

Many thanks to Robert Meijer for the fruitful discussions we had about experimental setups and for realising all kinds of modifications of laboratory equipment.

Abstract. Titania (anatase, Hombikat uv100) photocatalyst was coated onto a cordierite monolith and used in an internally illuminated monolith reactor (iimr) for photocatalytic oxidation of cyclohexane. Reactor temperature was kept constant at 25 °C, irradiance amounted $0.19\,\mathrm{mol\,h^{-1}\,m^{-2}}$ (wavelength range 230–388 nm) and irradiance limited bulk cyclohexanone production. The dry gas flow was in total 200 $\mathrm{mL\,min^{-1}}$ and consisted of equal parts nitrogen and air. Bulk production rates around $6 \cdot 10^{-6}\,\mathrm{mol\,h^{-1}}$ cyclohexanone were achieved for at least 7 hours under humid conditions. No mass transfer limitations were detected. All production rates were corrected for evaporation of cyclohexane.

The illuminated monolith produced cyclohexanone under dry conditions, no significant cyclohexanol production was observed. After 80 minutes of illumination under dry gas flow, the monolith deactivated, likely due to irreversible adsorption of carboxylates and carbonates.

Water vapour content of the air/nitrogen gas flow was varied. Water vapour enhanced product desorption from the monolith surface, likely by competitive adsorption. Cyclohexanone bulk production rate depended linearly on relative humidity. For relative humidity > 20 %, a deactivated monolith produced bulk cyclohexanone and cyclohexanol; water vapour decreased selectivity towards cyclohexanone.

Hydroxyl radicals formed due to water vapour played a minor role in maintaining activity: cyclohexanol bulk production rate dependency on humidity was nonlinear. We think that hydroxyl radicals were not able to remove carboxylates and carbonates from the monolith surface significantly: once the monolith deactivated under dry gas flow, water vapour was not able to restore activity under dry conditions to any extent.

Contents

CHAPTER 1

Introduction

Cyclohexanone is a raw material for the production of polyamide-6 (nylon). Cyclohexanone is industrially prepared from cyclohexane by oxidation at 140–180 °C and 8–20 bar. (Musser, 2000) Conversion has to be kept low in order to minimise production of other oxidation products such as cyclohexanol. Photocatalytic oxidation of cyclohexane could achieve higher selectivity of cyclohexanone at lower temperatures than the currently industrially applied processes.

Photocatalytic oxidation reactions are a promising energy-saving alternative to conventional oxidation reactions, such as the oxidation of cyclohexane. Absorption of light by the photocatalyst provides sufficient energy to enable oxidation at low temperatures (20–80 °C). Before photocatalytic oxidation reactions can be employed on industrial scale, the following challenges have to be faced:

- immobilisation of the photocatalyst, thus eliminating filtration steps,
- efficient illumination of the photocatalyst, and
- stable production (activity of the photocatalyst) at an economically acceptable level.

The issues of immobilisation and efficient illumination can be addressed using an internally illuminated monolith reactor (IIMR). (Du et al., 2008) The performance of this novel reactor in the photocatalytic oxidation of cyclohexane was determined once by Du et al. (2008, Figure 10) at 50 °C and two experiments were done by Carneiro et al. (2010, Figure 15). The exact reactor conditions for these three experiments are not clear to us.

This research aims at further optimising and modelling the performance of the IIMR. The photocatalytic oxidation of cyclohexane was chosen as a model reaction for photocatalytic oxidation in this work, due to its industrial relevance. Furthermore, cyclohexane is more practical in a laboratory environment than e.g. benzene, which is highly carcinogenic.

Regarding the short time available for this work, we chose to focus on the influence of water vapour on the performance of the IIMR. Contradictory effects of water vapour on photocatalytic oxidation reactions in general have been reported by others. (Henderson, 2011, pp. 249-252) There is no information available on the effect of water vapour on the performance of the IIMR in the photocatalytic oxidation of cyclohexane. This work explores the influence of water vapour on the performance of the IIMR in the photocatalytic oxidation of cyclohexane.

Following sections provide some background on photocatalysis to the reader.

1.1. The photocatalyst

A catalyst is a material that increases the rate of a chemical reaction by lowering the activation energy without being consumed or changed in the process itself. A photocatalyst is a catalyst that needs photons (light) to be catalytically active. The quantum yield is a measure for how much molecules are produced by the photocatalyst for one absorbed photon and is usually much less than 1.

Examples of oxides and sulphides being used as a photocatalyst are: TiO_2, ZnO, CeO_2, ZrO_2, SnO_2, CdS, ZnS. Titania shows in general highest activity and quantum yield. Titania is stable at employed photocatalytic conditions and for a catalyst inexpensive[1]. Titania can exist in different forms (rutile, anatase, brookite, etc.) of which anatase shows highest activity. Anatase is metastable: formation of rutile is thermodynamically favoured, but at temperatures below 600 °C anatase formation is kinetically favoured. (Herrmann, 2005)

The band-gap for bulk anatase titania is 3.2 eV (Henderson, 2011, p. 188), which corresponds to a wavelength threshold of 388 nm. Thus, titania is not able to absorb visible light; UV light up to 388 nm is necessary.

---

[1] Industrial price of titania: 2.50–2.75 € kg^{-1} for northwest Europe 2^{nd} quarter 2011, according to ICIS (www.icis.com)

Hombikat UV100 is a widely used 100 % anatase TiO_2 catalyst and has shown good initial activity. (Carneiro et al., 2010) Therefore, it is considered a good standard to use in this work. Degussa P-25 (70% anatase, 30 % rutile TiO_2) was also considered, but its percentage anatase may vary between batches, thus rendering itself difficult as a standard. Solaronix S450 has shown good regenerability when it is deactivated (Carneiro et al., 2010), but due to its high price was rejected for this work.

1.2. Heterogeneous photocatalysis

Using a photocatalyst and light, chemical oxidation-reduction reactions can be catalysed. Heterogeneous photocatalysis consists of the following steps:

(1) Liquid-phase transfer of reactants
(2) Adsorption of reactants (e.g. electron-acceptor A and electron-donor D) onto the catalyst surface: $\mathrm{A\,(l) \rightarrow A\,(ads)}$ and $\mathrm{D\,(l) \rightarrow D\,(ads)}$
(3) Reaction of reactants while adsorbed on the catalyst surface: $\mathrm{A\,(ads) \rightarrow P_1\,(ads)}$ and $\mathrm{D\,(ads) \rightarrow P_2\,(ads)}$
(4) Desorption of products: $\mathrm{P_1\,(ads) \rightarrow P_1\,(l)}$ and $\mathrm{P_2\,(ads) \rightarrow P_2\,(l)}$
(5) Liquid-phase transfer of products

These steps are the same as in conventional heterogeneous catalysis. But for photocatalysis, reaction (step 3) is not thermally activated. Instead, the following photoelectronic events activate photocatalysed chemical reactions (Herrmann, 2005) (Herrmann, 2010, pp. 462-463):

(1) Absorption of photons by the solid catalyst.
(2) Creation of photo-induced electrons ($\mathrm{e^-}$) and holes ($\mathrm{p^+}$) by a photon ($h\nu$): $h\nu \rightarrow \mathrm{e^-} + \mathrm{p^+}$
(3) Electron transfer reactions: $\mathrm{A\,(ads) + e^- \rightarrow A^{\bullet -}\,(ads)}$ and $\mathrm{D\,(ads) + p^+ \rightarrow D^{\bullet +}\,(ads)}$

Oxide and sulphide semiconductors are known to act as a photocatalyst. Such a semiconductor can absorb photons that are of equal or bigger energy than the photocatalyst's band-gap energy. The absorbed photon separates charge: an electron is promoted from its valence band to the conduction band, leaving behind a hole in the valence band. These photon-generated electrons and holes (electron vacancies) can transfer to adsorbed reactants. Radicalised reactants can undergo chemical reactions like in any other heterogeneously catalysed process. (Herrmann, 2005) (Carp et al., 2004)

Note that photochemistry is not taking place in pure photocatalysis: absorbed photons will not change the catalyst material irreversibly. As photons are absorbed by the photocatalyst, photoelectrons and photoholes are generated. Transfer of a photoelectron to an adsorbed species combined with transfer of an electron from an adsorbed species to a photohole will return the photocatalyst to its original state. (Herrmann, 2005)

1.2.1. General mechanism of photocatalytic oxidation.

Multiple possible electron transfer reactions in photocatalysis have been described in literature, see for example Hoffmann et al. (1995, pp. 73-74), Carp et al. (2004, pp. 65-67) and De Lasa et al. (2005, Ch. 1). For this work, we will aggregate the mechanism of photocatalysis on a less detailed level.

A typical photocatalytic system consists of oxygen, water and an organic substance (denoted R). As explained before, the illuminated photocatalyst contains photon-generated electrons and holes.

Oxygen is the main electron-acceptor, leading to superoxide radicals: $\mathrm{O_2\,(ads) + e^- \rightarrow O_2^{\bullet -}\,(ads)}$. This is the rate-determining step for most photocatalytic processes.

Water can donate an electron to a hole: $\mathrm{H_2O\,(ads) + h^+ \rightarrow OH^\bullet\,(ads) + H^+\,(ads)}$, thus forming a hydroxyl radical and a proton. A superoxide radical can combine with a proton into a hydroxyl radical: $\mathrm{2O_2^{\bullet -}\,(ads) + 2H^+\,(ads) + h\nu \rightarrow O_2\,(ads) + 2OH^\bullet\,(ads)}$ (this occurs via the formation and homolytic scission by light of hydrogen peroxide H_2O_2).

An organic molecule can donate an electron to a hole, yielding a positively charged organic radical: $\mathrm{R\,(ads) + h^+ \rightarrow R^{\bullet +}\,(ads)}$. These organic radicals can react with a.o. hydroxyl radicals or superoxide radicals, resulting in oxidised organic compounds.

Electrons and holes created by light on the photocatalyst can recombine, thus dissipating heat E and/or generating photons: $\mathrm{e^-} + \mathrm{p^+} \rightarrow E + h\nu$.

1.2.2. Photocatalytic oxidation of cyclohexane. The described general mechanism can be applied to the photocatalytic oxidation of cyclohexane to cyclohexanone. Cyclohexanone is a.o. formed by the reaction of an organic radical $R^{\bullet+}$ (ads) with a superoxide radical $O_2^{\bullet-}$ (ads). Thus, increasing oxygen concentration can increase cyclohexanone formation. Cyclohexanol on the other hand is a.o. formed by the reaction of a cyclohexyl radical $R^{\bullet+}$ (ads) with a hydroxyl radical $OH^{\bullet}$ (ads). Increasing availability of water could therefore increase cyclohexanol production. (Almquist and Biswas, 2001)

Note that hydroxyl radicals can form cyclohexyl radicals $R^{\bullet+}$ (ads). Thus, water can increase in equal amounts cyclohexanone and cyclohexanol production when one considers only the increased formation of cyclohexyl radicals. Cyclohexanol production however will increase more in reality, due to the described reaction of cyclohexyl radicals with hydroxyl radicals. (Almquist and Biswas, 2001)

1.3. Chemical compounds

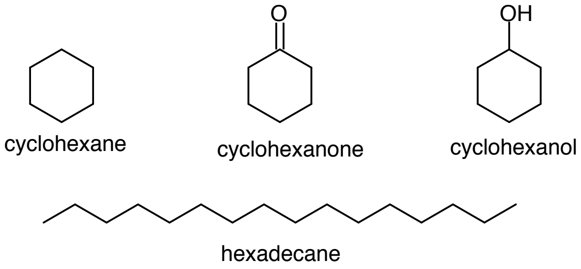

Figure 1.3.1 — Structural formulas of chemical compounds used in this work

Table 1.3.1 lists the chemicals that are involved in the photocatalytic oxidation of cyclohexane, plus hexadecane. See Figure 1.3.1 for their structural formulas. Hexadecane evaporates very little compared to the other compounds (see the vapour pressures). Therefore, hexadecane will be used for estimation of the evaporation of cyclohexane, see Section 2.5.6.

Note that cyclohexane exhibits a high vapour pressure and low explosion limits. This makes cyclohexane a potential explosion hazard, for which precautionary measures should be taken.

Table 1.3.1 — Chemical compounds that are used in this work. Explosion limits are listed in volume-percent.

Compound	Explosion limits (v%)	Boiling point (°C)	Vapour pressure @ 20 °C (bar)	CAS
cyclohexane	1.2–8.4	80.7	0.10	110–82–7
cyclohexanone	1.1–8.1	155.7	$3 \cdot 10^{-3}$	108–94–1
cyclohexanol	1.2	160.8	$1 \cdot 10^{-3}$	108–93–0
hexadecane	n/a	287	$< 7 \cdot 10^{-6}$	544–76–3

1.4. Determination of irradiance

The energy of a photon E can be estimated using the well-known relation

$$E = \frac{hc}{\lambda} \tag{1.4.1}$$

where h denotes Planck's constant, c the speed of light and λ the wavelength of the photon. Using this relation, the band-gap energy of anatase titania can be converted into the maximum effective photon wavelength for photocatalysis using anatase titania (see Section 1.1). And determined irradiances can be converted into moles of photons (of known wavelength).

1.5. Influence of process parameters

Several process parameters can be varied when using the IIMR for photocatalytic oxidation of liquid cyclohexane using gaseous air, nitrogen and water vapour:

- temperature,
- irradiance of the photocatalyst,
- liquid cyclohexane flow,
- gas flows (air, nitrogen and water vapour), and
- geometry of the monolith.

Reactor performance is determined by:

- kinetics,
- mass transfer, and
- light transfer.

To make optimal use of the photocatalyst, we want the IIMR to be able to operate in a regime that is limited by kinetics. We should experimentally check whether the performance of the IIMR is limited by mass transfer or light transfer. This depends on the values of the process parameters.

1.5.1. Experimentally determined cyclohexanone production rates. Table 1.5.1 lists photocatalytic oxidation of cyclohexane experiments done using Hombikat UV100 and resulting performance from literature. These experiments are comparable to the experiments that were done in this work. TIR denotes a top illumination reactor, that is a reactor in which a slurry of catalyst and reactant is agitated and illuminated from the top of the liquid surface.

Table 1.5.1 — Performance of Hombikat UV100 for photocatalytic oxidation of cyclohexane. *Initial* denotes the initial rate directly after start of the experiment. *Final* is the more or less stable rate that applies to most of the experimental time. *Average* is the average production over the total experiment time.

Reactor	Reference	Temperature (°C)	Cyclohexanone production ($10^{-5}\,\mathrm{mol\,h^{-1}}$) Initial	Final	Average
TIR	Du et al. (2008, p. 125 fig. 9)		42	7.8	11
IIMR	Du et al. (2008, p. 126 fig. 10)	50	5.2	0.79	1.4
TIR	Carneiro et al. (2009, p. S325 fig. 1)		4.3	1.3	2.2

1.5.2. Mass transfer. The IIMR can only be operated in film-flow regime. Pangarkar et al. (2008, Table 4) suggest that the monolith used in this work can yield a value for specific surface area times liquid mass transfer coefficient $k_\mathrm{L}a$ as low as 0.01 s^{-1} in film flow. Since pure cyclohexane is used in this work, only a possible mass transfer limitation in oxygen needs to be considered. When air saturates cyclohexane, bulk concentration of oxygen c_{O_2} is $2.3 \cdot 10^{-3}\,\mathrm{mol\,L^{-1}}$. Suppose that the concentration of oxygen at the liquid/solid interface $c_{\mathrm{O}_2}^{\mathrm{i,LS}}$ decreases 1 % due to the photocatalytic oxidation reaction.[2] The mass transfer rate of oxygen to the interface $J \cdot a$ will be then

$$\begin{aligned} J\,a &= -k_\mathrm{L}a\left(c_{\mathrm{O}_2} - c_{\mathrm{O}_2}^{\mathrm{i,LS}}\right) \\ &= -0.01\,\mathrm{s}^{-1}\left(c_{\mathrm{O}_2} - 0.99c_{\mathrm{O}_2}\right) \\ &= -0.01\,\mathrm{s}^{-1} \cdot 0.01c_{\mathrm{O}_2} \\ &= -0.01\,\mathrm{s}^{-1} \cdot 0.01 \cdot 2.3 \cdot 10^{-3}\,\mathrm{mol\,L^{-1}} \\ &= -2.3 \cdot 10^{-7}\,\mathrm{mol\,L^{-1}\,s^{-1}} \\ &= -8.3 \cdot 10^{-4}\,\mathrm{mol\,L^{-1}\,h^{-1}} \end{aligned} \tag{1.5.1}$$

---

[2] A decrease of 1 % in oxygen content of the interface film will not yield a big decrease in reaction rate (suppose first order-behaviour in oxygen: only 1 % decrease in reaction rate). The liquid-phase mass transfer of oxygen from the bulk to the interface depends on the concentration difference between interface and bulk: a 1 % decrease in oxygen content yields a relatively small mass transfer. Thus, this hypothetical case of 1 % decrease in oxygen content represents minimal mass transfer rate of oxygen and a minimal decrease in reaction rate.

This mass transfer rate is sufficient to oxidise $8.3 \cdot 10^{-4}\,\mathrm{mol\,L^{-1}\,h^{-1}}$ of cyclohexane. This is one order of magnitude higher than the measured production rates by others (see Table 1.5.1, we assume these rates are not limited by mass transfer). Thus, it is expected that the reactor operation will not be mass transfer-limited. However, we need to keep in mind that catalytic improvement of one order of magnitude could render the system limited by mass transfer.

Furthermore, we want to estimate whether it is possible to operate the reactor system in closed mode without oxygen depletion limiting the reaction rate significantly. Closed mode means that no gas is flowing in or out the system during illumination. The liquid is pre-saturated with oxygen before illumination. Solubility of oxygen in cyclohexane is $12.4 \cdot 10^{-4}\,(\text{mole fraction}) \cdot \mathrm{atm}^{-1}$ around room temperature (Wild et al., 1978). When 0.9 L liquid cyclohexane is pre-saturated with a mixture of equal parts air and nitrogen, and $1 \cdot 10^{-5}\,\mathrm{mol\,h^{-1}}$ oxygen is consumed by the photocatalytic reaction in closed mode (see Section 4.3.2), it lasts 1 hour before 1 % of the dissolved oxygen is consumed from the bulk. Therefore, we think that closed mode operation should be possible for at least 1 hour without affecting reaction rate more than 1 % (assuming first-order behaviour in oxygen).

1.5.3. Temperature. The influence of temperature on overall photocatalytic reaction rate is different from the effects of temperature in conventional catalytic processes. Since a photocatalytic reaction is activated by photons, its true activation energy is zero.

The photocatalytic reaction occurs on the surface of the photocatalyst; reactants have to adsorb on this surface and products have to desorb for the overall photocatalytic reaction to be sustainable. Thus, the apparent activation energy determined in experiments measuring e.g. liquid bulk product concentrations is not zero but some $\mathrm{kJ\,mol^{-1}}$. This apparent activation energy reflects the role of physical adsorption and desorption processes.

Physical adsorption (without dissociation) is always exothermic. Following Le Chatelier's principle: decreased temperature implies more adsorbed molecules. Increased temperature leads to less adsorption (desorption is favoured). Different cases can be distinguished for the influence of temperature on overall photocatalytic reaction rate, see Table 1.5.2. Note that "overall (photocatalytic) reaction rate" denotes not only the photocatalytic reaction itself, but the total system of adsorption, photocatalytic reaction(s) and desorption. At low temperature, strong adsorption of product B limits the reaction rate. Determined apparent activation energy E_{exp} is equal to the desorption enthalpy of B. At high temperature, strong desorption of reactant A limits the reaction rate. Experimentally determined activation energy is equal to the activation energy of adsorption of A. At moderate temperatures, adsorption of both product and reactant are in between the two previous cases, leading to a high overall reaction rate and a experimentally determined activation energy equal to the photocatalytic activation energy, which is about 0. (Herrmann, 2005)

Note that this discussion does not take other compounds, such as water, into account. Water adsorption at low temperatures is shown to be significant by Almeida et al. (2011) such that it influences the cyclohexanone production rate in photocatalytic oxidation of cyclohexane.

Table 1.5.2 — Influence of temperature on overall photocatalytic reaction rate

Low temperature (< 0 °C)	low rate, $E_{\mathrm{exp}} = \Delta H_{\mathrm{B}}^{\mathrm{des}}$
Moderate temperature (> 20, < 70 °C)	high rate, $E_{\mathrm{exp}} = E_{\mathrm{reaction}} \approx 0$
High temperature (> 70 °C)	low rate, $E_{\mathrm{exp}} = E_{\mathrm{A}}^{\mathrm{ads}}$

CHAPTER 2

Materials & methods

This chapter describes the materials & methods used in this work, including analysis methods and calculation procedures.

All chemicals used in this work were obtained at Sigma-Aldrich and used as received (unless otherwise stated). Hombikat UV100 was kindly provided by Sachtleben and used as received.

2.1. Internally illuminated monolith reactor system

The internally illuminated monolith reactor (IIMR) developed by Du et al. (2009, Ch. 6) was used in this work, see Figure 2.1.1 for a schematic drawing. This batch reactor consists of a glass vessel that can contain a titania-coated monolith of about 23 cm long and 4.2 cm in diameter. For illumination of the photocatalyst that was coated onto the monolith walls, fibres were inserted into the monolith channels from the bottom of the reactor vessel, see Figure 2.1.2 for a photograph. Liquid cyclohexane was recirculated from a 1 L storage tank over the reactor using a gear pump (see Appendix C for calibration information). A spraying device sprayed cyclohexane on top of the monolith channels. Liquid samples can be taken from the storage vessel using a tube connected to a 10 mL plastic syringe. A constant temperature water bath kept the storage vessel at a constant temperature. A trace of hexadecane was added to the storage vessel to estimate the evaporation of cyclohexane from the IIMR. See Figure 2.1.3 for a photograph of the reactor vessel of the IIMR while in illuminated operation.

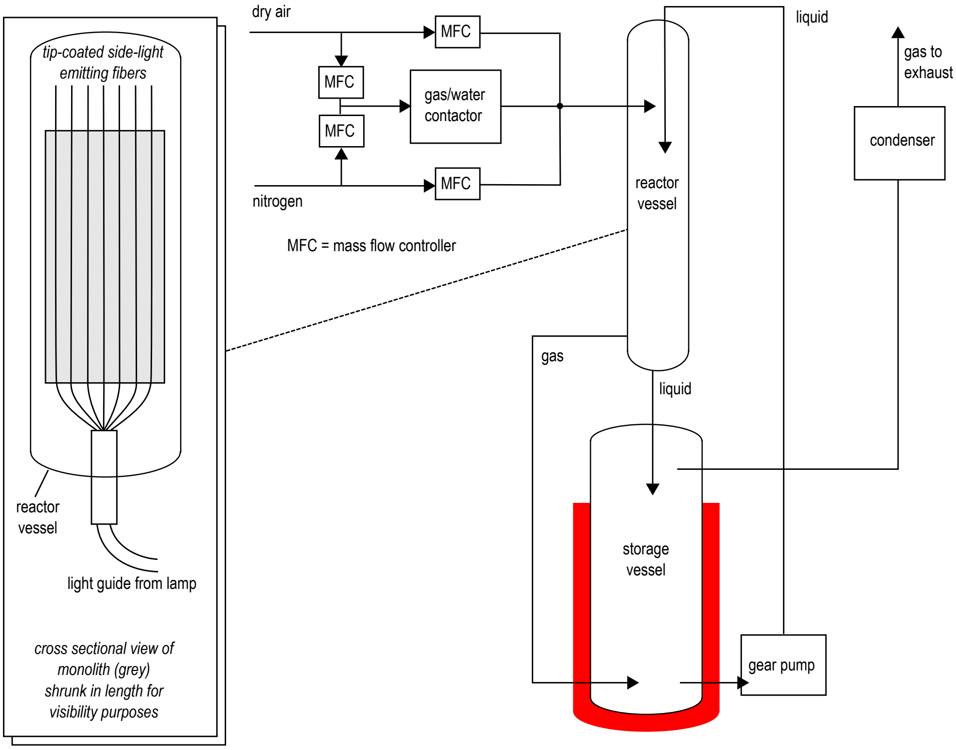

Figure 2.1.1 — Schematic drawing of the internally illuminated monolith reactor system (IIMR). Parts in red are heated by water from a constant temperature bath. A cross-sectional zoom of the reactor including monolith and fibres is displayed at the left side of the figure.

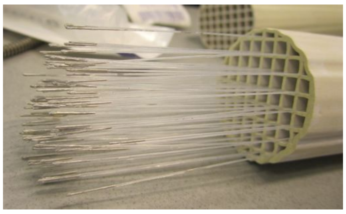

Figure 2.1.2 — Photograph of side-light emitting fibres sticking out of the monolith. At the left side the silver-coloured coating of the end of the fibres is visible.

A mixture of water vapour, air and nitrogen was fed to the reactor vessel at the top. The composition of this gas mixture was controlled using four mass flow controllers (see Appendix C for calibration information). The air that was fed to the setup was dried by a Drierite® gas-drying unit[1] (not shown in Figure 2.1.1). Part of the air and nitrogen flows can be directed to a flask filled with water, where the gases bubble through the water, thus taking up water vapour. Note that this gas/water contactor and the two preceding MFC's were installed only after IIMR session 7 of this work. A relative humidity sensor (Sensirion SHT71) determines humidity of the gas flow entering the reactor. After passing through the reactor vessel, the gas flow enters the storage vessel from the bottom and bubbles through cyclohexane. A tap water-cooled condenser is located just before the gas exhaust to minimise loss of cyclohexane.

Gear pump and mass flow controllers (MFC 1 and 2) were controlled by a PC running LabVIEW 2010. Temperature sensors (K-type thermocouples) are located at the top and bottom of the reactor vessel and in the storage vessel. Reactor conditions (temperatures, flows) were logged by

---

[1] Drierite® consists for 98 % of the drying agent calcium sulphate ($CaSO_4 \cdot 0.5H_2O$), and for 2 % of the moisture indicator cobalt dichloride ($CoCl_2$).

Figure 2.1.3 — Photograph of the reactor vessel of the IIMR while in illuminated operation.

the LabVIEW software. The reactor vessel was at atmospheric pressure due to the open connection of the system to the exhaust.

It was made sure that enough ventilation is available to stay at all times below the explosion limits of cyclohexane (see Section 1.3), also in the event of a total spill of cyclohexane contained by the IIMR.

2.2. Lamp and fibres

Tip-coated side-light emitting fibres (SpectraPartners) were used to illuminate the channels of the monolith contained by the IIMR. Each fibre had been coated at the end with aluminium to reflect light coming out of the fibre back into the fibre, see Figure 2.1.2. The fibres emit light along their length since the coating of the fibres had been removed. The bundle of side-light emitting fibres was connected to a fibre bundle that was connected to a 100 W mercury lamp system (HP-100 from Dr. Gröbel, containing an Osram HBO R 103W/45 lamp). Throughout this report, the fibre bundle connected to the lamp is denoted “first fibre bundle”. The fibre bundle connected to the first bundle is called “second fibre bundle” and illuminates the monolith. See Figure 2.2.1 for the spectrum plot determined for the light shining from the first fibre bundle connected to the lamp. See Appendix D, Section D.1 for a spectrum plot of the complete wavelength range of the lamp. By varying the distance between the two fibre bundles, the illumination could be dimmed.

The irradiance (wavelength range 220.75–400 nm) of light coming out of the fibres was determined using a photospectrometer (USB4000 from Ocean Optics). This photospectrometer was calibrated radiometrically using a calibration lamp (Ocean Optics DH-2000-CAL). Light emitted by the fibres was collected using a cosine corrected irradiance probe (CC-3-UV from Ocean Optics).

A holder for probe and fibre was designed to let the probe steadily look at a well-defined part of the fibre. The holder was made from black plastic to prevent detection of scattered light. A clamp connects the holder to a stand for steadiness. A cloth was used to cover the setup for background light. See Appendix D, Section D.2 for a photograph and design of the holders.

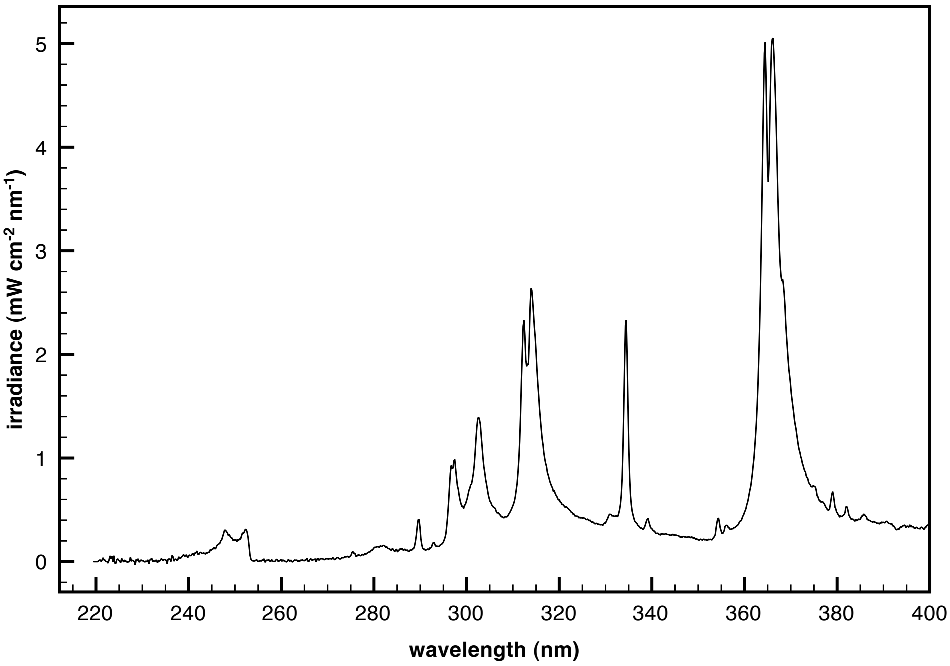

Figure 2.2.1 — Irradiance as a function of wavelength (220–400 nm) of the light exiting the first fibre bundle connected to mercury lamp system Dr. Gröbel HP100. The probe was held at approximately 1 cm from the end of the fibre bundle.

2.3. Quantitative analysis by gas-liquid chromatography

We had to determine the composition of liquid sampled from the IIMR, in order to determine the conversion and evaporation of cyclohexane. Gas-liquid chromatography has been used before for this purpose by a.o. Du et al. (2008). See Appendix G for some background information on gas-liquid chromatography (often called "gas chromatography").

2.3.1. Gas-liquid chromatograph. An Agilent 7820A gas-liquid chromatograph (GC) was employed in this work to determine the concentrations of cyclohexanone, cyclohexanol and hexadecane in cyclohexane sampled from the IIMR. The GC is equipped with a capillary column HP-5 from Agilent[2] and a flame ionization detector (FID). An automated liquid sampler (Agilent ALS 7693A) injects 1 µL using a 10 µL standard syringe. The ALS used cyclohexane for rinsing the syringe. Helium was used as carrier gas, hydrogen as FID fuel and nitrogen for make-up. Plastic-capped 2 mL glass vials from Chromacol were used.

We prepared solutions of cyclohexanone in cyclohexane to identify the retention time of cyclohexanone, see Section G.2.1. Standard solutions containing all three components (cyclohexanone, cyclohexanol and hexadecane) were analysed to determine optimal GC settings (see Table 2.3.1) and GC column temperature program (see Table 2.3.2) by trial-and-error. The gas-liquid chromatograph needs in total 40 minutes to analyse one sample and cool down before another sample can be analysed.

2.3.2. Response factor determination. The standard solutions were also used to determine the response factors (see Appendix G). It was verified regularly whether the response factors had changed by redoing GC analysis of standard samples.

EzChrom Elite Compact 3.3.2 SP2 software from Agilent performed the integration of peak areas for all solutions. The integration settings are listed in Table 2.3.3 and the compound retention times used for integration in Table 2.3.4.

Resulting peak areas of cyclohexanol, cyclohexanone and hexadecane for the standard solutions were plotted versus concentration and linearly regressed. Average relative standard uncertainty in standard solution preparation u'_{sp} was estimated for all solutions, the biggest uncertainty obtained was used in further calculations for sake of simplicity. Standard deviations s_{lr} arising from linear

---

[2] Column length 30 m, 0.320 mm diameter, 5 % phenyl methyl siloxane film 0.25 µm, part no. 19091J-413.

Table 2.3.1 — GC settings

Setting	Value
Injection mode	Splitless
Inlet temperature	200 °C
Inlet pressure	0.63434 bar
Purge flow to split vent	80 mL min^{-1} @ 0.75 min
Column flow	2.1283 mL min^{-1} @ 30 °C, 0.63434 bar; 33.624 cm s^{-1}
FID temperature	300 °C
FID hydrogen flow	30 mL min^{-1}
FID air flow	400 mL min^{-1}
FID constant column + make-up flow	27.121 mL min^{-1}
FID data logging frequency	20 Hz

Table 2.3.2 — GC column temperature program

Heating rate (°C min^{-1})	Temperature (°C)	Hold time (min)	Time (min)
0	30	1.5	1.5
1	40	3	14.5
20	200	2	24.5
post-run	250	2	

Table 2.3.3 — GC integration settings

Event	Start time (min)	Stop time (min)	Value
Integration off	0	11.7	0
Peak width	0	22	0.2
Threshold	0	22	500
Valley to valley	12.3	12.75	0
Valley to valley	13	13.8	0
Integration off	013.8	22.4	0
Peak width	22	60	0.05
Threshold	22	60	10000
Integration off	23.2	60	0

Table 2.3.4 — GC compound retention times

Compound	Retention time (min)	Window (min)
Cyclohexanol	12.6	0.643
Unknown compound	12.8575	0.643
Cyclohexanone	13.2	0.651083
Hexadecane	22.62	0.5

regression were calculated. Uncertainties u'_{sp} and s_{lr} lead to a confidence interval for future samples of unknown concentration, see Section G.1.1.

2.4. Monolith

Titania acts as a photocatalyst and was coated onto a monolith in this work, following the procedure described in this section. See Table 2.4.1 for the characteristics of the cordierite monolith that was used. See Figure 2.4.1 for a view from above the monolith.

2.4.1. Preparation of the coating solution. The monolith was coated with anatase titania (Hombikat UV100, kindly provided by Sachtleben). The coating procedure is based on work done by Du et al. (2008) and Leite Pimenta Carneiro et al. (2010, Chapter 9, pp. 157-158).

45 mL titanium(IV) isopropoxide ($C_{12}H_{28}O_4Ti$) was slowly added to 500 mL of demineralised water while stirring. Addition speed was around 0.5 mL min^{-1}, using a peristaltic pump and a

Table 2.4.1 — Monolith characteristics

Material	Cordierite
Type	Cylinder
Manufacturer	Corning
Length	22 cm
Diameter	42.8 mm
Channel type	Square
Channel side length	4 mm
Channel wall thickness	1 mm

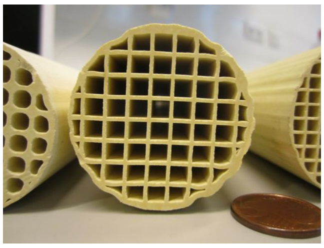

Figure 2.4.1 — Top view of the monolith. Next to the monolith is a 5 eurocent coin.

flexible silicone tube (5.8/3.4 mm outer/inner diameter). The watery solution of titanium(IV) isopropoxide was kept at 40 °C using a heating plate equipped with thermostat.

5 mL of nitric acid for catalysing the hydrolysis reaction was added drop by drop with a Pasteur pipette. A solution containing white flocks was obtained. The resulting solution was stirred overnight (at least 16 hours) at 80 °C. To prevent the evaporation of all the liquid during the night, around 100 mL water was added.

100 g Hombikat UV100 was added to the white homogenous solution and vigorously stirred using a hand blender (Philips HR1363 600 W) for fifteen minutes. Meanwhile, the monolith was dried at 150 °C in a furnace for several hours.

2.4.2. Coating the monolith. The coating mixture was shaken in order to ensure homogenisation. When cooled down, the monolith was put in a 500 mL measuring cylinder. Coating mixture was added to the measuring cylinder until the monolith was fully submerged. During ten minutes of contact between monolith and coating mixture, the monolith was pulled out somewhat and pushed back repeatedly to facilitate mixing of the coating solution. For another ten minutes the monolith was submerged the other way down, to minimise uneven partitioning of the coating.

Immediately after taking the monolith out from the coating solution, it was held horizontally, while continuously rotating the monolith around its longest axis to prevent coating solution from accumulating. Pressurised air was used to remove excessive liquid from the monolith channels. Hot air from a hairdryer (Principal A168 2000 W) dried the monolith further.

Once the coating had been applied and the monolith showed no visible liquid, calcination at 450 °C for 15 minutes (heating rate $40\,\mathrm{K\,min^{-1}}$) was performed in a furnace. Once cooled down, the monolith was dipped again in the coating solution and the other steps of the coating procedure were repeated in order to create additional layer(s). Three layers in total were coated onto the monolith, to obtain a layer thickness of around 27 µm according to Du et al. (2008, p. 124).

2.5. Operation of the IIMR

A monolith coated with TiO_2 was used in the Internally Illuminated Monolith Reactor (IIMR) for photocatalytic oxidation of liquid cyclohexane. The following procedure was carried out to test the photocatalytic activity.

2.5.1. Preparing the IIMR for operation. Cyclohexane was dried overnight by adding 100 g of 4Å molecular sieves (4–8 mesh) to 5 L of cyclohexane.

The outside of the monolith was sanded using sandpaper to decrease the outer diameter to 42.80 mm in order to fit inside the reactor vessel. The side-light emitting fibres were inserted in the channels of the monolith (two fibres per channel). The combination of monolith and fibres was inserted into the reactor vessel using a steel stick to give some support to the monolith while lowering it into the reactor vessel.

The liquid spraying device at the top of the reactor vessel should be disassembled once every few reactor sessions, to remove possibly present solid particles. Such particles can cause clogging, resulting in less or no liquid flow at all.

The temperature bath was turned on and time was taken to let the liquid in the storage tank and reactor reach a stable temperature. The mercury lamp was turned on (but not connected to the reactor) to let it warm up for at least 30 minutes. The storage tank of the IIMR was filled with 0.8–1.0 L of cyclohexane, measured by a 0.5 L measuring cylinder. Around 0.02 mL hexadecane was added to the storage tank if not already contained by the tank, to estimate the evaporation of cyclohexane. The pump was turned on at 3000 rpm (1.6 $\mathrm{L\,min^{-1}}$) to mix the liquid cyclohexane and hexadecane and to speed up temperature stabilisation. A sample was taken from this initial solution (see Section 2.5.3), in order to know the hexadecane concentration that corresponds to the measured total liquid volume.

Gas flow was turned on at a desired rate and was given 15 minutes to pre-saturate the liquid with oxygen if required.

2.5.2. Reactor conditions. The reactor can be operated in two modes: open and closed mode. For open mode, a controllable mixture of nitrogen, air and water vapour was supplied to the reactor. Closed mode denotes that the outlet of the reactor was capped by a balloon and no gases were supplied to the reactor. Closed mode minimises evaporation of cyclohexane during reactor operation. Temperature was kept constant around 25 °C in most cases. Liquid flow was 1.6 $\mathrm{L\,min^{-1}}$ (pump setting 3000 rpm, unless stated otherwise) and the total liquid volume was kept between 0.8 and 1 L (during preparation of each session fresh cyclohexane was added if necessary; there was no addition of liquid during a session). Gas humidity was varied throughout the experiments, total dry flow was kept constant around 200 $\mathrm{mL\,min^{-1}}$ and dry air/nitrogen content was around 50/50, unless stated otherwise.

Irradiance was kept constant during experiments, unless otherwise stated. The lamp system has a shutter. This shutter does not block the light coming from the lamp completely. When illumination had to be stopped, the shutter was closed and then the first fibre was disconnected from the second fibre.

2.5.3. Sampling. Samples of the liquid bulk were taken at desired times. It was made certain that a sample was taken every time a parameter changed in reactor operation. For example: when connecting the light guide to the reactor, a sample was taken. Or, when gas flows are changed, a liquid bulk sample was taken.

At the top of the storage tank of the IIMR is a syringe port for taking samples of storage tank liquid. A 10 mL plastic syringe was always connected to this port. Before taking a sample, the plunger of the syringe was pulled and pushed three times to refresh the liquid already contained by the syringe and tubing. Then, the plunger was pulled a fourth time, and the time was noted. The syringe was unscrewed and 1 mL of liquid was inserted into a 2 mL GC vial. The vial was capped by a plastic screw-cap. The syringe was reconnected to the sampling port and remaining liquid was discharged into the storage tank.

One syringe lasts about ten sampling actions. Friction of the plunger to the syringe wall increases during usage, up to a certain point that one breaks the plunger. Thus, a syringe was replaced by a new one when the operator felt the friction became too much.

2.5.4. End of operation. IIMR operation was finished by turning off the pump, the lamp (we left the fan of the lamp system running for some time to cool down!), the gases and the temperature bath. The liquid was taken out of the storage vessel and we determined the volume of liquid before storing it inside a capped erlenmeyer flask.

2.5.5. GC analysis of samples. We analysed samples by gas-liquid chromatography (see Section 2.3) the same day in duplicate, in a randomised order. Randomisation of the analysis order ensures that possible trends in analysis deviations will not enhance experimental trends, but will result in random effects. Resulting peak surface areas of each duplicate were compared, a third GC analysis was performed when two areas of a duplicate differed significantly more than the average difference of other samples. Such a third (or even fourth or fifth) GC analysis of a certain sample pointed which determined peak area(s) is/are the outlier(s). Outliers were neglected in further calculations. The average peak surface area of each duplicate was used in further calculations. Note that the duplicates were not used to estimate the random error in peak surface areas.

To minimise confidence intervals of IIMR sample concentrations, the linear regression done in GC response factor determination for standard solutions (see Section 2.3.2) was redone for each IIMR experiment. Only standard solutions covering the GC peak area range of zero up to the experiment's maximum peak area were used in the regression, to minimise standard deviation s_{lr} originating from linear regression.

Each liquid sample for GC analysis is about 1 mL. Since the total amount of samples taken is small compared to total reactor volume (around 1.5 %), the decrease in reactor volume from sampling was neglected in calculations.

2.5.6. Calculation of reactor concentrations. The liquid concentrations of cyclohexanone, cyclohexanol and hexadecane contained by the IIMR were determined using GC analysis of liquid samples. It was assumed that hexadecane does not evaporate from the reactor liquid due to its low vapour pressure, see Section 1.3. Thus, from the increase in concentration of hexadecane c_{HED} from moment t_1 to t_2, the volume of reactor liquid $V_{\mathrm{L}}^{t_2}$ at time t_2 can be calculated when the volume at time t_1 is known:

$$V_{\mathrm{L}}^{t_2} = \frac{V_{\mathrm{L}}^{t_1} c_{\mathrm{HED}}^{t_1}}{c_{\mathrm{HED}}^{t_2}} \tag{2.5.1}$$

Vapour pressure of cyclohexanone and cyclohexanol are respectively 3 % and 1 % of the vapour pressure of cyclohexane at 20 °C (see Section 1.3). Therefore, cyclohexanone and cyclohexanol were assumed not to evaporate from the reactor liquid. Measured concentrations of cyclohexanone and cyclohexanol c_m were converted to hypothetical concentrations c_h in the hypothetical case of no evaporation taking place:

$$c_h = \frac{c_m V_{\mathrm{L}}^{t_2}}{V_{\mathrm{L}}^{t_1}} \tag{2.5.2}$$

Combination of both equations yields:

$$c_h = \frac{c_m c_{\mathrm{HED}}^{t_1}}{c_{\mathrm{HED}}^{t_2}} \tag{2.5.3}$$

For most reactor sessions the trend in increase of hexadecane concentration was close in size to the random error in hexadecane concentration. Therefore, hexadecane concentration data were linearly regressed before using the data for the correction for evaporation of cyclohexanone and cyclohexanol concentrations.

The uncertainties in peak areas for one GC sample were assumed to be related, and the uncertainties between different samples were thought to be independent. Uncertainty Δ_{c_h} in hypothetical reactor concentration c_h (see Section 2.5.6) was calculated using (see Appendix E for more information):

$$\Delta_{c_h} = \sqrt{\left(c_{\mathrm{HED}}^{t_1}\right)^2 \left(\left| \frac{1}{c_{\mathrm{HED}}^{t_2}} \right| \Delta_{c_m} + \left| -c_m \left(c_{\mathrm{HED}}^{t_2}\right)^{-2} \right| \Delta_{c_{\mathrm{HED}}^{t_2}} \right)^2 + \left(\frac{c_m}{c_{\mathrm{HED}}^{t_2}} \right)^2 \left(\Delta_{c_{\mathrm{HED}}^{t_1}} \right)^2} \tag{2.5.4}$$

2.5.7. Monolith regeneration procedure. After around 80 minutes of illumination (see Section 3.3), the monolith shows no production of cyclohexanone or other components anymore under dry illuminated conditions. Throughout this work this is called a deactivated monolith. Whenever required, the monolith was removed from the IIMR and dried by application of a hairdryer and pressurised air. The dry monolith was placed inside a furnace that heats it at $40\,\mathrm{K\,min^{-1}}$ to 450 °C for 15 minutes under air, this regenerated the monolith.

2.6. Physical adsorption equilibrium of cyclohexanone

Physical adsorption equilibrium of cyclohexanone on titania-coated monolith was determined in order to get an idea of the consumption of cyclohexanone from the liquid bulk by adsorption on the monolith. This was done for both the monolith contained by IIMR as well as for a slice of fresh monolith contained by a beaker. The amount of adsorbed cyclohexanone $n_{\text{ads}}^{t_1}$ on the monolith can be calculated from the equilibrium bulk concentration $n_{\text{L}}^{t_1}$ and the initial bulk concentration:

$$n_{\text{ads}}^{t_1} = n_{\text{L}}^{t_0} - n_{\text{L}}^{t_1} \tag{2.6.1}$$

After 2–3 hours at constant temperature, we assumed adsorption equilibrium was reached (this assumption was checked after GC analysis by the trend in cyclohexanone concentration decrease). Some cyclohexanone was added to the liquid bulk solution to determine another equilibrium composition.

2.6.1. Monolith contained by the IIMR. A regenerated monolith was assumed to contain no adsorbed compounds ($n_{\text{ads}}^{t_0} = 0\,\text{mol}$). Cyclohexane containing $n_{\text{L}}^{t_0}$ moles of cyclohexanone was used as start solution in the IIMR. We determined initial composition by taking a sample for GC analysis from the IIMR storage vessel. Then, liquid circulation over the monolith was started and periodically a 1 mL sample from the liquid bulk was taken (e.g. once per 30 minutes). No gas was flowing nor was the monolith illuminated.

Note that when cyclohexanone was added to cyclohexane, this was done using a vessel outside the IIMR that can be shaken or stirred. The IIMR itself does not contain a stirrer or other means to homogenise the cyclohexane solution without the liquid contacting the monolith.

2.6.2. Slice of monolith. The slice of titania-coated monolith was never illuminated and served as a blank for determining the influence of illumination on adsorption behaviour. We put 200 mL of fresh cyclohexane in a 250 mL beaker and immersed a 1 cm slice of monolith. A watch glass was put on top of the beaker to decrease evaporation, see Figure 2.6.1 for a photograph. Now and then we stirred the system by moving the monolith slice using pincers. 1 mL liquid samples were taken for analysis by GC. Cyclohexanone was added to the beaker after a few hours to determine another equilibrium composition, see Section 3.3.3.

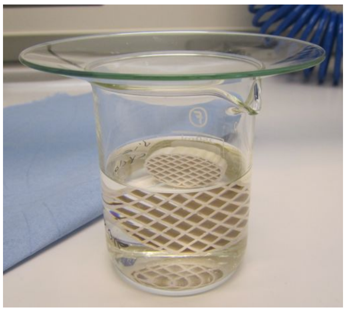

Figure 2.6.1 — Photograph of a slice of monolith immersed in cyclohexane contained by a 250 mL beaker that is covered by a watch glass.

CHAPTER 3

Results

3.1. Determination of irradiance from side-light emitting fibres

Irradiance emitted from a side-light emitting fibre connected to the HP-100 mercury lamp (Dr. Gröbel) that is used with the IIMR was determined to be $1 \cdot 10^{-4}\,\mathrm{W\,m^{-1}}$ fibre for wavelength range 230–388 nm. This value was determined by measurement at 7 cm from the end of a dirty, used fibre. In total, 100 fibres are used in the IIMR and their length is 23 cm each. Total amount of photons emitted in wavelength range 230–388 nm by the 100 fibres was at least $2 \cdot 10^{-2}\,\mathrm{mol\,h^{-1}}$. Conversion from irradiance to photon flux is done using Equation 1.4.1 (assuming each photon is of wavelength 300 nm).

Measurement of irradiance at the start of the fibre yielded double values, which is in agreement with Du et al. (2009, p. 137). Averaging this over the whole fibre yields $3 \cdot 10^{-2}\,\mathrm{mol\,h^{-1}}$ as estimation for the total amount of photons emitted by the 100 fibres. The illuminated surface area of the monolith is estimated at $0.16\,\mathrm{m^2}$, irradiance is thus $0.19\,\mathrm{mol\,h^{-1}\,m^{-2}}$.

3.2. Quantitative GC analysis of standard solutions

Twelve standard solutions (see Section G.2.1) containing known amounts of cyclohexanone, cyclohexanol and hexadecane in cyclohexane were analysed by gas-liquid chromatography. Four solutions (no. 4, 6 10 and 11) were analysed three times.

After analysis, the peaks in the chromatograms corresponding to cyclohexanone, cyclohexanol and hexadecane were integrated by software. Figure 3.2.1 shows the peak area versus concentration of the compound in each standard solution. Drawn lines represent the linear regression that was carried out on the total set of standard solutions.

A plot of residuals of the regression showed alternating positive and negative residuals, thus indicating linearity. The residuals increased with concentration.

Standard solutions 6, 9 and 10 were analysed again one month later. No change in peak area was observed, thus indicating that over one month time, GC response factors do not change significantly.

3.3. Photocatalysis using IIMR

3.3.1. Reactor sessions 1 & 2. Two reactor sessions were done using the same coated monolith under conditions listed in Table 3.3.1.

Table 3.3.1 — Reactor conditions for reactor sessions 1 and 2. The gas/liquid contactor was not installed yet.

Condition	Unit	Session 1	Session 2
Liquid temperature	°C	25	26
Air flow	$\mathrm{L\,min^{-1}}$	4.649	0.312
Nitrogen flow	$\mathrm{L\,min^{-1}}$	0	0.333
Liquid origin	n/a	910 mL cyclohexane	919 mL cyclohexane
Monolith origin	n/a	freshly coated	from session 1
Notes	n/a	All liquid has been evaporated	Non-evaporated components from session 1?

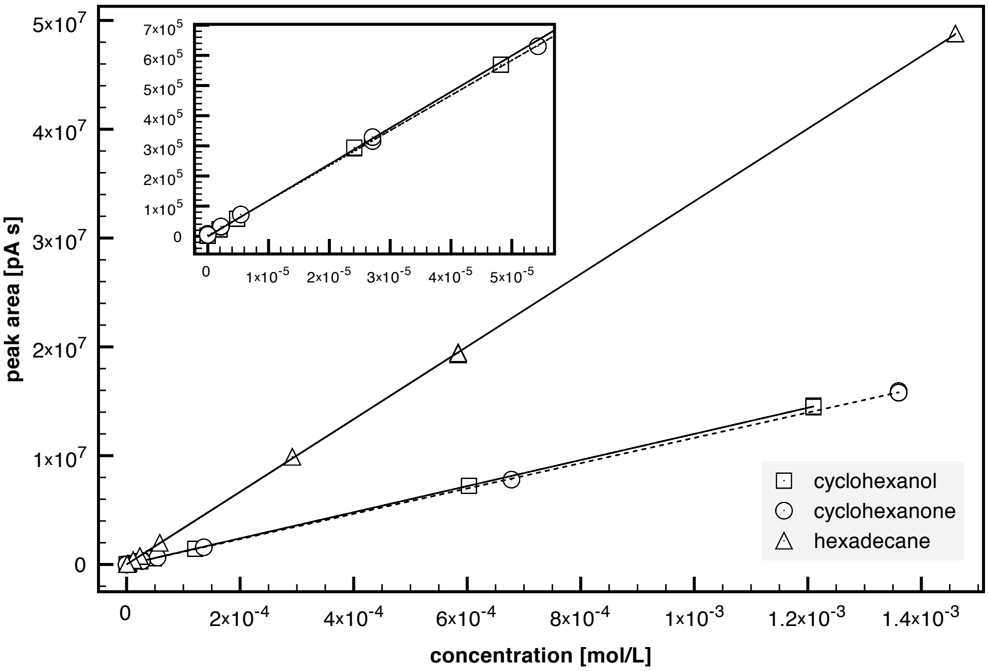

Figure 3.2.1 — Gc peak areas versus concentration of standard solutions for the compounds cyclohexanone, cyclohexanol and hexadecane. The inset is a zoomed view of the same graph at low concentration for cyclohexanone and cyclohexanol (the axes are set in the same units as the axes of the main graph). Drawn lines represent linear regression of the data (the dotted line represents cyclohexanone).

Liquid bulk concentrations of cyclohexanone and cyclohexanol in the iimr versus time are plotted in Figure 3.3.1 and 3.3.2. These concentrations are corrected for the evaporation of cyclohexane (Equation 2.5.3).

During reactor session 1, cyclohexanone concentration decreased when the reactor system was not illuminated (until time 34.5 min., Figure 3.3.1). Directly after turning on the light, cyclohexanone concentration increased. After 40 minutes of illumination (time = 75 min.) the rate of cyclohexanone production decreased. The concentration of cyclohexanone stabilised after 80 minutes of illumination (time = 120 min.). Cyclohexanone concentration started decreasing after 100 minutes of illumination. Cyclohexanol concentration was stable during the whole reactor session 1 at a significantly smaller level than cyclohexanone.

Reactor session 2 was carried out using the same monolith of reactor session 1, which was left in place inside the reactor. Session 2 starts at high cyclohexanone and cyclohexanol concentrations (compared to session 1), the explanation for this will be discussed in Section L.4.

During illumination, cyclohexanone concentration decreases, the monolith seems to be deactivated. Without illumination, cyclohexanone concentration decreased faster than during illumination, both at start of reactor session 2 as well as from 130 until 150 min.

Cyclohexanol concentration decreased throughout the whole reactor session at decreasing rate, regardless of illumination state.

3.3.1.1. *Specific observations.* All the cyclohexane has been evaporated in reactor session 1 around time = 205 minutes, evaporation was thus on average $0.2\,\mathrm{L\,h^{-1}}$. After this first session, the monolith showed some black spots, as if it was burned.

Between the end of reactor session 1 and the start of reactor session 2, concentrations of cyclohexanone and cyclohexanol increased tenfold. Hexadecane concentration was at the start of session 2 the same as at the start of session 1.

Both monolith and glass reactor wall show black stains.

3.3.2. Reactor sessions 3 & 4. The monolith from session 2 was regenerated (see Section 2.5.7) an reinserted into the iimr. Reactor session 3 was conducted at the conditions listed in Table 3.3.2 with this monolith. Reactor session 4 was conducted using fresh cyclohexane, see Table 3.3.2.

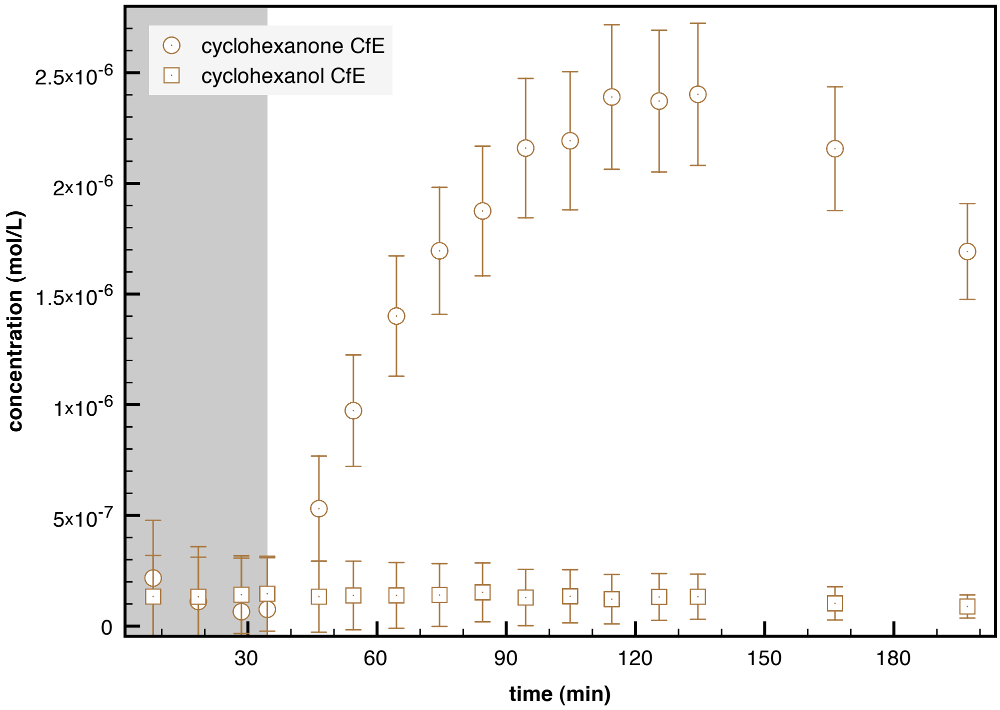

Figure 3.3.1 — Reactor session 1: liquid bulk concentrations of cyclohexanone and cyclohexanol (corrected for evaporation) versus time. From 34.5 min. the reactor was illuminated.

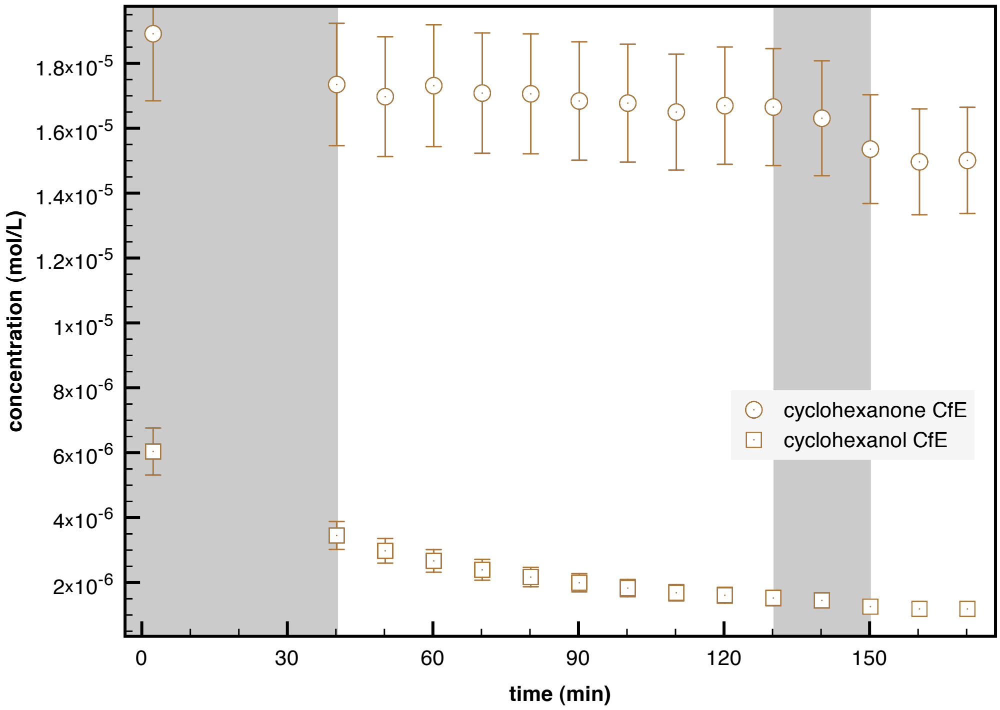

Figure 3.3.2 — Reactor session 2: liquid bulk concentrations of cyclohexanone and cyclohexanol (corrected for evaporation) versus time. From 40 min. until 130 min. the reactor was illuminated, as well as from 150 min. until the end.

Figure 3.3.3 shows the for evaporation corrected liquid concentration of cyclohexanone versus time (circular points) for session 3. During illumination (all but grey-coloured timer intervals) cyclohexanone concentration increases.

Table 3.3.2 — Reactor conditions for reactor sessions 3 & 4. The gas/liquid contactor was not installed yet.

Condition	Unit	Session 3	Session 4
Liquid temperature	°C	25	30–35
Air flow	$\mathrm{L\,min^{-1}}$	0.312	0.312
Nitrogen flow	$\mathrm{L\,min^{-1}}$	0.333	0.333
Liquid origin	n/a	750 mL from session 2 and 179 mL cyclohexane	895 mL cyclohexane
Monolith origin	n/a	from session 2, regenerated	from session 3, regenerated

Liquid flow was increased at around time = 60 min. (light blue-coloured time interval), by increasing pump speed. Increased pump speed leads to increased reactor temperature, which can be seen from the blue line showing the average[1] reactor temperature (right vertical axis). During the period of increased liquid flow, cyclohexanone concentration rises at the same rate as before the period. After the period of increased liquid flow (time = 75 min., 50 minutes of illumination) however, cyclohexanone production rate decreases.

Illumination was dimmed at around time = 95 min. (light yellow-coloured time interval). Cyclohexanone concentration decreases during this period of dimmed illumination. When illumination is switched off (grey-coloured intervals), cyclohexanone concentration decreases faster than during dimmed illumination.

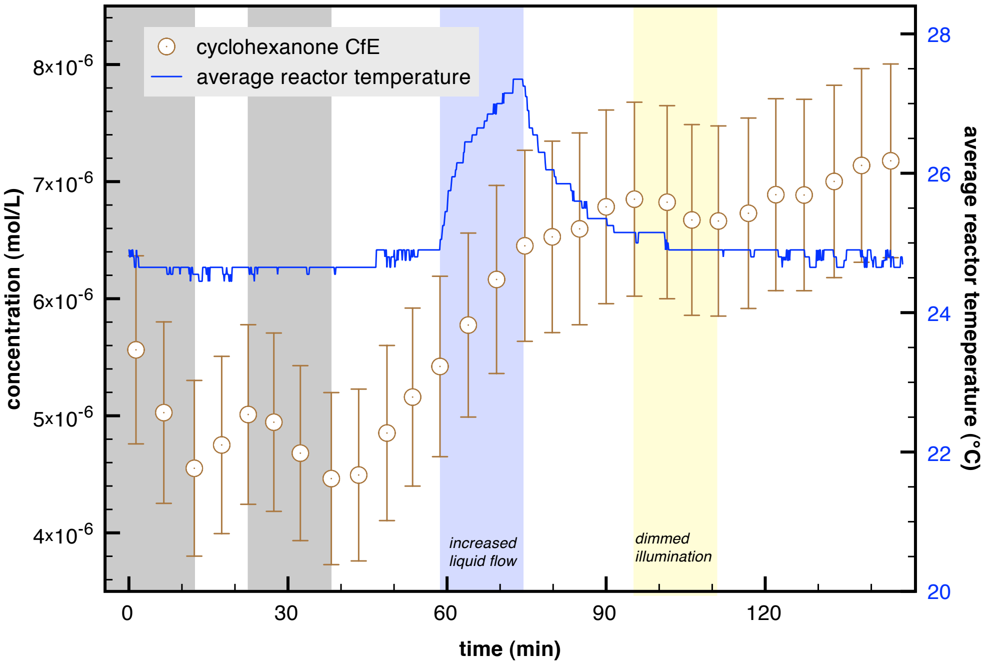

Figure 3.3.3 — Reactor session 3: liquid bulk concentrations of cyclohexanone (circular points, corrected for evaporation) versus time. The reactor was illuminated during the whole experiment, except for the grey-coloured time intervals. The liquid flow was increased from 1.6 to 2.2 $\mathrm{L\,min^{-1}}$ during the blue-coloured time period, the illumination was dimmed for the yellow-coloured time interval. The blue line denotes average reactor temperature (right vertical axis).

Figure 3.3.4 shows the development in liquid bulk concentration of cyclohexanone and average reactor temperature for reactor session 4. Due to failure of the thermostat of the constant temperature bath, average reactor temperature drops from 35 °C to 31 °C halfway the reactor

---

[1] The average of the temperature values obtained from the sensors installed at top and bottom of the reactor vessel.

session. This temperature change does not seem to influence the development of the liquid bulk cyclohexanone concentration.

When the illumination is dimmed (yellow-coloured time interval), cyclohexanone production rate decreased. When undimming the illumination after 30 minutes of illumination, the original cyclohexanone production rate is not restored. Cyclohexanone production rate continues to decrease until a more or less stable level of production is reached at $t = 60\,\mathrm{min}$.

Increasing (blue-coloured time period) nor decreasing liquid flow (green-coloured time period) influences cyclohexanone production rate.

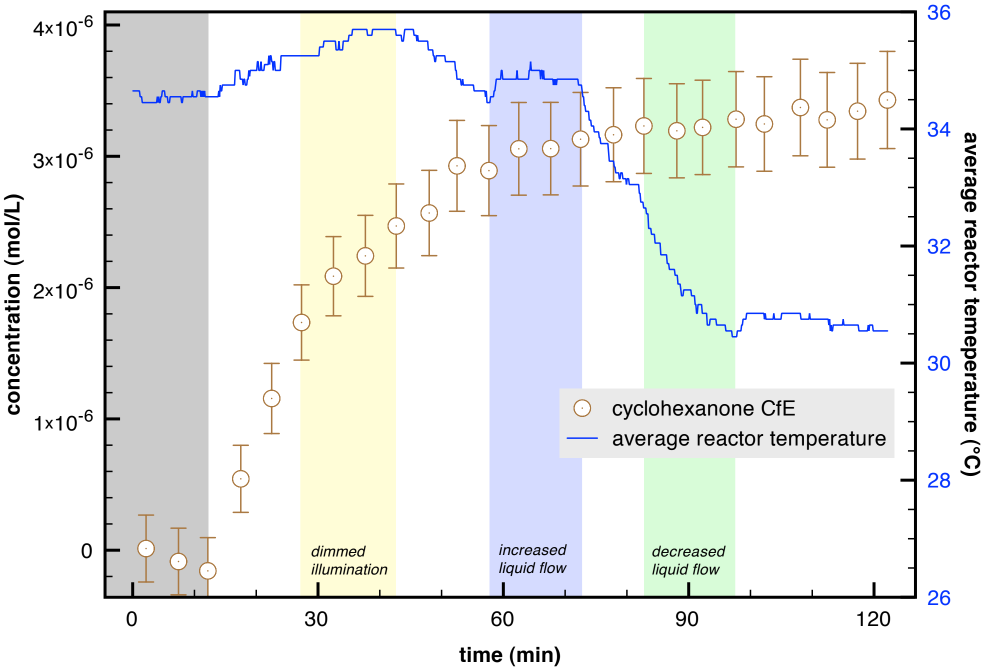

Figure 3.3.4 — Reactor session 4: liquid bulk concentrations of cyclohexanone (circular points, corrected for evaporation) versus time. The reactor was illuminated during the whole experiment, except for the grey-coloured time interval. The liquid flow was increased from 1.6 to 2.2 $\mathrm{L\,min^{-1}}$ during the blue-coloured time period, the illumination was dimmed for the yellow-coloured time interval. The green-coloured interval denotes a decrease in liquid flow from 1.6 to 1.0 $\mathrm{L\,min^{-1}}$. The blue line denotes average reactor temperature (right vertical axis).

3.3.2.1. *Specific observations.* At 1.6 $\mathrm{L\,min^{-1}}$ liquid flow (reactor session 3) it was observed that not much liquid was pumped down the monolith, less than during previous reactor sessions. In the preparation for reactor session 4, no liquid could be sprayed at the top of the reactor. Disassembly of the spraying device revealed clogging caused by solid particles, presumably from the coating and the monolith. The procedure (see Section 2.5) was adapted for prevention of clogging.

Cyclohexanol concentration is stable around $(1 \pm 1) \cdot 10^{-7}\,\mathrm{mol\,L^{-1}}$ for both reactor session 3 and 4.

White powder was observed to be in cyclohexane used in the IIMR. This white powder could be titania that had been eroded from the monolith.

3.3.3. Physical adsorption sessions 5–9 and beaker session 1. IIMR sessions 1–4 showed consumption of cyclohexanone from the liquid bulk when the monolith was not illuminated. Therefore, we wanted to test how much cyclohexanone can be consumed from the bulk by adsorption phenomena. The detailed results of IIMR sessions 5–9 done without illumination on cyclohexanone adsorption are given in Appendix I. The results from a session using a never illuminated coated slice of monolith in a beaker are also found there.

The results show that physical adsorption of cyclohexanone on the monolith decreases when UV-illumination is longer ago. Regeneration of the monolith does not yield an increase of adsorption.

Physical adsorption experiments of a slice of monolith (never illuminated by UV) do not show adsorption.

3.3.4. Closed mode IIMR sessions 10–12. Liquid cyclohexane contained by the IIMR was pre-saturated by flowing 223 mL min^{-1} air and 199 mL min^{-1} nitrogen for at least fifteen minutes. The gas flows were stopped and the outlet of the reactor was capped by a balloon to create a closed system. Illumination of the titania-coated monolith yielded cyclohexanone production rates of $(6.5 \pm 0.5) \cdot 10^{-6}$ mol h^{-1}. Cyclohexanol was produced at approximately 1/3 of the rate of cyclohexanone (sessions 11 & 12) up to 1/2 (session 10). See Figure 3.3.5 for a concentration plot of a typical experiment, and Appendix J for the other plots of closed mode IIMR sessions. No deactivation can be seen from these closed mode IIMR sessions.

Concentrations were not corrected for evaporation since hexadecane concentration did not follow a clear trend, due to little evaporation. The monolith (from physical adsorption experiment 9) was not regenerated before, nor in between the closed mode experiments. Liquid cyclohexane from the previous session was used, plus fresh cyclohexane if necessary. The amount of cyclohexanone contained by the liquid bulk at the end of a session was determined to be in line with the amount of cyclohexanone at the start of a successive session in closed mode. The humidity sensor of the IIMR pointed an average relative humidity of 55 % during closed mode experiments.

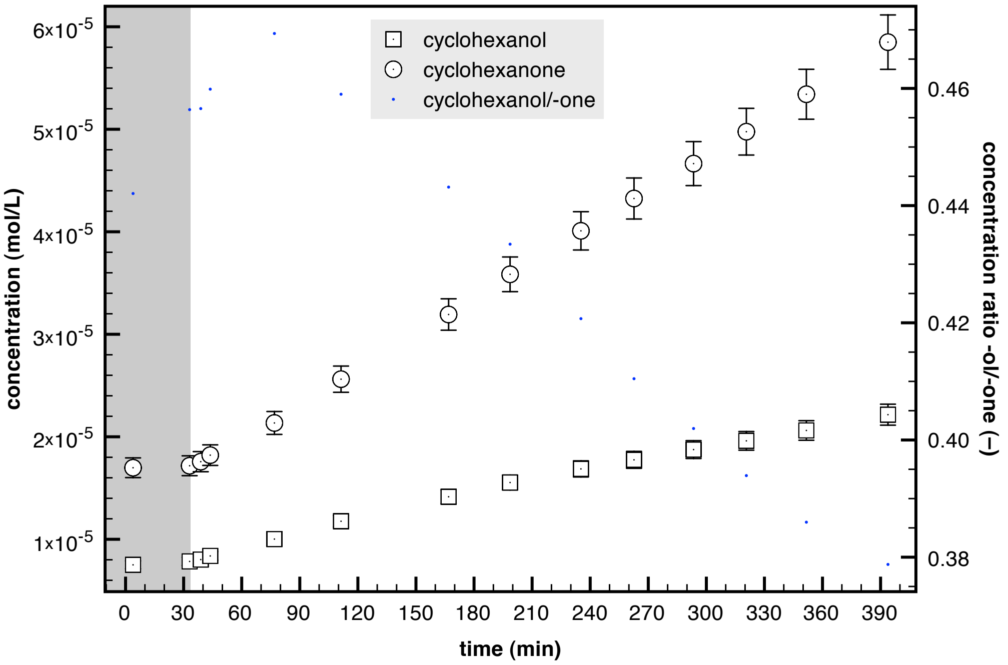

Figure 3.3.5 — Reactor session 11 (closed mode): liquid bulk concentrations of cyclohexanone and cyclohexanol versus time. The closed reactor was illuminated during the whole experiment, except for the grey-coloured time interval. The blue dots denote the liquid bulk concentration of cyclohexanol divided by cyclohexanone (right vertical axis).

3.3.5. Open mode IIMR sessions 13–19 & 30. IIMR sessions 13–19 & 30 were conducted using humidified gas flows of which the dry part amounts 200 mL min^{-1}, about 50 % nitrogen and 50 % air. See Figures 3.3.6–3.3.13 for the concentrations of cyclohexanone and cyclohexanol during IIMR sessions 13–19 and 30[2].

The monolith (from closed mode IIMR session 12) was not regenerated before, nor in between the open mode experiments (unless stated otherwise). Liquid cyclohexane from the previous session was used (unless otherwise stated). Some fresh cyclohexane was added if necessary to attain a total liquid volume of 0.8–1 L.

The amount of cyclohexanone contained by the liquid bulk at the end and start of successive sessions were determined to be constant for all open mode sessions, except for sessions 16–17.

---

[2] Session numbers 20–29 were not used for any experiments done for practical reasons.

Before the start of session 17, humidified gas had flown over the monolith. Increased liquid bulk concentrations of cyclohexanone and cyclohexanol at the start of session 17 (compared with preceding session 16 more than doubled) were determined, see Figures 3.3.9 and 3.3.10 for more information.

Reactor session 13 (Figure 3.3.6) was done at constant humidity (RH 57 %), and includes a dark period at the end to see the effect of humid conditions at darkness. During illumination the bulk concentrations of cyclohexanone and cyclohexanol increase, and these concentrations decrease slightly when the monolith is not illuminated.

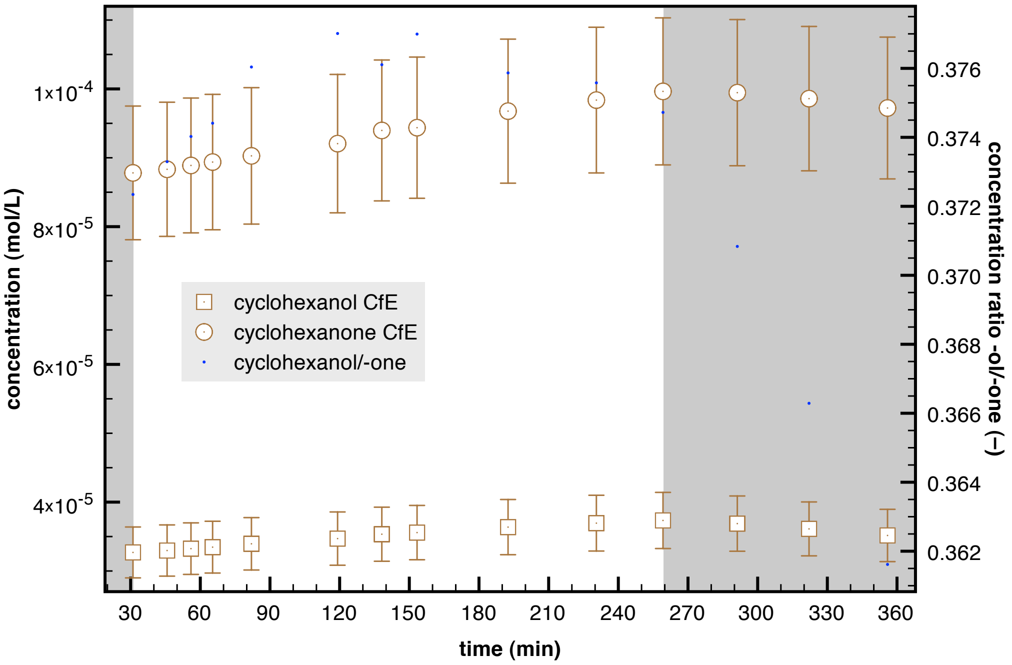

Figure 3.3.6 — Reactor session 13: liquid bulk concentrations of cyclohexanone and cyclohexanol (corrected for evaporation) versus time. Humidified gas was used (57 % relative humidity), from 20 min. before start of the session. The reactor was illuminated during the whole experiment, except for the grey-coloured time intervals. The blue dots denote the liquid bulk concentration of cyclohexanol divided by cyclohexanone (right vertical axis).

Reactor session 14 (Figure 3.3.7) started under dry conditions, to see whether the monolith that was producing in the previous session under humid conditions would produce under dry conditions, e.g. because there was still water existent in the IIMR system (for example, water dissolved in the liquid cyclohexane). No cyclohexanone/cyclohexanol production is observed during dry illumination, liquid bulk concentrations even decrease. The rate of cyclohexanone decrease at dry conditions is constant up to time 120 min. After 120 min., the decrease rate changed. Session 14 is concluded under humid conditions, for which production is observable.

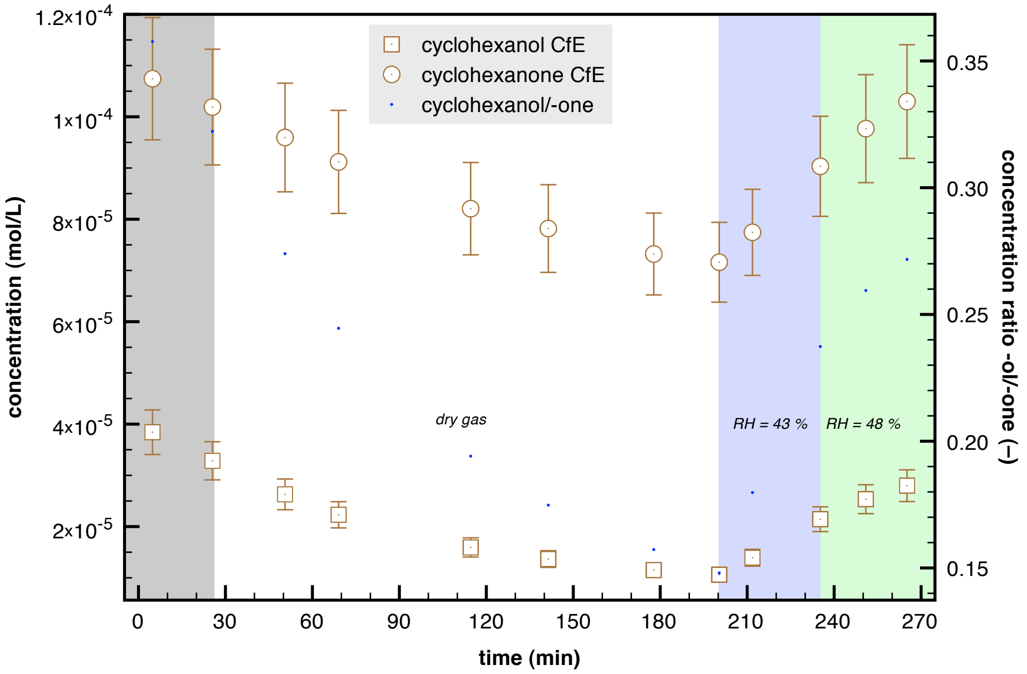

Figure 3.3.7 — Reactor session 14: liquid bulk concentrations of cyclohexanone and cyclohexanol (corrected for evaporation) versus time. The reactor was illuminated during the whole experiment, except for the grey-coloured time interval. Coloured time intervals denote a certain level of humidification of gas. The blue dots denote the liquid bulk concentration of cyclohexanol divided by cyclohexanone (right vertical axis).

The monolith was regenerated after session 14, and the IIMR was dried by nitrogen. Session 15 (Figure 3.3.8) started with dry conditions and fresh cyclohexane, to check whether bulk cyclohexanone production is produced after regeneration. During dry illumination, bulk production of cyclohexanone and little production of cyclohexanol are observed. When water vapour is added (RH 49 %) the liquid bulk concentrations of both cyclohexanone and cyclohexanol increase steadily.

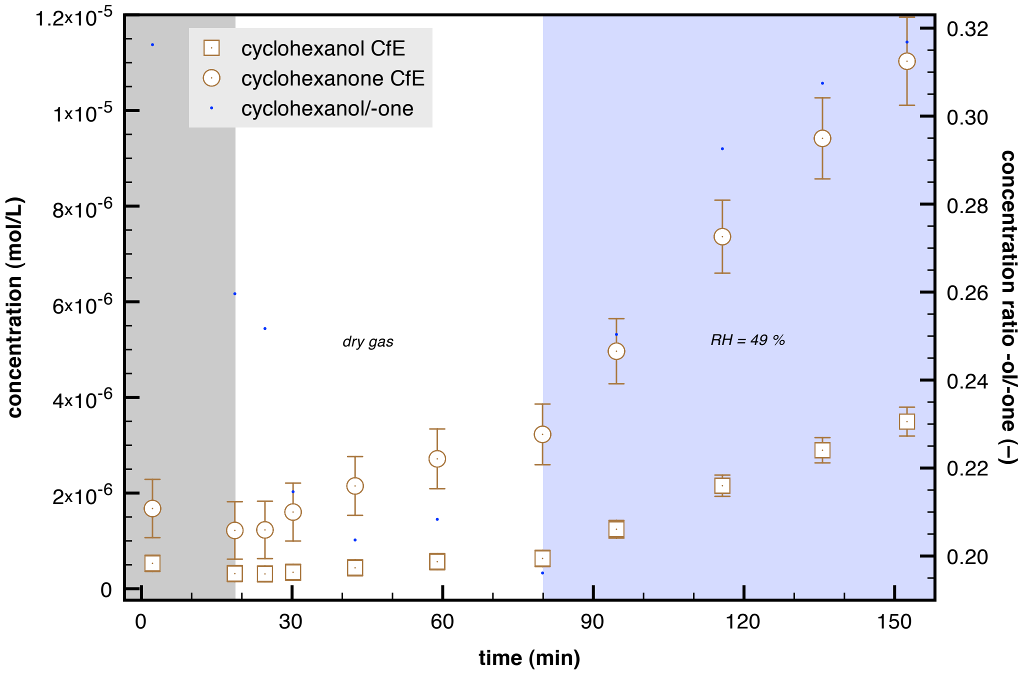

Figure 3.3.8 — Reactor session 15: liquid bulk concentrations of cyclohexanone and cyclohexanol (corrected for evaporation) versus time. The monolith was regenerated and the system was dried by nitrogen for four hours. Fresh cyclohexane was used. Dry gas was used, except for the blue-coloured time interval (49 % relative humidity of the gas). The reactor was illuminated during the whole experiment, except for the grey-coloured time interval. The blue dots denote the liquid bulk concentration of cyclohexanol divided by cyclohexanone (right vertical axis).

Session 16 (Figure 3.3.9) is carried out at dry conditions and at low humidity (RH 9 %). Both the dry period before and after the humid time interval show a decrease in cyclohexanone and cyclohexanol bulk concentrations. For humid conditions (RH 9 %) both concentrations increase steadily.

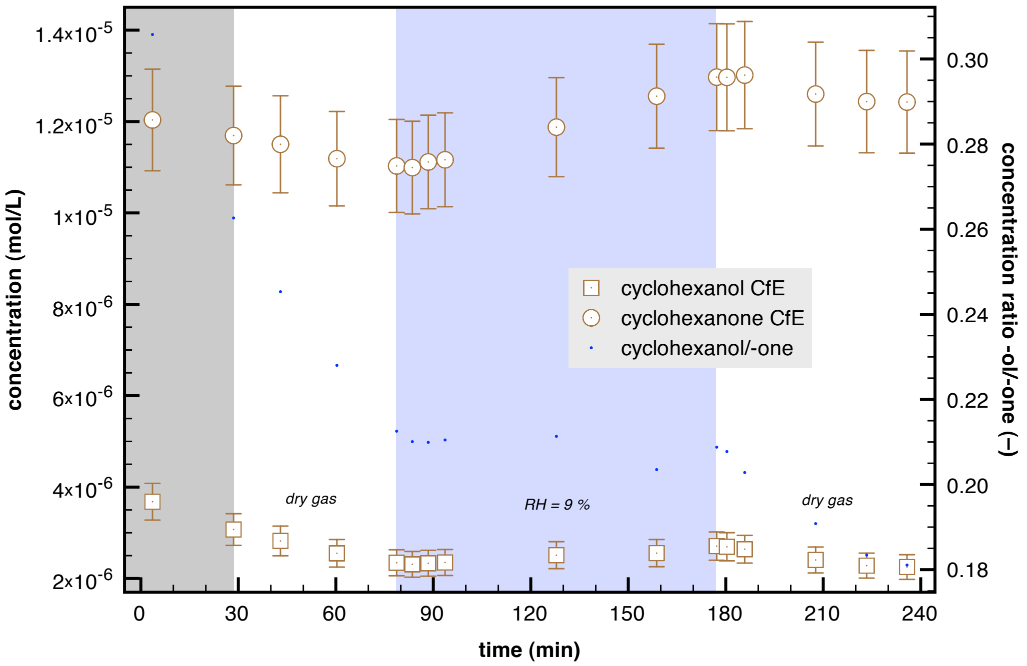

Figure 3.3.9 — Reactor session 16: liquid bulk concentrations of cyclohexanone and cyclohexanol (corrected for evaporation) versus time. The reactor was illuminated during the whole experiment, except for the grey-coloured time interval. Coloured time intervals denote a certain level of humidification of gas. The blue dots denote the liquid bulk concentration of cyclohexanol divided by cyclohexanone (right vertical axis).

IIMR session 17 (Figure 3.3.10) starts at high humidity (RH 93 %) and following that, the humidity is decreased twice. This session was done to see the effect of high humidity, and the effect of decreasing the humidity during an experiment. The initial concentration of cyclohexanone is 2.2 times as high as the final concentration in session 16, indicating desorption of cyclohexanone during humid darkness (see Section 4.3.2.3). Note that 830 mL liquid from session 16 was used, plus an additional 205 mL fresh cyclohexane.

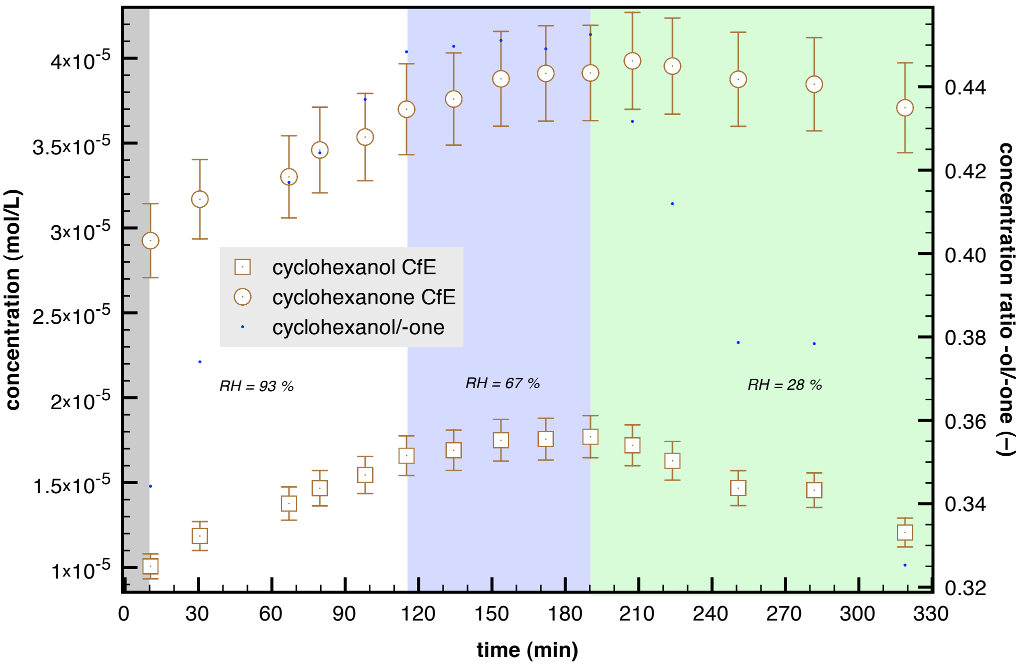

Figure 3.3.10 — Reactor session 17: liquid bulk concentrations of cyclohexanone and cyclohexanol (corrected for evaporation) versus time. The reactor was illuminated during the whole experiment, except for the grey-coloured time interval. Coloured time intervals denote a certain level of humidification of gas. From before the start of this session, humidified gas (93 % relative humidity) had flown through the system for 30 min. The blue dots denote the liquid bulk concentration of cyclohexanol divided by cyclohexanone (right vertical axis).

Session 18 (Figure 3.3.11) was carried out at low to moderate humidities, starting with dry conditions. Humidity was on purpose increased, decreased and then increased to different levels. Production of bulk cyclohexanone and cyclohexanol can be seen, except for the dry dark period and the illuminated period with RH 6 %, for which liquid bulk concentrations decreased.

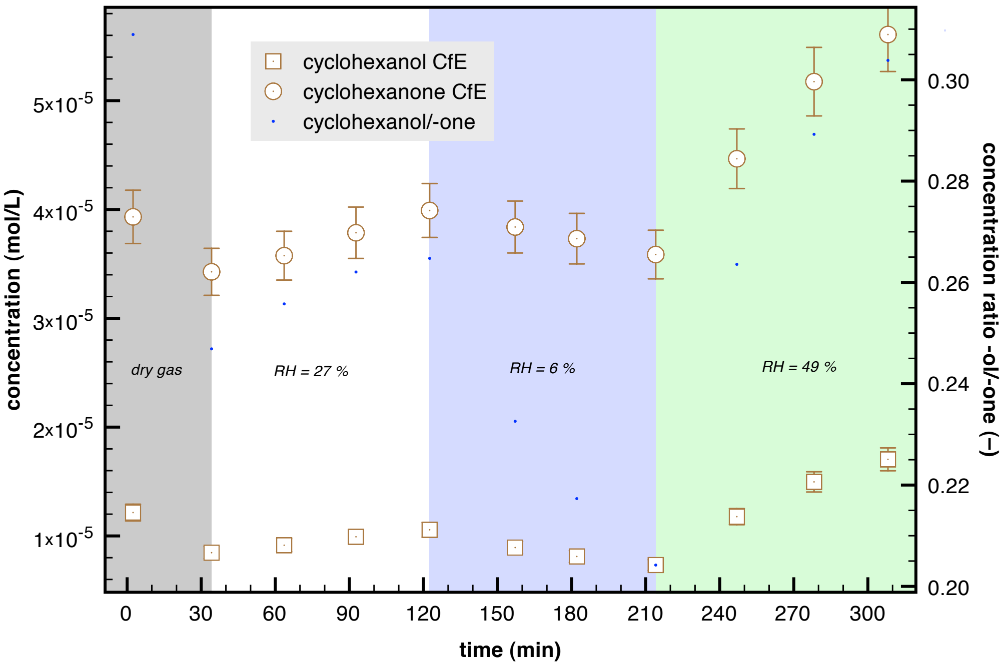

Figure 3.3.11 — Reactor session 18: liquid bulk concentrations of cyclohexanone and cyclohexanol (corrected for evaporation) versus time. The reactor was illuminated during the whole experiment, except for the grey-coloured time interval. The IIMR (including the monolith) was dried by nitrogen for 45 min. before the start of this session. Coloured time intervals denote a certain level of humidification of gas. The blue dots denote the liquid bulk concentration of cyclohexanol divided by cyclohexanone (right vertical axis).

IIMR session 19 (Figure 3.3.12) was done at 52 % RH for six hours to determine the long-term stability of cyclohexanone bulk production. The IIMR was dried by nitrogen overnight before the start of session 19. Two different bulk production rates can clearly be observed for both cyclohexanone and cyclohexanol. After around 120 minutes of production, both rates decrease to another stable level. No reactor conditions were changed, therefore we think this decrease in production is caused by a change in surface occupation of the monolith, see Section 4.3.2.

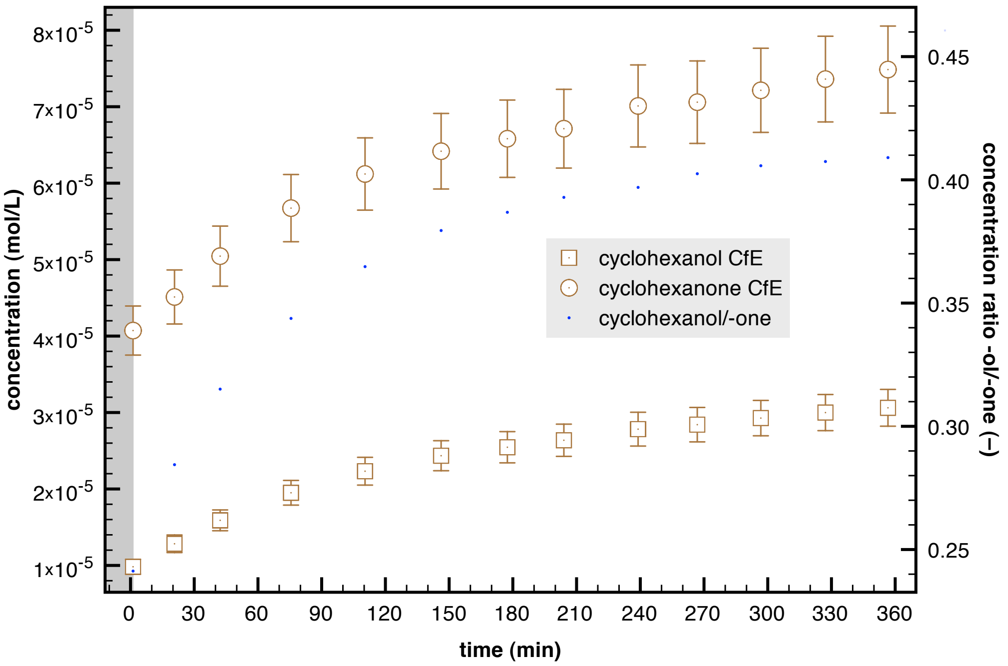

Figure 3.3.12 — Reactor session 19: liquid bulk concentrations of cyclohexanone and cyclohexanol (corrected for evaporation) versus time. The reactor was illuminated during the whole experiment, except for the grey-coloured time interval. The gas relative humidity was 52 %. The IIMR (including the monolith) was dried by nitrogen overnight before the start of this session. The blue dots denote the liquid bulk concentration of cyclohexanol divided by cyclohexanone (right vertical axis).

IIMR session 30 (Figure 3.3.13) was conducted to check whether drying by nitrogen overnight could make the monolith produce cyclohexanone under dry conditions. Unfortunately, it clearly does not produce cyclohexanone nor cyclohexanol at dry illumination after drying overnight. For humid illumination, production of both compounds can be observed. The production at RH 69 % decreases after a while.

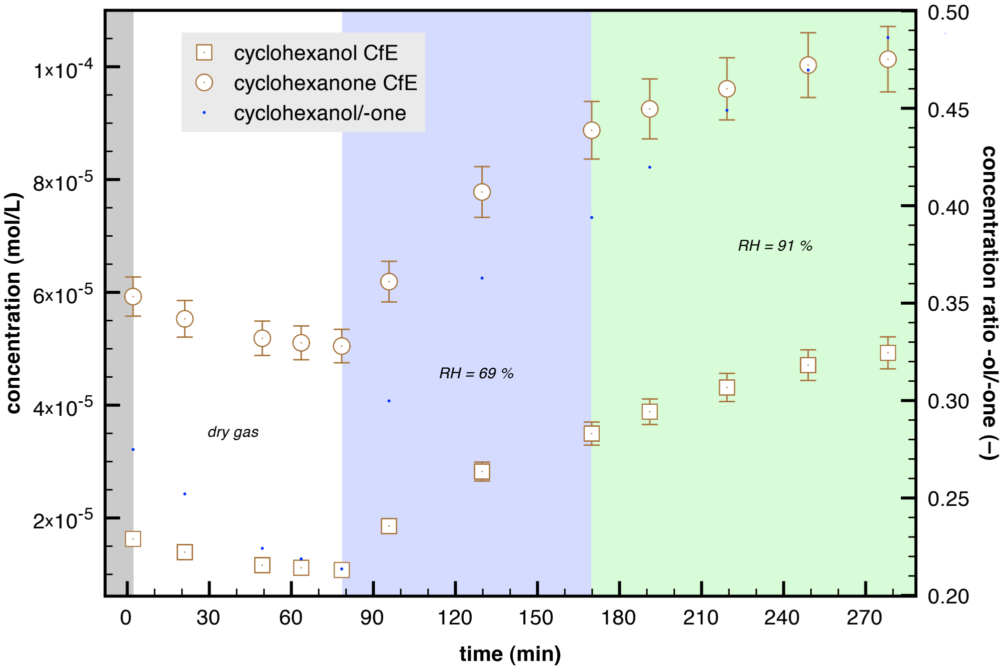

Figure 3.3.13 — Reactor session 30: liquid bulk concentrations of cyclohexanone and cyclohexanol (corrected for evaporation) versus time. The reactor was illuminated during the whole experiment, except for the grey-coloured time interval. The IIMR (including the monolith) was dried by nitrogen overnight before the start of this session. Coloured time intervals denote a certain level of humidification of gas. The blue dots denote the liquid bulk concentration of cyclohexanol divided by cyclohexanone (right vertical axis).

CHAPTER 4

Discussion

4.1. Determination of irradiance by side-light emitting fibres

Irradiance of side-light emitting fibres was determined to estimate whether the conversion of the IIMR is limited by the amount of photons supplied by the fibres. Therefore, a rough estimation of the minimum irradiance available was conducted. Irradiance was measured at the end of an old fibre, this will underestimate the total irradiance since light emission at the end will be less than at the lamp-side of the fibre. And irradiance of a dirty, used fibre will be less than irradiance from a new, clean fibre.

Determined amount of $3{\cdot}10^{-2}\,\mathrm{mol\,h^{-1}}$ ($0.19\,\mathrm{mol\,h^{-1}\,m^{-2}}$) photons in wavelength range 230–388 nm is comparable to the irradiance per surface area Du et al. (2008, p. 126) use with an IIMR and with a side light fibre reactor. Note that Du et al. (2008, p. 126) mention a top illumination reactor and annular slurry reactor that employ higher values for irradiance.

Our irradiance is a factor 580 times bigger than maximal determined rate of cyclohexanone production using an IIMR (see Table 1.5.1).

4.2. Quantitative GC analysis of standard solutions

A set of twelve standard solutions was prepared by sequential dilution of one solution of cyclohexane containing weighed amounts of cyclohexanone, cyclohexanol and hexadecane. Analysis by gas chromatography of these standard solutions yields a linear correlation for peak area and concentration of each dissolved compound. Therefore, we conclude that developed GC method can be used to determine concentrations of cyclohexanone, cyclohexanol and hexadecane in cyclohexane.

No change in GC response can be detected after one month, thus indicating that used GC detection method is stable for at least one month.

The used GC column (HP-5 from Agilent) is a non-polar column. Peaks of cyclohexanone and cyclohexanol are difficult to separate from an in-between non-polar compound. Thus, we recommend to try a different, probably more polar column type to improve separation and thus reduce analysis time. Du et al. (2008) and Carneiro et al. (2009) have used a more polar column (Chrompack CPwax52CB) than we have.

4.3. Photocatalysis using IIMR

Photocatalytic oxidation of cyclohexane was conducted using the IIMR, at different humidities of the gas flow. Closed mode sessions (without any gas flow) were also conducted. Liquid bulk concentrations of cyclohexanone and cyclohexanol were monitored using GC, see Section 3.3 and Appendix J for the resulting concentration plots. The system was checked for production rate limitations caused by irradiance and liquid flow. Liquid flow does not influence the production rate of bulk cyclohexanone around $1.6\ \mathrm{L\,min^{-1}}$. Undimmed irradiance of $3\cdot10^{-2}\,\mathrm{mol\,h^{-1}}$ photons in wavelength range 230–388 nm limited the cyclohexanone production rate. Unfortunately, no IIMR experiments could be found in literature in which production limitation by irradiance was tested like done in this work. No influence of temperature fluctuations on reaction rates could be observed for sessions 1–4. See Appendix L for more discussion on this.

4.3.1. Monolith deactivation and regeneration under dry gas flow. Using a freshly coated monolith with TiO_2 (reactor session 1), cyclohexanone is produced for 80 minutes when illuminated at dry conditions. After 80 minutes, cyclohexanone bulk concentration decreases. The same monolith in combination with fresh cyclohexane from the shelf (reactor session 2) results immediately in a similar decrease in cyclohexanone bulk concentration. We think that after 80 minutes of illumination, the monolith is deactivated. Heating the monolith to 450 °C for 15 minutes (see Section 2.5.7) restores cyclohexanone productivity of the illuminated monolith (reactor sessions 3 and 4). Note that no cyclohexanol is produced under dry gas flow.

Carneiro et al. (2011) show by ATR-FTIR that adsorbed carboxylates and carbonates accumulate on the surface of Hombikat UV100 and Solaronix "S450" during irradiation at dry conditions. Carboxylates decrease the photocatalytic activity of TiO_2 (Du et al., 2006). Carboxylates and carbonates are formed by successive oxidation reactions of adsorbed cyclohexanone. In the end, carboxylates and carbonates can be oxidised to carbon dioxide and water. Another route of carboxylate/carbonate formation via cyclohexylperoxide might also play a role. (Carneiro et al., 2010, p. 203) Carboxylates and carbonates could be responsible for the deactivation of the monolith in this work. Heating the monolith in air will burn carboxylates and carbonates off, therefore restoring photocatalytic activity.

Besides carboxylates and carbonates, adsorbed cyclohexanone, cyclohexanol and water influence bulk cyclohexanone productivity. These compounds will also burn/evaporate off the monolith when heated.

Carneiro et al. (2010, p. 205) were not able to restore activity of powdery Hombikat by heat treatment at 400 °C for 1 h (Solaronix "S450" could be regenerated however). It could be that 400 °C is too low for all inhibiting species to burn, or that coated Hombikat behaves differently from Hombikat in the form of powder. Sintering during heat treatment could be suppressed for coated Hombikat.

4.3.2. The influence of water vapour. IIMR sessions conducted under humid conditions (RH $>$ 20 %) show that water vapour prevents deactivation of the monolith. Stable cyclohexanone production is possible for at least 6 hours when water vapour is added to the gas flow (reactor sessions 13–19 & 30). It is not possible to reactivate the monolith activity at dry conditions by applying humid gas flow in advance, see Figures 3.3.9 and 3.3.13. Carneiro et al. (2011, p. 130) obtained the same type of results for illumination of Solaronix "S450" powder in a top illuminated slurry reactor (TIR): humidified gas flow yielded sustainable cyclohexanone bulk production. They also tested Hombikat UV100, but these particles agglomerated due to the water vapour, thus decreasing active surface area. This turned out to be detrimental for activity.

Operation of the IIMR in closed mode (reactor sessions 10–12) yields stable cyclohexanone production too (maximum tested duration 7 hours). During closed mode operation, the humidity sensor of the IIMR reports 55 % relative humidity. We think that humid air from the surroundings of the system diffuses into the system during closed mode operation. Note that in open mode, there is gas flow that creates some overpressure, thus preventing air from the laboratory entering the system. Due to the glass/glass connections and flexible tubing connected to steel, the IIMR cannot be considered gas-tight. The humidity is likely the cause for stability of cyclohexanone bulk production in closed mode.

Figure 4.3.1 displays bulk cyclohexanone production rates versus relative humidity. Cyclohexanol/cyclohexanone production rate ratios are also shown (blue dots, right axis). Negative production rates (consumption from the liquid bulk, by adsorption onto the monolith surface) are plotted, but their production rate ratios are omitted. The rates were determined by linear regression of the liquid bulk concentrations of cyclohexanone. See Appendix K for the raw data.

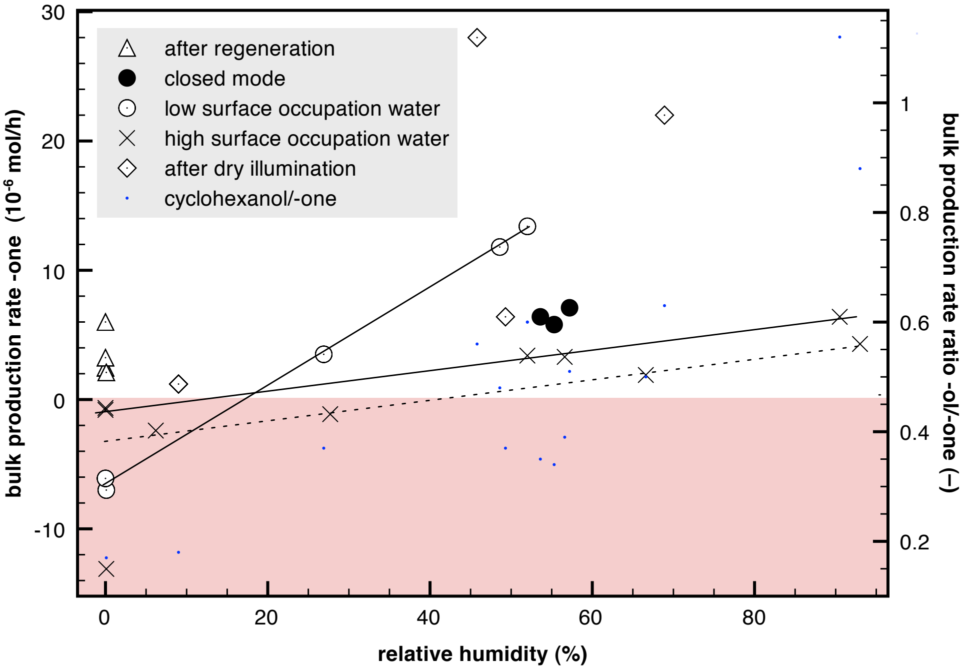

Figure 4.3.1 — Liquid bulk production rates of cyclohexanone (corrected for evaporation) versus relative humidity. The blue dots denote the liquid bulk production rate of cyclohexanol divided by that of cyclohexanone (right vertical axis). Triangles denote rates at dry conditions obtained directly after regeneration of the monolith. Solid circles are from closed mode experiments, and crosses are from the experiments from which we think surface occupation of water has reached a high value. Tilted squares denote rates obtained after a period of illumination under dry conditions. Production rate ratios of negative rates are not shown. The lightly red-coloured area denotes negative production rates. The three manually drawn lines are for visibility purposes only. Both lines connecting the crosses are of exactly the same slope.

In general, water vapour enhances photocatalytic activity, but more detailed effects of water vapour can be identified. Therefore, cyclohexanone production rates are categorised according to reactor operation mode and monolith history. Cyclohexanone production rates displayed by a triangle in Figure 4.3.1 were observed directly after regeneration of the monolith, under dry conditions.[1] Production rates obtained in closed mode are denoted by solid circles.

Some (parts of) IIMR sessions were preceded by a period of humidified gas flow.[2] Monolith surface occupations of water of these humid experiments were considered to have reached a high value. Their cyclohexanone production rates are marked by a cross in Figure 4.3.1. Open circles denote rates that were obtained after a period of dry gas flow, and for which no decrease in activity had been seen yet.

The distinction between high and low surface occupation of water can be quite arbitrary since we did not measure water occupancy directly. See for example Figure 3.3.12: the monolith of session 19 was dried overnight, and showed up to 80 minutes a stable bulk cyclohexanone production (at 52 % RH). After that point in time, cyclohexanone production decreased to a lower (but stable) level. We think that the monolith surface adsorbed water from the humidified gas flow. The first rate is classified as obtained for a surface low in water occupancy (open circle), the second rate is thought to represent a surface rich in water content (cross).

The qualifications "high" and "low" in water surface occupation should be regarded in relation to the circumstances: when a highly occupied surface at 10 % RH gas flow is brought under 90 % RH gas flow, the surface is lowly occupied initially at the new 90 % RH conditions. This is because

---

[1] Sessions 1, 3, 4 and 15.

[2] Sessions 13, 14 (until 120 min.), 16 (dry periods), 17, 18 (RH 6 %), 19 from time 150 min. and session 30 from time 150 min.

the water occupancy corresponding to adsorption equilibrium at 10 % RH is far less compared to the water occupancy corresponding to adsorption equilibrium at 90 % RH. [3]

Production rates obtained at humidified conditions that were seen following on a period of illumination at dry gas flow are marked by a tilted square. [4]

Detailed effects of water vapour that can be identified from Figure 4.3.1 will be discussed in following paragraphs.

4.3.2.1. *Water vapour increases activity and decreases selectivity.* Production rate of cyclohexanone increases for increasing humidity. The blue dots show that the increase in cyclohexanone production rate comes at the cost of a decrease in selectivity towards cyclohexanone. Water vapour enhances both cyclohexanone as well as cyclohexanol production rate, the latter increasing relatively more. We think that water vapour dissolves in liquid cyclohexane, and then adsorbs at the monolith surface (which is covered by a liquid film of cyclohexane). Note that water that has been dissolved in the liquid phase during previous humid conditions is not sufficient (at dry conditions) to yield comparable effects as water vapour, see for example reactor session 14 (Figure 3.3.7).

Some adsorbed water could be converted into hydroxyl radicals (see Section 1.2.1). These hydroxyl radicals improve reaction rates. Hydroxyl radicals can convert inhibiting species such as carboxylates at the catalyst surface into carbon dioxide, thus preventing deactivation of the monolith. Ameen and Raupp (1999) for example detected that water vapour converts adsorbed species involved in photocatalytic gas-phase *o*-xylene degradation into carbon dioxide.

But as previously stated, it is not possible to regenerate the activity of the monolith under dry conditions by using water vapour in advance (see Figures 3.3.9 and 3.3.13). Therefore, it is not likely that a significant amount of the adsorbed carboxylates is converted into free sites by hydroxyl radicals at humidified conditions. Another possible explanation is that free sites created by carboxylate degradation were occupied by cyclohexanol and cyclohexanone from the bulk immediately, thus inhibiting activity at dry conditions. Bulk concentrations of these products were significantly lower in sessions using a regenerated monolith under dry conditions than in the sessions employing dry gas flow after humid gas flow. An experiment employing a deactivated monolith and fresh cyclohexane (low content of cyclohexanone and cyclohexanol) could show whether carboxylate degradation by water-vapour induced hydroxyl radicals lead to significant activity under dry conditions. This was not done in this work, see also Section 5.3 for this recommendation.

Significant amounts of bulk cyclohexanol were produced at humid conditions, while at dry conditions virtually no cyclohexanol was produced. Increasing humidity results in cyclohexanol production increasing relatively more than cyclohexanone production. This could be due to increasing concentrations of hydroxyl radicals, see Section 1.2.2.

4.3.2.2. *Water inhibits activity by surface occupation.* Experiments for which a high surface occupation of water should be assumed (crosses), show lower cyclohexanone production rate than experiments of lower surface water content (open circles, RH > 20 %). Both categories of rates show a linear dependence on relative humidity, which is visualised by the two manually drawn lines in the plot. Increasing humidity of the gas phase has a less strong effect (smaller slope of the plot) on the cyclohexanone production rate for surfaces highly occupied by water. We think that water occupies sites at the surface that are otherwise used for the reactions involved in cyclohexanone production. Thus, the higher the water surface occupation, the lower the bulk cyclohexanone productivity since water occupies production sites at the catalyst surface. Then cyclohexane adsorption is limited by water, thus decreasing cyclohexanone production.

Session 17 (Figure 3.3.10) showed a consumption of cyclohexanone at 28 % relative humidity from 210 min. Session 18 was carried out the next day and started with 30 min. of dry gas flow without liquid in the system, and then another 30 min. of dry gas flow when cyclohexane was pumped around the non-illuminated IIMR. After this drying period, humid gas flow (27 % RH) and

---

[3] An example of this can be seen in IIMR session 18 (Figure 3.3.11). During the period of illumination at RH 27 % the monolith surface is considered to contain not much water, due to the history of dry gas flow. During the period of RH 6 %, the monolith surface is considered to be occupied with water heavily, due to the history of a significant higher humidity before. Illumination at higher humidity (RH 49 %) follows, then the monolith surface is considered to contain (relatively) low amounts of water, due to the lower humidity used before.

[4] Rates from sessions 14 (from 120 min.), 15, 16 and 30.

illumination resulted in cyclohexanone production. This result shows that dry gas flow can remove water from the monolith surface, thus increasing cyclohexanone productivity at humid conditions. Note that drying of the monolith does not result in regeneration of activity at dry conditions, see session 30 (Figure 3.3.13).

Two lines were drawn parallel to each other in Figure 4.3.1. The dotted line connects the rates obtained for surfaces that were illuminated at significant higher humidity ($>$ 9 % RH) previously (except for the rate obtained at 93 % RH, the highest humidity used). The lowest cyclohexanone rate displayed by the plot (lower left corner) was also preceded by significantly higher humidity. We think that going from high to a lower humidity, water desorbs from the surface, yielding free sites at the surface. These free sites are then occupied by a.o. cyclohexanone that adsorbs from the bulk, thus giving a lower rate of bulk cyclohexanone production. We think this lower rate can be seen until water adsorption equilibrium has been reached: then the rate increases to the parallel solid line.

Cyclohexanone bulk production rates obtained in closed mode (solid circles) are in between the rates of surfaces of low and high water occupation. We ascribe this difference to the different experimental conditions used. For closed mode, we think humid air from the surroundings could enter the IIMR. Therefore, the concentration of oxygen will have been higher for closed mode than for the open mode experiments which were done at 1:1 air/nitrogen flow.

4.3.2.3. *Water enhances desorption of cyclohexanone.* During illumination of a deactivated monolith under dry gas flow, cyclohexanone is consumed from the bulk (negative bulk production rate). The tilted squares in Figure 4.3.1 show that addition of water vapour after dry illumination yields an increased production rate of bulk cyclohexanone. This rate is above the level of cyclohexanone production of experiments without a history of illumination under dry conditions. We think that the cyclohexanone that was consumed from the bulk during dry illumination, was adsorbed by the monolith surface (see Section 4.3.3). This adsorbed cyclohexanone is desorbed from the monolith surface during humid illumination. We subtracted the amount of adsorbed cyclohexanone during dry illumination from the production rates during humid conditions after dry illumination. These calculations yield rates that are in line with the rates denoted by open circles in Figure 4.3.1, thus supporting our thought that water enhances desorption of cyclohexanone.

The rate of $6.4 \cdot 10^{-6}\,\mathrm{mol\,h^{-1}}$ for 49 % RH obtained after a period of dry illumination (tilted square) is a special case: the monolith was regenerated and dried before session 15. Production of cyclohexanone was observed during illumination under dry gas flow, thus it makes sense that the rate of cyclohexanone production under humidified conditions is not higher than the other humidified rates. This production rate of session 15 (humidified part) is in between the rates of highly and lowly water-occupied surfaces. This could indicate that the surface was moderately occupied by water after dry illumination.

Humidified gas flow during darkness enhances desorption too. This can be seen from the cyclohexanone bulk concentration development between session 16 and 17. Humidified gas flow without illumination resulted in an increased cyclohexanone concentration. Cyclohexanol bulk concentration increased as well. Carneiro et al. (2011) have shown that humidified gas enhances desorption of cyclohexanone from Solaronix “S450”, at both dark and illuminated conditions.

How exactly water vapour enhances desorption of cyclohexanone cannot be deducted from the results of this work. Competitive adsorption could play a role, like Almquist and Biswas (2001) suggest.

4.3.2.4. *Dry productivity of a regenerated monolith.* Cyclohexanone rates determined at dry conditions after regeneration (triangles) do not show a trend in time. These bulk production rates are from session 1, 3, 4 and 15. Session 15 yields the lowest bulk production rate of cyclohexanone, but is close to the others. Session 4 yields the highest rate, further away from the other values. Loose white powder was found in the liquid circulating the IIMR. We think that this loss of titania-coating does not influence the productivity of the monolith significantly, since productivity of the most recent session (15) is close to the first sessions (1 and 3).

4.3.2.5. *Cyclohexanol production.* Figure 4.3.2 displays production rates of cyclohexanol versus relative humidity in the same manner as Figure 4.3.1 does. The same trends can be observed from Figure 4.3.2 as for the case of cyclohexanone production (see previous sections). Difference is that the trends for surfaces low and high in water occupation (denoted by circles and crosses) are less linear than for cyclohexanone. This could be due to the non-first order reaction rate behaviour, as suggested by Section 1.2.2.

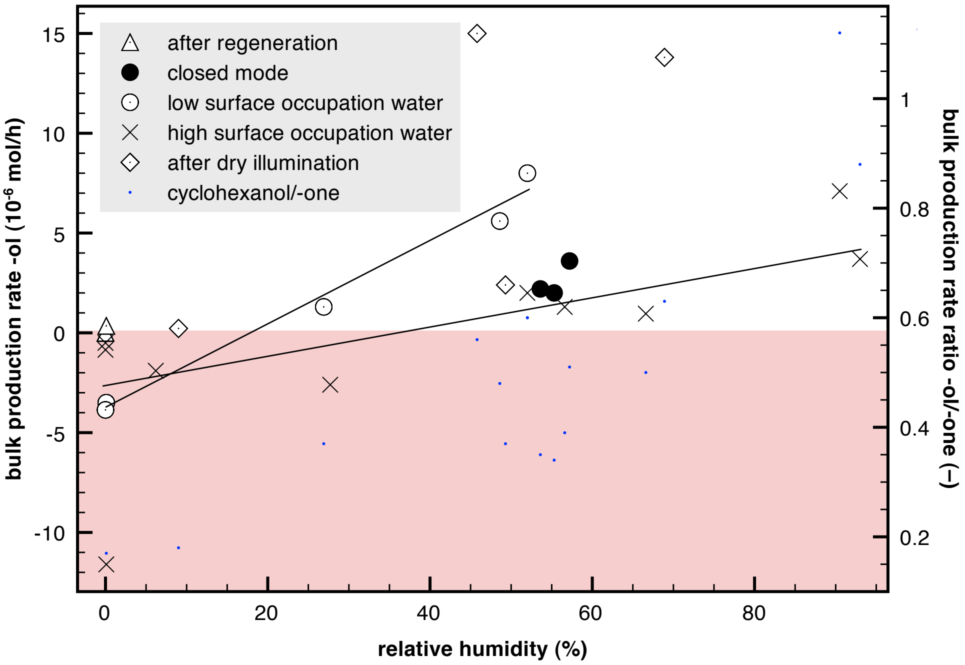

Figure 4.3.2 — Liquid bulk production rates of cyclohexanol (corrected for evaporation) versus relative humidity. The blue dots denote the liquid bulk production rate of cyclohexanol divided by that of cyclohexanone (right vertical axis). Triangles denote rates at dry conditions obtained directly after regeneration of the monolith. Solid circles are from closed mode experiments, and crosses are from the experiments from which we think surface occupation of water has reached a high value. Tilted squares denote rates obtained after a period of illumination under dry conditions. Production rate ratios of negative rates are not shown. The lightly red-coloured area denotes negative production rates. The two manually drawn lines are for visibility purposes only.

4.3.2.6. *Conclusions on the influence of water vapour.* For good readability, we summarise now the conclusions we have drawn in this section on the influence of water vapour on photocatalytic cyclohexanone production.

Water vapour enhances desorption of cyclohexanone from the illuminated and from the dark monolith surface. During illumination of the monolith, water vapour prevents bulk cyclohexanone production from ceasing. More water vapour leads to increasing bulk cyclohexanone production. This comes at the price of decreasing selectivity towards cyclohexanone; bulk cyclohexanol is produced relatively more.

We think that water adsorbs from the liquid bulk at the monolith surface, and then enhances somehow the desorption of other compounds such as cyclohexanone and cyclohexanol. On the other hand, adsorbed water decreases the number of sites available for cyclohexane adsorption, thereby limiting cyclohexanone production eventually.

Let us rephrase this while looking at Figure 4.3.3, where surface occupations are schematically visualised in relation to the rate-RH plot of cyclohexanone. Note that cyclohexane is not shown on the surfaces, but will be abundant since the liquid bulk is almost pure cyclohexane.

Bulk cyclohexanone production for a dry surface that is illuminated at humid conditions depends strongly on the humidity; this is represented by the steepest line. Drawings *c* and *e* show that the surface is lowly occupied with water. Over time, more and more water will adsorb at the monolith surface, until adsorption equilibrium has been reached. The less steep line reflects this equilibrium situation, drawings *a* and *d* show a lot of adsorbed water at the surface, and less free sites and less adsorbed cyclohexanone and cyclohexanol than *c* and *e*. Due to the adsorbed water, less surface sites are involved in cyclohexanone production and thus less additional cyclohexanone can be desorbed by increasing the amount of water vapour. In other words: less free surface sites are available for cyclohexane adsorption, thus limiting cyclohexanone production.

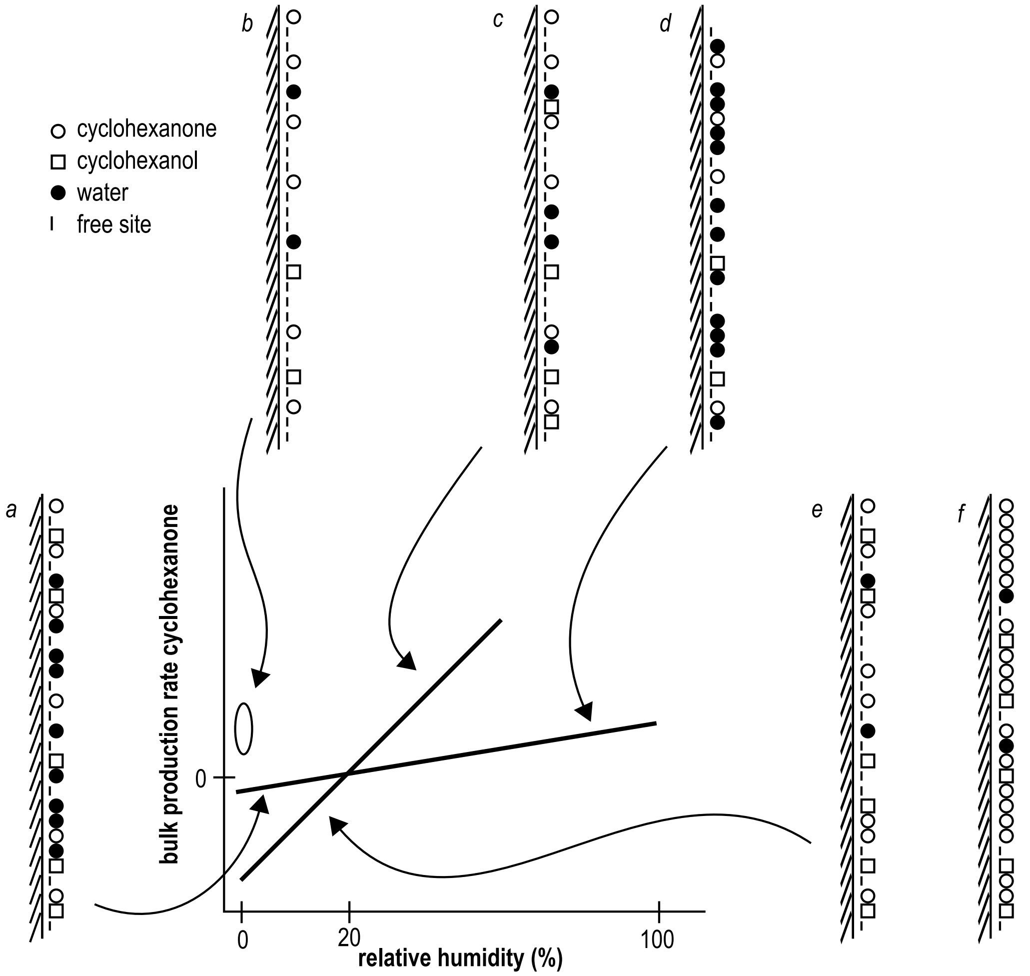

Figure 4.3.3 — Schematic representation of the monolith surface for different positions in the rate-RH plot of cyclohexanone (Figure 4.3.1). The drawings of surfaces from left to right represent: RH $<$ 20 % high water content (*a*), regenerated surface dry conditions (*b*), RH $>$ 20 % low water content (*c*), RH $>$ 20 % high water content (*d*), RH $<$ 20 % low water content (*e*) and a deactivated surface under dry conditions (*f*, not shown in plot).

Monolith surfaces at low humidity of the gas phase will show less adsorbed water and thereby more adsorbed cyclohexanone and cyclohexanol (due to more free sites available for product adsorption) than monolith surfaces at high humidity. This can be seen from comparing drawings *a* to *d* and from comparing drawings *e* to *c*. For low humidity (RH $<$ 20 %) there is too little water vapour available to make the deactivated monolith surface produce bulk cyclohexanone; it even adsorbs cyclohexanone.

Around 20 % RH, the trend lines for surfaces low in water content and surfaces high in water content cross each other, around a production rate of zero. Below 20 % RH, a relatively dry surface (drawing *e*) adsorbs more bulk cyclohexanone than a wet surface (drawing *a*). The dry surface has more free sites available for adsorption of cyclohexanone, cyclohexanol and water due to the lower water occupancy. Water adsorption is less important than cyclohexanone/cyclohexanol adsorption due to the low humidity. Eventually after enough time, the dry surface will have become relatively wet (due to water adsorption) and will have adsorbed cyclohexanone and cyclohexanol, thus the dry surface of drawing *e* will eventually become like drawing *a* (and will show lower adsorption of bulk cyclohexanone as showed in the plot). Note that for both cases *a* and *e* there is net adsorption of cyclohexanone from the bulk; there is too little water vapour available to desorb more cyclohexanone from the surface than is being adsorbed.

The same process applies to humidities $>$ 20 % RH with the difference that water adsorption is more important than adsorption of cyclohexanone and cyclohexanol because of the high humidity.

Dry surface *c* will become occupied more by water after time, and less occupied by cyclohexanone and cyclohexanol due to water adsorption. Thus, dry surface *c* will become wet surface *d* after enough time and will desorb less cyclohexanone than *c* did.

Figure 4.3.3 also shows a regenerated monolith surface that is producing bulk cyclohexanone (active monolith, drawing *b*) at dry conditions. After 80 min. of dry illumination the monolith deactivates, the surface is thought to become like shown in drawing *f*. This surface is highly occupied by reaction products cyclohexanone and cyclohexanol. Furthermore, little produced water is adsorbed on the surface and there is very few free sites available for cyclohexane adsorption. It could be that carboxylates and carbonates are also adsorbed, but as shown by this work these compounds do not play a major role.

4.3.3. Physical adsorption of cyclohexanone and cyclohexanol. All the observations presented and discussed in Appendix I lead us to the thought that bulk cyclohexanone decrease (like observed under dark periods of further illuminated IIMR sessions) is favoured by a history of illumination of the monolith. The longer ago this illumination, the less the concentration cyclohexanone decreases. And without any illumination ever occurred, no significant cyclohexanone decrease can be determined (experiment of slice of monolith in beaker). It is known that illumination can change adsorption properties of titania, e.g. the photo-induced hydrophilic effect (Fujishima et al., 2008).

When not illuminated, cyclohexanone and cyclohexanol concentrations decrease for open mode dry experiments. We think that the monolith adsorbs cyclohexanone and cyclohexanol. This results in a decrease in liquid bulk concentrations under dark conditions because there is no production of these compounds by the photocatalyst. During illumination, adsorption will not likely result in a decrease in liquid bulk concentrations: production by the photocatalyst outweighs adsorption.

For closed mode experiments 10 & 11, cyclohexanone and cyclohexanol concentrations are stable during darkness. The availability of water vapour could play a role here: when water has occupied most of the free sites on the monolith surface, less free sites are available for adsorption of cyclohexanone and cyclohexanol.

Start concentration of cyclohexanone of session 30 is decreased 20 % in comparison to the final concentration of preceding session 19, due to physical adsorption during the dark illumination period before the start of session 30.

4.3.4. This work compared to other work. Dry reactor sessions of this work show a decline in cyclohexanone production rate after 40–50 minutes of illumination. Du et al. (2008, p. 126 fig. 10) determined a stable increase in cyclohexanone concentration for over 50 minutes of illumination under presumably dry conditions, at 50 °C. Figure 4.3.4 shows the real liquid bulk concentrations for reactor session 1 (see for other graphs of real bulk concentrations Appendix H). These uncorrected concentrations show a stable increase in cyclohexanone after 60 minutes of illumination. It is not clear whether Du et al. corrected cyclohexanone concentrations for evaporation of cyclohexanone. Looking at the similarities between the uncorrected concentrations of cyclohexanone of this work and the cyclohexanone concentrations determined by Du et al., we suggest that Du et al. might not have corrected for cyclohexane evaporation. Note that work done by Carneiro et al. (2010, p. 203) does show a decrease of production rate after 150 min in a slurry reactor.

Another explanation for the lack of deactivation in the work done by Du et al. (2008, p. 126 fig. 10) could be that there was water vapour existent in the system, for example because there was no gas flow into the system (however, looking at the text of the article this seems unlikely), thus introducing moist from the laboratory atmosphere.

A third explanation could be the higher temperature (50 °C) employed by Du et al., this work uses 25 °C. On the other hand, this work showed that temperature fluctuations of 5 °C (reactor sessions 3 and 4) do not result in a significantly different cyclohexanone production rate. See Section L.2 for more discussion on effects of temperature.

Furthermore, the production plot by Du et al. shows a stable production rate of $7.9 \cdot 10^{-6}\,\mathrm{mol\,h^{-1}}$ during 230 min. Comparing this to the rates seen in this work (see Figure 4.3.1) we think this is comparable to the bulk production we obtained in closed mode. Therefore, we think that Du et al. operated the IIMR under humid conditions, possibly in closed mode.

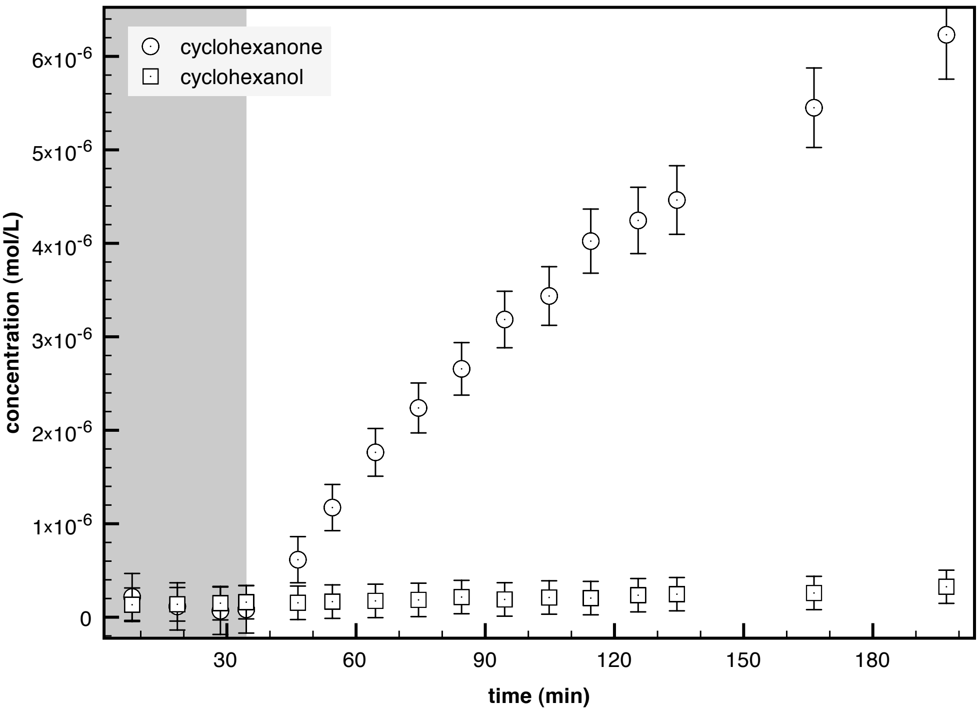

Figure 4.3.4 — Reactor session 1: real liquid bulk concentrations of cyclohexanone and cyclohexanol (not corrected for evaporation) versus time. From 34.5 min. the reactor was illuminated.

We did not determine a significant change in cyclohexanol concentration for reactor session 1. Du et al. (2008, p. 126 fig. 10) showed cyclohexanol production comparable to cyclohexanone production. Cause for this difference might be in the higher temperature used by Du et al. and/or in the existence of water vapour.

CHAPTER 5

Conclusions and recommendations

5.1. Main conclusion on water vapour

We have investigated the influence of water vapour on the performance of an internally illuminated monolith reactor (IIMR) in photocatalytic oxidation of cyclohexane. We conclude that water vapour prevents deactivation of the photocatalyst Hombikat UV100 coated onto a cordierite monolith in bulk cyclohexanone production for relative humidity > 20 %. Increasing relative humidity of the gas flow increases the bulk production rate of cyclohexanone linearly. This increased cyclohexanone production comes at the price of a more than proportional increase in bulk cyclohexanol production, thus decreasing selectivity towards cyclohexanone.

We think the production enhancement by water vapour is mainly due to altered adsorption/desorption behaviour of cyclohexanone, possibly by competitive adsorption. However, hydroxyl radicals will certainly play a role (albeit minor), as can be concluded from the non-linear dependency of bulk cyclohexanol production on relative humidity.

5.2. Other conclusions

We have not detected mass transfer limitations for the used IIMR. Applied irradiance of $3 \cdot 10^{-2}\,\mathrm{mol\,h^{-1}}$ photons in wavelength range 230–388 nm limited the production rate of cyclohexanone.

Operation under dry gas flow deactivates the monolith after 80 minutes of illumination. Regeneration of the monolith (450 °C for 15 minutes) restores cyclohexanone productivity of the illuminated monolith under dry conditions.

Closed mode operation yields stable cyclohexanone productivity due to humid air from the surroundings entering the IIMR via leakages.

The coated monolith lost some titania during operation, but this did not influence the activity of the monolith significantly.

Physical adsorption of cyclohexanone and cyclohexanone on the titania-coated monolith was influenced by the history of illumination of the monolith. The more recent the illumination, the more adsorption of these compounds was observed. A slice of never illuminated titania-coated monolith did not show adsorption.

5.3. Recommendations

This section lists some recommendations we make that are directly connected to the current setup and work. Chapter 6 contains suggestions for future work, i.e. recommendations on a more broader basis.

We recommend to do more IIMR sessions in open mode and conditions employed in this work to support the concluded dependencies of bulk cyclohexanone production rate on relative humidity more firmly and precisely. Especially around RH 10 %, 20 %, 40 % and 80 % more results are needed (see Figure 4.3.1). For RH < 20 %, a very long experiment is interesting to see whether adsorption of cyclohexanone from the bulk will come to an end.

Furthermore, an IIMR session that starts using fresh cyclohexane, a deactivated monolith and humid conditions for a short period can show whether humid conditions really do not regenerate the monolith by the degradation of adsorbed carboxylates by hydroxyl radicals. This short period of humid operation should be followed directly by operation under dry gas flow, to check whether activity is (partially) restored and thus the monolith is regenerated or not. The fresh cyclohexane is necessary to exclude the possibility of deactivation under dry conditions by the adsorption of reaction products like cyclohexanone and cyclohexanol (see Section 4.3.2.1 for more information).

The IIMR is not gas-tight at the moment of writing. A gas-tight IIMR introduces the possibility of exploring different humidities of the gas phase in closed mode IIMR operation. Then the dependency of cyclohexanone bulk production rate on relative humidity for closed mode sessions can be explored. This possibly makes experiments also more precise, since evaporation of cyclohexane can be kept at an absolute minimum.

Another recommendation for minimising evaporation of cyclohexane is to install cyclohexane saturators in the line of incoming gas flow of the IIMR. A third option could be to change from the highly evaporating cyclohexane to a less evaporating reactant, such as methylcyclohexane.

Current work lacks a method for determining gas-phase composition of the outlet of the IIMR. Therefore, it can be that we are producing carbon dioxide, which should be taken into account for determining production selectivity towards cyclohexanone. We thus recommend to install a gas-liquid chromatograph for regular determination of the gas-phase composition of the IIMR during operation.

This work also lacks a method for determination of monolith surface occupancies during operation. We recommend to find a suitable (spectroscopic) technique (e.g. ATR-FTIR) that gives a clear view of the compounds adsorbing at the monolith surface during IIMR operation.

The cyclohexanone bulk production of the current setup is limited by irradiance. Therefore, we recommend to increase irradiance to at least $3\,\mathrm{mol\,h^{-1}\,m^{-2}}$, this value corresponds to the maximum for linear dependency of reaction rate on irradiance according to Leite Pimenta Carneiro et al. (2010, p. 201). We recommend to include a means of dimming the irradiance in a controllable manner. LED (light-emitting diode) could be an energy-saving alternative to the currently used mercury lamp, since LED is capable of emitting photons of certain discrete wavelengths, thus making more effectively use of electricity. There should preferably be no coupling of fibre bundles to minimise loss of light. When coupling is necessary, special paste of a refractive index similar to the fibres should be applied in coupling.

Used fibres in this work are not durable. The tip-coating gets loose over time, and the fibres are easily broken. We recommend to explore ways to endure the tip-coating and fibres itself.

We recommend to explore other IIMR operation parameters besides humidity. Oxygen content of the gas flow, temperature and irradiance can be varied. If it is determined that at certain conditions the performance of the IIMR is limited by mass transfer, it can be useful to change monolith geometry and flow conditions to explore other regimes than film flow (such as Taylor flow) for enhanced mass transfer.

The titania coated on the monolith should be analysed. There is a slice of coated monolith that has never been used in the IIMR available, as well as the coated monolith that is used in the IIMR. Common techniques like scanning electron microscopy can reveal whether the monolith has been homogeneously coated, thickness of the coating, and durability (by comparing the slice with the used monolith).

A good analysis of performance of the IIMR should include a mass balance. Therefore, dead volumes in the IIMR should be minimised, to be able to exactly measure the amount of liquid contained by the IIMR. The current setup cannot be emptied totally because of these dead volumes, e.g. in the metal tubing from gear pump up to the reactor. Analysis of the gas-phase is of course also necessary for a good mass-balance. The adsorbed components on the monolith itself should also be analysed for a closed mass-balance. This could be done together with the (spectroscopic) technique to analyse the surface occupancies during operation. Alternatively, the monolith could after operation be analysed by thermogravimetric analysis (TGA).

Risk analysis & evaluation of the IIMR should be evaluated regularly. Most important point of concern currently is the thermostat of the constant temperature water bath. When this thermostat breaks or gets disconnected, the bath will heat the water infinitely. Thus, a new bath or protective measurement should be installed that stops (the bath from) heating whenever the thermostat gets disconnected or breaks down.

CHAPTER 6

Suggestions for future work

We give suggestions for future work in this chapter. These recommendations are broader than the current work and setup (Section 5.3). We conclude this chapter with an outlook.

It is possible to create a monolith that consists of titania only. It is recommended to obtain such an anatase monolith, thereby eliminating the need for coating a ceramic monolith.

The fibres are a weak point of the IIMR. In order to illuminate the surface of the monolith, it could be an option to create a UV-transparent monolith and illuminate the photocatalyst from the side of the monolith. Like Du et al. (2008, p. 127) show this is not optimal when considering the concentration profiles of reactants and photons, since these are coming from the opposite direction. But the elimination of the need for coating (and arising problems) could overcome the disadvantages posed by the concentration profiles.

We have shown that humid gas under dark conditions induces a fast desorption of cyclohexanone from the monolith surface. In designing an industrial process, this dark desorption behaviour should be considered to increase activity of the monolith. For example, one could alternate humid illuminated production with a (relatively short) period of dark humid desorption of reaction products, to increase production during the next illuminated production period. An extra consideration is the addition of a period of dry gas flow, to desorb water from the surface, thus freeing sites for cyclohexanone production.

For increased selectivity towards cyclohexanone, one could employ a short period of dry illumination. If this period is short enough (less than 80 minutes, probably around 5 minutes) formation of irreversibly deactivating species such as carboxylates and carbonates could be prevented because illumination time is too short to oxidise cyclohexanone further. This short period of dry illumination could then be followed by dark humid desorption and dry gas flow as described previously.

6.1. Outlook

This work showed options for improving the stability of cyclohexanone production by photocatalytic oxidation of cyclohexane using an internally illuminated monolith reactor. But at the end of a day of stable bulk cyclohexanone production, conversions are extremely low. At the best, we reach a production rate of $1 \cdot 10^{-5}\,\mathrm{mol\,h^{-1}}$ cyclohexanone. We used 1 L of cyclohexane, that is 9 moles. Thus, we are roughly 6 orders of magnitude from 100 % conversion.

Increasing cyclohexanone productivity with 5–6 orders of magnitude will cost a lot of effort and time. Of course, life is full of challenges, but perhaps it is wiser to shift the potential application focus of the IIMR from the chemical bulk industry towards the fine chemicals industry. Then conversion is less important. For producing e.g. medicines, selectivity will be very important, and selectivity is what makes photocatalytic oxidation interesting.

Another option is to focus on the removal of trace compounds from e.g. waste streams (such as contaminated water). Then conversion of course has to be high, but since very little reactant is available the IIMR could do the job.

CHAPTER 7

List of abbreviations

Abbreviation	Meaning
ALS	Automatic liquid sampler (in use with a GC)
ATR-FTIR	Attenuated total reflectance Fourier transform infrared spectroscopy
CfE	Corrected for evaporation (for evaporation of cyclohexane in this work)
FID	Flame ionisation detector (detector for a GC)
GC	Gas-liquid chromatograph
HED	Hexadecane
IIMR	Internally illuminated monolith reactor
TIR	Top illumination reactor
RH	Relative humidity

CHAPTER 8

List of symbols

Symbol	Unit	Description
A	$\mathrm{m^2}$	Surface area available for mass transfer
a	$\mathrm{m^2\,m^{-3}}$	Specific surface area
c	$\mathrm{mol\,L^{-1}}$	Concentration
H	$\mathrm{J\,mol^{-1}}$	Enthalpy
J	$\mathrm{mol\,m^{-2}\,s^{-1}}$	Molar flux
K	*depends on reaction*	Reaction equilibrium constant
k_L, k_G	$\mathrm{m\,s^{-1}}$	Mass transfer coefficient
K_H	$\mathrm{mol\,m^3\,Pa^{-1}}$	Henry's law constant
M	$\mathrm{g\,mol^{-1}}$	Molar mass
m	–	Dimensionless solubility
n	mol	Amount of substance
P	Pa	Pressure or partial pressure
R	$\mathrm{J\,mol^{-1}\,K^{-1}}$	Gas constant
S	$\mathrm{J\,mol^{-1}\,K^{-1}}$	Entropy
T	K	Temperature
v	$\mathrm{m\,s^{-1}}$	Velocity
V	$\mathrm{m^3}$	Volume
δ	m	Film thickness
ρ	$\mathrm{kg\,m^{-3}}$	Density
Φ_m	$\mathrm{kg\,s^{-1}}$	Mass flow
Φ_v	$\mathrm{m^3\,s^{-1}}$	Volumetric flow
ω	rpm	Pump speed
[]	$\mathrm{mol\,L^{-1}}$	Concentration of a compound

Subscript	Description
ads	Adsorbed
app	Apparent
avg	Average
eq	Equilibrium
G	Gas phase
H_2O	Water
HED	Hexadecane
i	Interface
int	Initial
L	Liquid phase
v	Volumetric basis

Superscript	Description
$\varnothing$	Standard conditions (most stable form of compound at 1 bar and 25 °C)
sat	Saturation conditions

Bibliography

Almeida, A., November 2010. Cyclohexane photo-catalytic oxidation on tio2, an in situ atr-ftir mechanistic and kinetic study. Ph.D. thesis, Delft University of Technology.
URL `http://resolver.tudelft.nl/uuid:9fe64f7c-443e-4724-b9be-6d2b68d59872`

Almeida, A. R., Berger, R., Moulijn, J. A., Mul, G., 2011. Photo-catalytic oxidation of cyclohexane over tio2: a novel interpretation of temperature dependent performance. Physical Chemistry Chemical Physics 13 (4), 1345–1345.
URL `http://dx.doi.org/10.1039/c0cp00879f`

Almquist, C. B., Biswas, P., 06 2001. The photo-oxidation of cyclohexane on titanium dioxide: an investigation of competitive adsorption and its effects on product formation and selectivity. Applied Catalysis A: General 214 (2), 259–271.
URL `http://dx.doi.org/10.1016/S0926-860X(01)00495-1`

Ameen, M. M., Raupp, G. B., 05 1999. Reversible catalyst deactivation in the photocatalytic oxidation of diluteo-xylene in air. Journal of Catalysis 184 (1), 112–122.
URL `http://dx.doi.org/10.1006/jcat.1999.2442`

Bettencourt da Silva, R. J. N., Camões, M. F., 2010. The quality of standards in least squares calibrations. Analytical Letters 43 (7), 1257–1257.
URL `http://dx.doi.org/10.1080/00032710903518674`

Carneiro, J. T., Berger, R., Moulijn, J. A., Mul, G., September 2009. An internally illuminated monolith reactor: Pros and cons relative to a slurry reactor. Catalysis Today 147 (Supplement 1), S324–S329.
URL `http://dx.doi.org/10.1016/j.cattod.2009.07.041`

Carneiro, J. T., Moulijn, J. A., Mul, G., 07 2010. Photocatalytic oxidation of cyclohexane by titanium dioxide: Catalyst deactivation and regeneration. Journal of Catalysis 273 (2), 199–210.
URL `http://dx.doi.org/10.1016/j.jcat.2010.05.015`

Carneiro, J. T., Yang, C.-C., Moulijn, J. A., Mul, G., 01 2011. The effect of water on the performance of tio2 in photocatalytic selective alkane oxidation. Journal of Catalysis 277 (2), 129–133.
URL `http://dx.doi.org/10.1016/j.jcat.2010.10.019`

Carp, O., Huisman, C. L., Reller, A., 2004. Photoinduced reactivity of titanium dioxide. Progress in Solid State Chemistry 32 (1-2), 33–177.
URL `http://dx.doi.org/10.1016/j.progsolidstchem.2004.08.001`

de Lasa, H., Serrano, B., Salaices, M. (Eds.), 2005. Photocatalytic Reaction Engineering. Springer US.
URL `http://dx.doi.org/10.1007/0-387-27591-6`

Du, P., Carneiro, J. T., Moulijn, J. A., Mul, G., 01 2008. A novel photocatalytic monolith reactor for multiphase heterogeneous photocatalysis. Applied Catalysis A: General 334 (1-2), 119–128.
URL `http://dx.doi.org/10.1016/j.apcata.2007.09.045`

Du, P., Moulijn, J. A., DelftChemTech, TU Delft, D. U. o. T., February 2009. Catalysis engineering of light induced dye degradation and cyclohexane photo-oxidation.
URL `http://resolver.tudelft.nl/uuid:288516cb-0364-448b-a160-b30dac0988ab`

Du, P., Moulijn, J. A., Mul, G., Maart 2006. Selective photo(catalytic)-oxidation of cyclohexane: Effect of wavelength and tio2 structure on product yields. Journal of Catalysis 238 (2), 342–352.
URL `http://dx.doi.org/10.1016/j.jcat.2005.12.011`

Foo, K. Y., Hameed, B. H., 01 2010. Insights into the modeling of adsorption isotherm systems. Chemical Engineering Journal 156 (1), 2–10.
URL `http://dx.doi.org/10.1016/j.cej.2009.09.013`

Fornasini, P., 2009. The Uncertainty in Physical Measurements. Springer New York, New York, NY.
URL `http://dx.doi.org/10.1007/978-0-387-78650-6`

Fujishima, A., Zhang, X., Tryk, D. A., 12 2008. Tio2 photocatalysis and related surface phenomena. Surface Science Reports 63 (12), 515–582.
URL `http://dx.doi.org/10.1016/j.surfrep.2008.10.001`

Guiochon, G., Guillemin, C. L., 1988. Quantitative gas chromatography: for laboratory analyses and on-line process control. Elsevier.

Henderson, M. A., 06 2011. A surface science perspective on photocatalysis. Surface Science Reports 66 (6-7), 185–297.
URL `http://dx.doi.org/10.1016/j.surfrep.2011.01.001`

Herrmann, J. M., 2005. Heterogeneous photocatalysis: state of the art and present applications in honor of pr. r.l. burwell jr. (1912–2003), former head of ipatieff laboratories, northwestern university, evanston (ill). Topics in Catalysis 34 (1-4), 49–65.
URL `http://dx.doi.org/10.1007/s11244-005-3788-2`

Herrmann, J.-M., 09 2010. Photocatalysis fundamentals revisited to avoid several misconceptions. Applied Catalysis B: Environmental 99 (3-4), 461–468.
URL `http://dx.doi.org/10.1016/j.apcatb.2010.05.012`

Hibbert, D., Gooding, J., 2006. Data analysis for chemistry: an introductory guide for students and laboratory scientists. Oxford University Press.
URL `http://books.google.com/books?id=d7v7jLAAcbcC`

Hoffmann, M. R., Martin, S. T., Choi, W., Bahnemann, D. W., 01 1995. Environmental applications of semiconductor photocatalysis. Chemical Reviews 95 (1), 69–96.
URL `http://dx.doi.org/10.1021/cr00033a004`

Leite Pimenta Carneiro, J. T., Moulijn, J. A., Mul, G., ChemE, TU Delft, D. U. o. T., April 2010. Application of semiconductor photocatalysis for organic synthesis: from photons to the process.
URL `http://resolver.tudelft.nl/uuid:a5f58400-98eb-41f4-9065-e17e5ce2dd96`

Musser, M. T., 2000. Ullmann's Encyclopedia of Industrial Chemistry. Wiley-VCH Verlag GmbH, Ch. Cyclohexanol and Cyclohexanone.
URL `http://dx.doi.org/10.1002/14356007.a08_217`

Pangarkar, K., Schildhauer, T. J., van Ommen, J. R., Nijenhuis, J., Kapteijn, F., Moulijn, J. A., 05 2008. Structured packings for multiphase catalytic reactors. Industrial & Engineering Chemistry Research 47 (10), 3720–3751.
URL `http://dx.doi.org/10.1021/ie800067r`

Wild, J. D., Sridhar, T., Potter, O. E., 06 1978. Solubility of nitrogen and oxygen in cyclohexane. The Chemical Engineering Journal 15 (3), 209–214.
URL `http://dx.doi.org/10.1016/0300-9467(78)80005-7`

APPENDIX A

Kinetics

For developing an overall model describing the performance of the IIMR, the influence of the following parameters on reaction kinetics is needed:

1. concentrations of oxygen, cyclohexane and water
2. adsorption equilibria of the involved compounds on the catalyst
3. irradiance

Almeida et al. (2011) have produced a micro-kinetic model, which was experimentally validated and fitted using ATR-FTIR spectroscopy. The titania surface was illuminated by $8.98 \cdot 10^{-9}\,\mathrm{Einstein\,cm^{-2}\,s^{-1}}$ at 375 nm by UV-LEDs during the experiments (Almeida, 2010, p. 25).

Next paragraphs describe the model from Almeida et al. (2011), including additional assumptions, and the implementation using Simulink 7.5 (part of MATLAB R2010a, from The MathWorks).

A.1. Micro-kinetic model from Almeida et al. (2011)

Bulk cyclohexane (Cyh) and water (H_2O) are assumed to be in equilibrium with respectively adsorbed cyclohexane (Cyh^*) and water (H_2O^*):

$$\mathrm{Cyh} + * \overset{K_{\mathrm{Cyh}}}{\rightleftharpoons} \mathrm{Cyh}^* \tag{A.1.1}$$

$$\mathrm{H_2O} + * \overset{K_{\mathrm{H_2O}}}{\rightleftharpoons} \mathrm{H_2O}^* \tag{A.1.2}$$

Free sites on the catalyst surface are denoted by $*$.

Adsorbed cyclohexane reacts with superoxide ion (O_2^-) forming adsorbed cyclohexanone (CyhO^*) and water:

$$\mathrm{Cyh}^* + \mathrm{O_2^-} \underset{{}^\bullet\mathrm{OH}}{\overset{k_1}{\rightarrow}} \mathrm{CyhO}^* + \mathrm{H_2O}^* \tag{A.1.3}$$

Adsorbed cyclohexanone can react further to adsorbed carboxylate ($C_6H_{11}O_2^*$):

$$\mathrm{CyhO}^* + {}^\bullet\mathrm{OH} \overset{k_2}{\rightarrow} \mathrm{C_6H_{11}O_2^*} \tag{A.1.4}$$

Adsorbed cyclohexane can react with superoxide ion and hydroxide radical (${}^\bullet OH$). This side-reaction forms adsorbed carboxylate and water:

$$\mathrm{Cyh}^* + \mathrm{O_2^-} + {}^\bullet\mathrm{OH} \overset{k_3}{\rightarrow} \mathrm{C_6H_{11}O_2^*} + \mathrm{H_2O}^* \tag{A.1.5}$$

Cyclohexanone will desorb from the catalyst surface, leaving behind a free site on the catalyst (denoted $*$):

$$\mathrm{CyhO}^* \overset{k_4}{\rightarrow} \mathrm{CyhO} + * \tag{A.1.6}$$

The equations describing chemical equilibria, production rates and the adsorption balance are listed in Table A.1.1. Necessary parameters are listed in Table A.1.2. Note that the total number of active sites is denoted N_{T} (mol), the total liquid reactor volume V_{R} and the fractional occupancy θ.

It is assumed that bulk water and bulk cyclohexane are always in equilibrium with their adsorbed counterparts. Cyclohexanone and carboxylates are not in adsorption equilibrium. The adsorption balance can be rewritten in terms of equilibrium (eq) and non-equilibrium (neq) species:

Table A.1.1 — Equations used in the micro-kinetic model of Almeida et al. (2011)

Equation	Description
$K_{\mathrm{Cyh}} = \frac{\theta_{\mathrm{Cyh}}}{[\mathrm{Cyh}]\theta^*}$	Cyclohexane adsorption equilibrium
$K_{\mathrm{H_2O}} = \frac{\theta_{\mathrm{H_2O}}}{[\mathrm{H_2O}]\theta^*}$	Water adsorption equilibrium
$\frac{V_{\mathrm{R}}}{N_{\mathrm{T}}} \frac{\mathrm{d}\,[\mathrm{CyhO}^*]}{\mathrm{d}t} = k_1 \theta_{\mathrm{Cyh}} \left[\mathrm{O}_2\right]^n - k_2 \theta_{\mathrm{CyhO}} - k_4 \left(\theta_{\mathrm{CyhO}} - K_{\mathrm{CyhO}} \left[\mathrm{CyhO}\right] \theta^*\right)$	Production rate adsorbed cyclohexanone
$\frac{V_{\mathrm{R}}}{N_{\mathrm{T}}} \frac{\mathrm{d}[\mathrm{H_2O}^*]}{\mathrm{d}t} = \left(k_1 + k_3\right) \theta_{\mathrm{Cyh}} \left[\mathrm{O}_2\right]^n$	Production rate adsorbed water
$\frac{V_{\mathrm{R}}}{N_{\mathrm{T}}} \frac{\mathrm{d}[\mathrm{C_6H_{11}O_2^*}]}{\mathrm{d}t} = k_2 \theta_{\mathrm{CyhO}} + k_3 \theta_{\mathrm{Cyh}} \left[\mathrm{O}_2\right]^n$	Production rate adsorbed carboxylates
$\frac{V_{\mathrm{R}}}{N_{\mathrm{T}}} \frac{\mathrm{d}[\mathrm{CyhO}]}{\mathrm{d}t} = k_4 \left(\theta_{\mathrm{CyhO}} - K_{\mathrm{CyhO}} \left[\mathrm{CyhO}\right] \theta^*\right)$	Production rate bulk cyclohexanone
$1 = \theta^* + \theta_{\mathrm{Cyh}} + \theta_{\mathrm{CyhO}} + \theta_{\mathrm{H_2O}} + \theta_{\mathrm{C_6H_{11}O_2}}$	Adsorption balance

Table A.1.2 — Parameters used in the micro-kinetic model of Almeida et al. (2011)

Parameter	Value	Description
K_x	$K_{x,296} \exp\left\{\frac{-\Delta H_{x,\mathrm{ads}}}{R}\left(\frac{1}{T} - \frac{1}{296\,\mathrm{K}}\right)\right\}$	Equilibrium constant of adsorption of compound x (cyclohexane, water or cyclohexanone)
$K_{\mathrm{Cyh},296}$	$0.31\,\mathrm{m^3\,mol^{-1}}$	Equilibrium constant of cyclohexane adsorption at 296 K
$\Delta H_{\mathrm{Cyh,ads}}$	$-34.4 \cdot 10^3\,\mathrm{J\,mol^{-1}}$	Enthalpy of cyclohexane adsorption
$K_{\mathrm{H_2O},296}$	$\frac{766\,\mathrm{m^3\,mol^{-1}}}{8.73}$	Equilibrium constant of water adsorption at 296 K[a]
$\Delta H_{\mathrm{H_2O,ads}}$	$-47.1 \cdot 10^3\,\mathrm{J\,mol^{-1}}$	Enthalpy of water adsorption
$K_{\mathrm{CyhO},296}$	$26.9\,\mathrm{m^3\,mol^{-1}}$	Equilibrium constant of cyclohexanone adsorption at 296 K
$\Delta H_{\mathrm{CyhO,ads}}$	$-36.9 \cdot 10^3\,\mathrm{J\,mol^{-1}}$	Enthalpy of cyclohexanone adsorption
k_i	$k_{i,296} \exp\left\{\frac{-E_{a,i}}{R}\left(\frac{1}{T} - \frac{1}{296\,\mathrm{K}}\right)\right\},\ i = 1 \ldots 4$	Reaction rate constants
$k_{1,296}$	$10.84\,\mathrm{m^3\,mol^{-1}\,s^{-1}}$	Reaction rate constant 1 at 296 K
$E_{a,1}$	$0\,\mathrm{J\,mol^{-1}}$	Activation energy of reaction 1
$k_{2,296}$	$0\,\mathrm{s^{-1}}$	Reaction rate constant 2 at 296 K
$E_{a,2}$	n.a.	Activation energy of reaction 2
$k_{3,296}$	$1.74 \cdot 10^{-3}\,\mathrm{m^3\,mol^{-1}\,s^{-1}}$	Reaction rate constant 3 at 296 K
$E_{a,3}$	$18.4 \cdot 10^3\,\mathrm{J\,mol^{-1}}$	Activation energy of reaction 3
$k_{4,296}$	$1286\,\mathrm{s^{-1}}$	Reaction rate constant 4 at 296 K
$E_{a,4}$	$0\,\mathrm{J\,mol^{-1}}$	Activation energy of reaction 4

---

[a] A private communication revealed that the equilibrium constant for water should be divided by 8.73 to account for inactive sites that adsorb water.

$$1 = \theta^* + \sum \theta_{\mathrm{eq}} + \sum \theta_{\mathrm{neq}} \tag{A.1.7}$$

Surface occupation of an equilibrium species i can be isolated as follows (j denotes other equilibrium species; $\sum \theta_{\mathrm{eq}} = \theta_i + \sum_{j \neq i} \theta_j$):

$$\begin{aligned}
1 =& \theta^* + \theta_i + \sum_{j \neq i} \theta_j + \sum \theta_{\mathrm{neq}} \\
1 =& \frac{\theta_i}{K_i\,[i]} + \theta_i + \sum_{j \neq i} K_j\,[j]\,\frac{\theta_i}{K_i\,[i]} + \sum \theta_{\mathrm{neq}} \\
1 =& \theta_i \frac{\left(1 + K_i\,[i] + \sum_{j \neq i} K_j\,[j]\right)}{K_i\,[i]} + \sum \theta_{\mathrm{neq}} \\
\theta_i =& \frac{\left(1 - \sum \theta_{\mathrm{neq}}\right) K_i\,[i]}{\left(1 + K_i\,[i] + \sum_{j \neq i} K_j\,[j]\right)} \\
\theta_i =& \frac{\left(1 - \sum \theta_{\mathrm{neq}}\right) K_i\,[i]}{\left(1 + \sum K_{\mathrm{eq}}\,[\mathrm{eq}]\right)}
\end{aligned} \tag{A.1.8}$$

This micro-kinetic model assumes the Langmuir monolayer adsorption model is applicable. Thus, all adsorption sites are considered to be equal and adsorption enthalpy is independent from surface occupancy θ.

Since pure cyclohexane will be used in this work, it is assumed that the concentration of bulk cyclohexane will be constant. It is assumed that most of the produced water is in the bulk phase. Therefore, bulk concentration of water is taken equal to the total amount of produced water divided by the reactor liquid volume V_R. From this, the catalyst surface occupation of water can be calculated using the water adsorption equilibrium (see Table A.1.1).

See Figure A.1.1 for a schematic representation of the implementation in Simulink. See Appendix B for the supporting MATLAB code. Ode15s was used as solver (variable-step size).

Current implementation of the model was used to make graphs of surface occupancy at different temperatures like Almeida et al. (2011) have done, see Figure A.1.2.

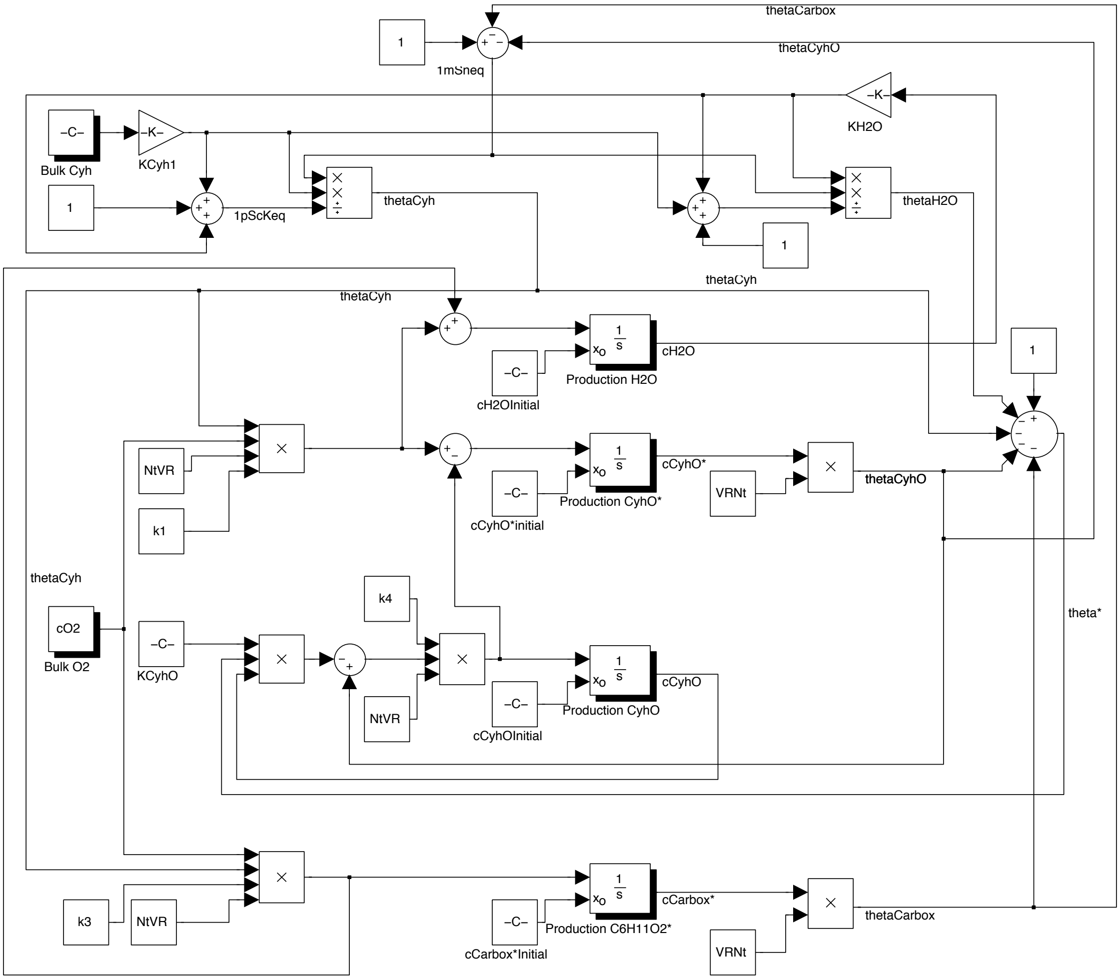

Figure A.1.1 — Implementation of the micro-kinetic model of Almeida et al. (2011) in Simulink

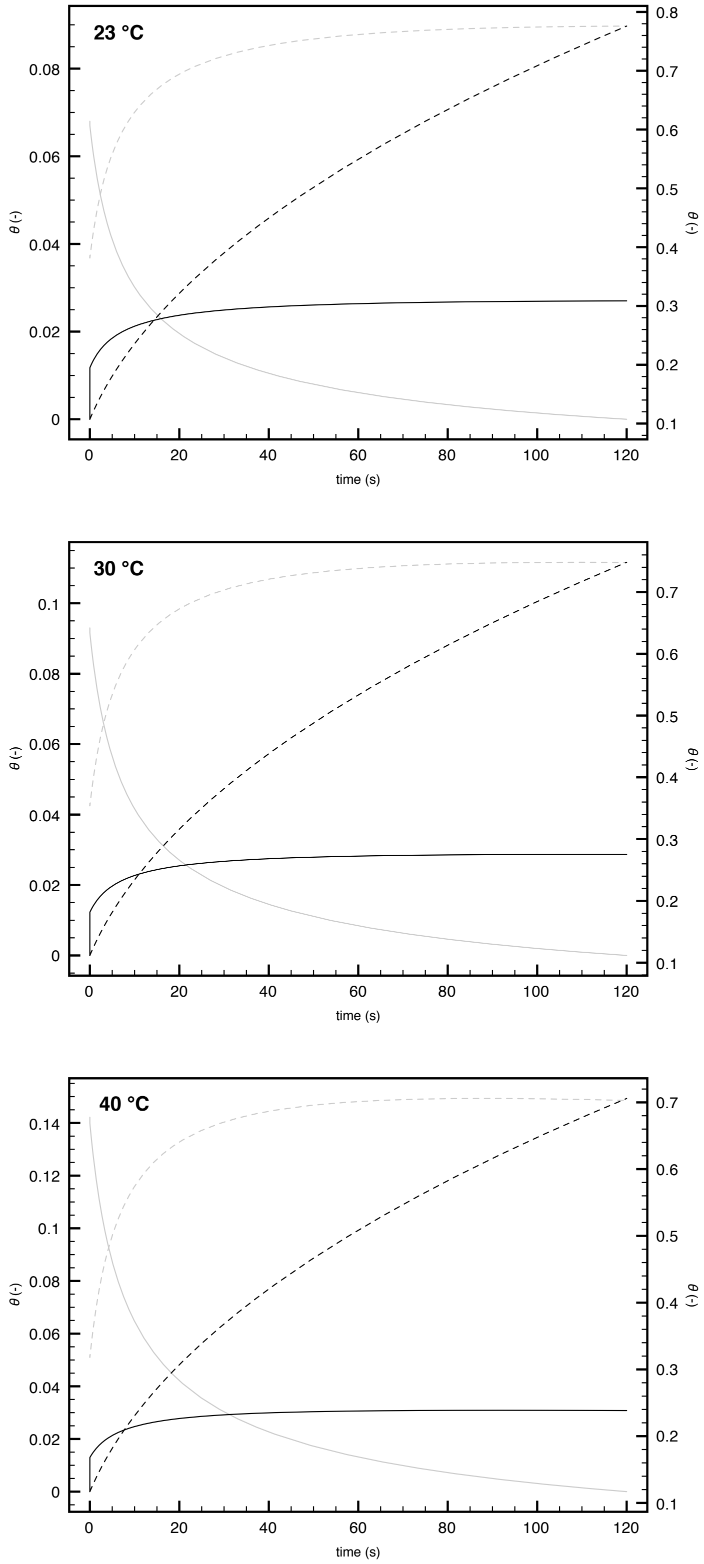

Figure A.1.2 — Surface occupancy of the catalyst surface according to the implementation of this work of the micro-kinetic model by Almeida et al. (2011) at three different temperatures. Cyclohexanone is denoted by the black line, carboxylates by the dashed black line, cyclohexane by the grey solid line and water by the grey dashed line. Grey lines (cyclohexane and water) are projected on the right y-axis.

APPENDIX B

Supporting MATLAB code implementation micro-kinetic model

```
% general assumptions:
% [O2] is stable at saturation concentration at all times
% the amount of cyclohexane is stable at all times (consumption is not
% taken into account)
% all produced water comes in the liquid solution, then theta is calculated

% all data are from A. Almeida, Cyclohexane photo-catalytic oxidation
% on TiO2, an in situ ATR-FTIR mechanistic and kinetic study, PhD thesis,
% Delft University of Technology, November 2010,
% http://resolver.tudelft.nl/uuid:9fe64f7c-443e-4724-b9be-6d2b68d59872.
% unless otherwise noted.


T = 273.15 + 25;

VR = 1.1e-6;
VRNt = VR / 4.9e-8;
%volume of reactor in m^3 divided by number of active sites in mol
NtVR = 1/VRNt;

cO2 = 0.002388400011e3; % mol/m^3 O2 concentration 0.002388400011e3

rhocyclohexane = 0.779e3;  % kg/m^3, src: http://en.wikipedia.org/wiki/Cyclohexane
MMcyclohexane = 84.160; % kg/kmol, src: http://en.wikipedia.org/wiki/Cyclohexane

cCyhInitial = rhocyclohexane/MMcyclohexane*1e3;
% concentration of pure cyclohexane in mol/m^3
cH2OInitial = NtVR + 2.5e-4*cCyhInitial;
% initial water content of reactor system in mol/m^3, NOTE: this is purely
% theoretical, adjusted to results from Ana Rita
cCyhOInitial = 0;
cCyhOAdsInitial = 0;
cCarboxAdsInitial = 0;

k1_296 = 10.84; % m^3 mol^-1 s^-1
Ea1 = 0;
k2_296 = 0; % s^-1
Ea2 = 0;
k3_296 = 1.74e-3; % m^3 mol^-1 s^-1
Ea3 = 18.4; % kJ mol^-1
k4_296 = 1286; % s^-1
Ea4 = 0;

k1 = k1_296*exp(-Ea1 * (1e3/8.314) * (1/T - 1/296));
k2 = k2_296*exp(-Ea2 * (1e3/8.314) * (1/T - 1/296));
k3 = k3_296*exp(-Ea3 * (1e3/8.314) * (1/T - 1/296));
k4 = k4_296*exp(-Ea4 * (1e3/8.314) * (1/T - 1/296));

dHCyhads = -34.4; % kJ mol^-1
KCyh_296 = 0.31; % m^3 mol^-1
KCyh = KCyh_296 * exp(-dHCyhads *  (1e3/8.314) * (1/T - 1/296));
dHH2Oads = -47.1; % kJ mol^-1
KH2O_296 = 766; % m^3 mol^-1
KH2O = (1/8.73) * KH2O_296 * exp(-dHH2Oads *  (1e3/8.314) * (1/T - 1/296));
% adapted for ratio 8.73 named in Athena code
dHCyhOads = -36.9; % kJ mol^-1
KCyhO_296 = 26.9; % m^3 mol^-1
```

```
KCyhO = KCyhO_296 * exp(-1 * dHCyhOads *  (1e3/8.314) * (1/T - 1/296));


%thetaCyhInitial = (KCyh*cCyhInitial)/(1+(KCyh*cCyhInitial + KH2O*cH2OInitial));
% initial cyclohexane coverage, assuming equilibrium
% and neglecting other compounds than cyclohexane and water.
% Furthermore, concentration decrease from absorption is neglected.
%thetaH2OInitial = (KH2O*cH2OInitial)/(1+(KCyh*cCyhInitial + KH2O*cH2OInitial));
%thetaFreeInitial = 1 - (thetaCyhInitial + thetaH2OInitial);


```

APPENDIX C

Calibration mass flow controllers and pump

C.1. Calibration mass flow controllers used before session 7

The mass flow controllers (Brooks 5850S) contained by the IIMR when there was no gas/liquid contactor yet (before IIMR session 7) were calibrated using a Bios Definer 220H calibration apparatus. This calibration devices corrects for real temperature and pressure. The displayed flow $\Phi_{v,i}^{\text{display}}$ was correlated to the real flow $\Phi_{v,i}$ in $\mathrm{L\,min^{-1}}$ (MFC 1) and $\mathrm{mL\,min^{-1}}$ (MFC 2) (20 °C, 760 mm Hg) for both controllers using linear regression ($R > 0.9999$):

$$\Phi_{v,1} = 1.77386 + 1032.72 \cdot \Phi_{v,1}^{\text{display}} \qquad 0.3\,\mathrm{L\,min^{-1}} < \Phi_{v,1}^{\text{display}} < 18.45\,\mathrm{L\,min^{-1}} \tag{C.1.1}$$

$$\Phi_{v,2} = 11.1859 + 1.07336 \cdot \Phi_{v,2}^{\text{display}} \qquad 150\,\mathrm{mL\,min^{-1}} < \Phi_{v,2}^{\text{display}} < 1500\,\mathrm{mL\,min^{-1}} \tag{C.1.2}$$

Mass flow controller 1 is used for air flow, MFC 2 is used for nitrogen flow.

C.2. Calibration pump

A gear pump (Micropump integral series model EG132-0024-U) is used for pumping liquid around the IIMR. This pump has been calibrated by filling a graduated cylinder and measure the time it takes to fill to about 450 mL. For pump speed setting ω of 500, 1000, ..., 5000 rpm flow measurements have been done in triplicate. Linear regression ($R > 0.99$) yields for liquid flow $\Phi_{v,l}$ ($\mathrm{mL\,s^{-1}}$):

$$\Phi_{v,l} = -3.66448 + 1.01099 \cdot 10^{-2} \cdot \omega \qquad 500\,\mathrm{rpm} < \omega < 5000\,\mathrm{rpm} \tag{C.2.1}$$

C.3. Calibration mass flow controllers used from session 7

The mass flow controllers (Brooks 5850S) of the IIMR (including the gas/liquid contactor) were calibrated using a Bios DryCal DC-lite calibration apparatus. This calibration devices does not correct for real temperature and pressure. The displayed flow $\Phi_{v,i}^{\text{display}}$ was correlated to the real flow $\Phi_{v,i}$ in $\mathrm{mL\,min^{-1}}$ for both controllers using linear regression ($R > 0.9999$):

$$\Phi_{v,\text{air dry}} = 7.92671 + 1.07774 \cdot \Phi_{v,\text{air dry}}^{\text{display}} \qquad 15\,\mathrm{mL\,min^{-1}} < \Phi_{v,\text{air dry}}^{\text{display}} < 600\,\mathrm{mL\,min^{-1}} \tag{C.3.1}$$

$$\Phi_{v,N_2\,\text{dry}} = 0.121023 + 0.994389 \cdot \Phi_{v,N_2\,\text{dry}}^{\text{display}} \qquad 30\,\mathrm{mL\,min^{-1}} < \Phi_{v,N_2\,\text{dry}}^{\text{display}} < 260\,\mathrm{mL\,min^{-1}} \tag{C.3.2}$$

$$\Phi_{v,\text{air wet}} = -0.498933 + 1.01867 \cdot \Phi_{v,\text{air wet}}^{\text{display}} \qquad 10\,\mathrm{mL\,min^{-1}} < \Phi_{v,\text{air wet}}^{\text{display}} < 100\,\mathrm{mL\,min^{-1}} \tag{C.3.3}$$

$$\Phi_{v,N_2\,\text{wet}} = -0.177733 + 1.02539 \cdot \Phi_{v,N_2\,\text{wet}}^{\text{display}} \qquad 10\,\mathrm{mL\,min^{-1}} < \Phi_{v,N_2\,\text{wet}}^{\text{display}} < 100\,\mathrm{mL\,min^{-1}} \tag{C.3.4}$$

Note that "air wet" and "N_2 wet" denote the MFC's that are used for the (dry) gases flowing towards the gas/liquid contactor. The calibration was done using the dry gases. For reference by future users of the setup we list tags and original calibration gases for used MFC's:

MFC	Tag	Originally calibrated for
air dry	T51479/002	air 0–1500 $\mathrm{mL\,min^{-1}}$
N_2 dry	F11043/004	C_3H_8 0–100 $\mathrm{mL\,min^{-1}}$
air wet	F11043/001	N_2 0–100 $\mathrm{mL\,min^{-1}}$
N_2 wet	F11043/003	O_2 0–100$\mathrm{mL\,min^{-1}}$

APPENDIX D

Illumination

D.1. Spectrum plot lamp HP100

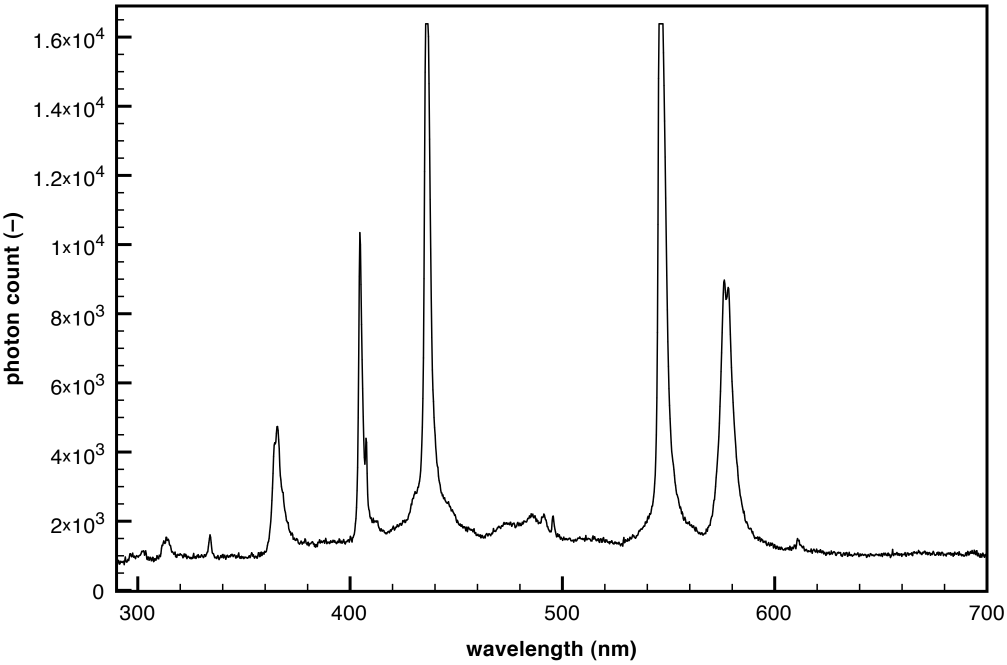

Figure D.1.1 — Photon count as a function of wavelength (300–700 nm) of the light exiting the mercury lamp system Dr. Gröbel HP100. The photon count from 700 until 1100 nm was negligible and is therefore not shown. This spectrum plot was determined using photospectrometer HR4000 from Ocean Optics.

D.2. Probe & fibre holder design

Figure D.2.1 is a photograph of three of the used holders for probe & fibre (see Section 2.2) and Figure D.2.2 displays the design for the holders. The second design (counted from the left for top-left drawing of Figure D.2.2) was used for the irradiance measurements reported. The first design allows light to reach the non-transmissive parts of the probe. The third design was not carried out due to technical difficulties.

Figure D.2.1 — Photograph of the used holders for fibre & probe. The left holder shows the hole for inserting the probe. The holder at the right side shows the hole for inserting the fibre.

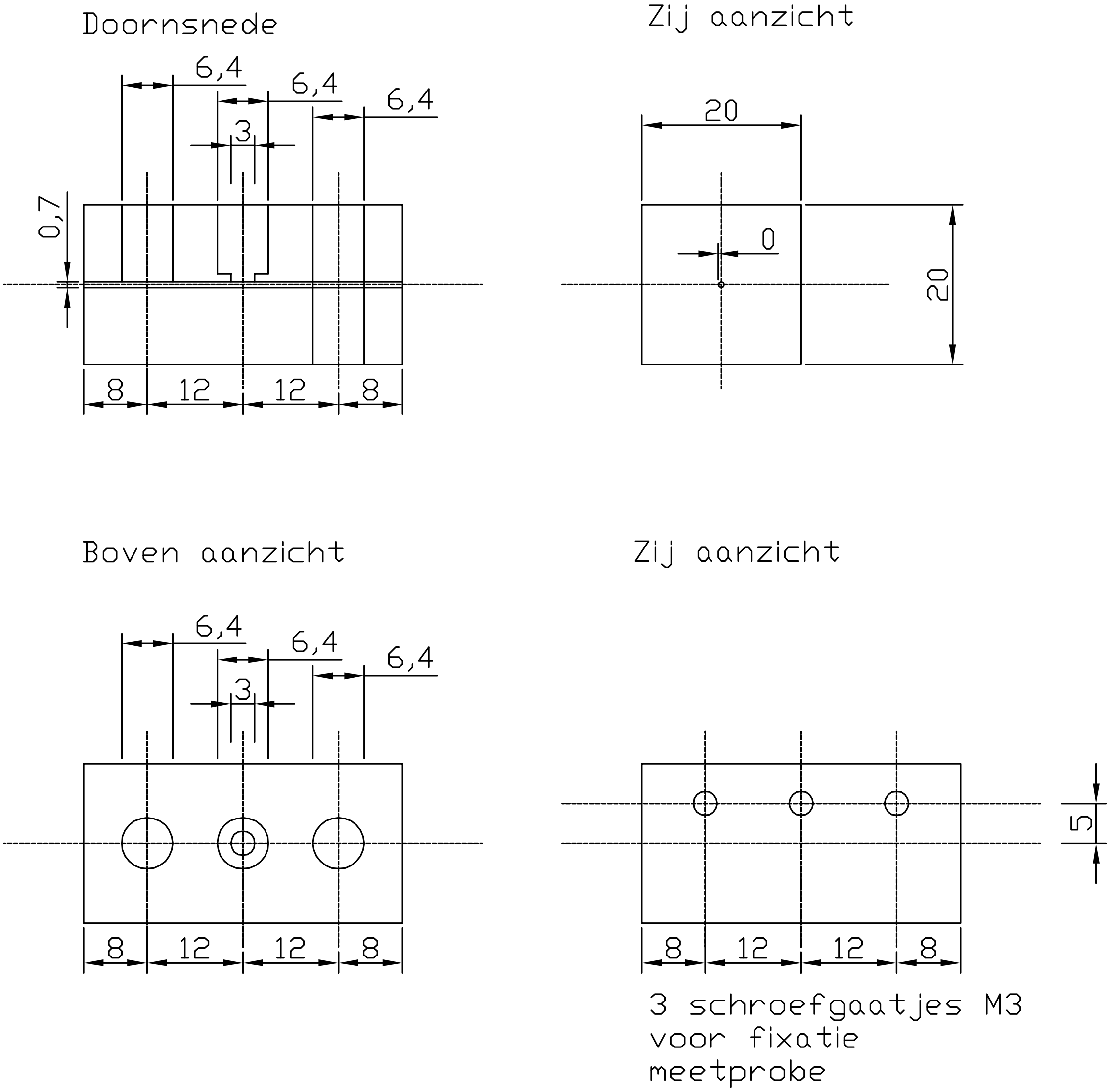

Figure D.2.2 — Design of the used holders for fibre & probe, three holders in one block of plastic. Top-left drawing displays a cross-section alongside the fibre, bottom-left drawing displays top-view (hole for probe), drawings at the right display side-views. Sizes are in mm.

APPENDIX E

Uncertainty estimation

Uncertainties Δ_x, Δ_y, Δ_z in respectively x, y, $z, \ldots$ that are independent from each other propagate in the function $Q\left(x, y, z, \ldots\right)$ according to

$$\Delta_Q \cong \sqrt{\left(\frac{\partial Q}{\partial x}\right)^2 \left(\Delta_x\right)^2 + \left(\frac{\partial Q}{\partial y}\right)^2 \left(\Delta_y\right)^2 + \left(\frac{\partial Q}{\partial z}\right)^2 \left(\Delta_z\right)^2 + \ldots} \tag{E.0.1}$$

where Δ_Q is the uncertainty in Q.

For the case that the uncertainties in x, y, $z, \ldots$ are related to each other, the maximum uncertainty in Q is estimated

$$\Delta_{Q,\mathrm{max}} \cong \left|\frac{\partial Q}{\partial x}\right| \Delta_x + \left|\frac{\partial Q}{\partial y}\right| \Delta_y + \left|\frac{\partial Q}{\partial z}\right| \Delta_z + \ldots \tag{E.0.2}$$

This and more information on error propagation is written by Fornasini (2009, Ch. 8).

APPENDIX F

Physical adsorption

The monolith will physically adsorb some of the components in the reaction mixture. Several adsorption models have been developed over time. The adsorption model by Langmuir is best known. It assumes that: (Foo and Hameed, 2010)

1. each adsorption site is equal and adsorbs with equal affinity (constant adsorption enthalpy)
2. the total number of adsorption sites does not change
3. maximum one layer of molecules adsorbs; one molecule per adsorption site
4. adsorbed species do not interact with each other
5. adsorbed species do not move around the surface

Langmuir adsorption for component i at constant temperature and equilibrium yields an isotherm:

$$\theta_i = \frac{K_\mathrm{L}\,[i]}{1 + K_\mathrm{L}\,[i]} \tag{F.0.3}$$

where θ_i denotes the fractional surface coverage of component i, K_L denotes the Langmuir isotherm constant and $[i]$ is the liquid bulk concentration of i.

APPENDIX G

Gas-liquid chromatography

G.1. Introduction

Gas-liquid chromatography can be used for determining the composition of a liquid mixture quantitatively. When a proper chromatogram is obtained in which the peaks of interest are separated properly, surface area A_i of such a peak is proportional to the amount of compound i in the injected sample. Thus, concentration $[i]$ can be related to response factor f_i for constant injection volume: (Guiochon and Guillemin, 1988, Ch. 13, 15)

$$[i] = f_i A_i \tag{G.1.1}$$

The response factor varies for each compound, detector type and carrier gas. Thus, analysis of samples should be followed by analysis of solutions of known composition. Then, the response factor can be determined. Unfortunately, this response factor can change in time, thus periodic reanalysis of the standard solutions can be necessary. (Guiochon and Guillemin, 1988, Ch. 13, 15)

GC analysis of a series of standard solutions (sometimes called "calibration solutions") of known concentration x_i yields peak area y_i for a certain compound that can be correlated:

$$y_i = a + bx_i + \epsilon_i \qquad i = 1 \dots n \tag{G.1.2}$$

ϵ_i denotes the error that is minimised using the least-squares method, thus yielding the line $\hat{y}_i = a + bx_i$. By inverting this equation, the concentration of the compound in unknown test solutions can be determined.

G.1.1. Uncertainty estimation. Relative standard uncertainty u'_{sp} arising from inaccuracies in the preparation of standard solutions can be be estimated. Standard deviation s_{lr} of the estimate of a concentration from GC peak area arising from linear regression can be calculated by

$$s_{\mathrm{lr}} \cong \frac{s_{y/x}}{b} \left[\frac{1}{m} + \frac{1}{n} + \frac{\left(\bar{y}_{\mathrm{t}} - \bar{y}\right)^2}{b^2 \sum_i \left(x_i - \bar{x}\right)^2} \right]^{1/2} \tag{G.1.3}$$

Where $s_{y/x}$ is the residual standard error from linear regression, n the total number of standard solution samples, $\bar{y}_{\mathrm{t}}$ the mean peak area of m samples of test solution, $\bar{y}$ the mean of samples of peak areas of standard solutions, $\bar{x}$ the mean of concentrations of samples of standard solutions. (Bettencourt da Silva and Camões, 2010)

Relative total standard uncertainty s'_{GC} of GC analysis is obtained by quadratically adding u'_{sp} and s'_{lr}:

$$s'_{\mathrm{GC}} = \sqrt{\left(u'_{\mathrm{sp}}\right)^2 + \left(s'_{\mathrm{lr}}\right)^2} \tag{G.1.4}$$

Note that $s'_{\mathrm{lr}} = s_{\mathrm{lr}}/\hat{x}_{\mathrm{t}}$; the absolute standard deviation divided by the estimated concentration of test solution. (Bettencourt da Silva and Camões, 2010)

An absolute 95 % confidence interval (CI) for GC analysis can be calculated using Student's t-distribution for $n-2$ degrees of freedom:

$$\mathrm{CI} = s_{\mathrm{GC}} \cdot t_{n-2}\,(95\%) = s'_{\mathrm{GC}} \cdot \hat{x}_{\mathrm{t}} \cdot t_{n-2}\,(95\%) \tag{G.1.5}$$

The limit of detection can be estimated by three times the standard deviation of multiple determinations of a blank sample. (Hibbert and Gooding, 2006, Ch. 5.8) Further information on the conditions under which this uncertainty estimation can be applied is written by Bettencourt da

Silva and Camões (2010). Hibbert and Gooding (2006, Ch. 5) have written an easily readable introductory text including an example on uncertainty estimation for calibration.

G.2. Calibration

This section describes the determination procedure for gas chromatography response factors f_i (see Equation G.1.1) of the compounds cyclohexanone, cyclohexanol and hexadecane in cyclohexane. Thus, peak areas for these compounds can be translated into concentrations.

A solution of weighed amounts (approximately 1 gram) of cyclohexanone, cyclohexanol and hexadecane in 25 mL cyclohexane was prepared. This solution was diluted using cyclohexane, 25 mL volumetric flasks and 1, 5 and 10 mL volumetric pipettes.

Gas chromatographic analysis of “pure” cyclohexane showed that minor amounts of cyclohexanone and cyclohexanol are existent in cyclohexane off the shelf. Thus, both the amount of compound n_c (cyclohexanone or cyclohexanol) that was weighed on purpose and the concentration c_0 of the volume of cyclohexane V_0 determine the actual concentration c of a standard solution of total volume V:

$$c = \frac{n_k + c_0 V_0}{V} \approx \frac{n_k}{V} + c_0 \tag{G.2.1}$$

This equation shows that all standard solutions have the same constant offset $\frac{c_0 V_0}{V} \approx c_0$ in their concentrations for cyclohexanone and cyclohexanol. Thus, surface areas of the peaks in the chromatograms will show also a constant offset. Linear regression of all peak areas versus intended concentration $(\frac{n_k}{V})$, including the intended zero concentration of cyclohexane, is possible. The offset in the equation resulting from this linear regression represents c_0.

G.2.1. Preparation of standard solutions. About 1 g of cyclohexanone, cyclohexanol and hexadecane were added to a 25 mL volumetric flask containing some cyclohexane (dried on zeolite). The exact amounts of the three compounds added were measured using a balance. Since cyclohexanol is quite viscous (melting point is 18 °C), the addition was done using a Pasteur pipette. After addition, the volumetric flask was filled up to 25 mL with cyclohexane (solution 1).

1 mL solution was diluted to 25 mL using cyclohexane (solution 2). This dilution is repeated two times, thus resulting in the most diluted solution (solution 4) being diluted 25^3 times in total.

5 mL of solution 2 is diluted to 25 mL (solution 5). 10 mL of solution 5 is diluted to 25 mL (solution 6). Solutions 7–10 are created in the same way, using solution 3 and 4 as start solutions.

Pure cyclohexane was also analysed by gas chromatography, to account for the cyclohexanone and cyclohexanol already present in ’pure’ cyclohexane. Since cyclohexane evaporates significantly, samples before and after the preparation of standard solutions were taken from the beaker containing cyclohexane for this preparation.

Note that used reagents were assumed to be pure, while in practice only ≥ 99 % pure reagents were used.

Note that no correction for air buoyancy in weighing was applied, since this correction is small compared to estimated relative standard uncertainty u'_{sp} which originates from inaccuracies in the preparation of standard solutions.

APPENDIX H

Real bulk concentrations IIMR sessions

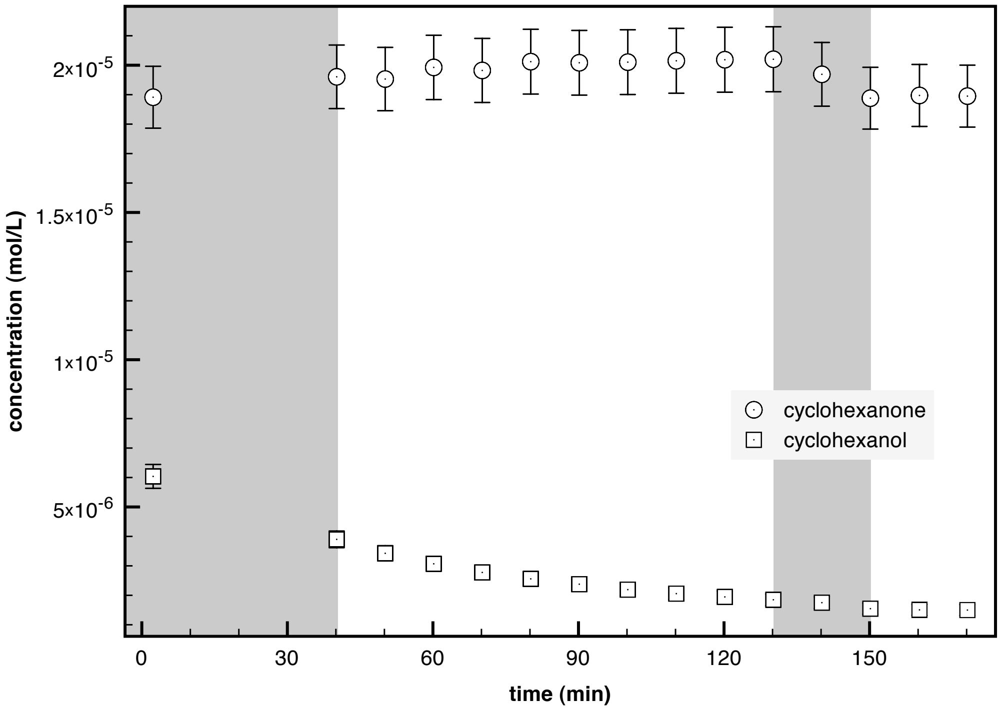

Figure H.0.1 — Reactor session 2: real liquid bulk concentrations of cyclohexanone and cyclohexanol (not corrected for evaporation) versus time. From 40 min. until 130 min. the reactor was illuminated, as well as from 150 min. until the end.

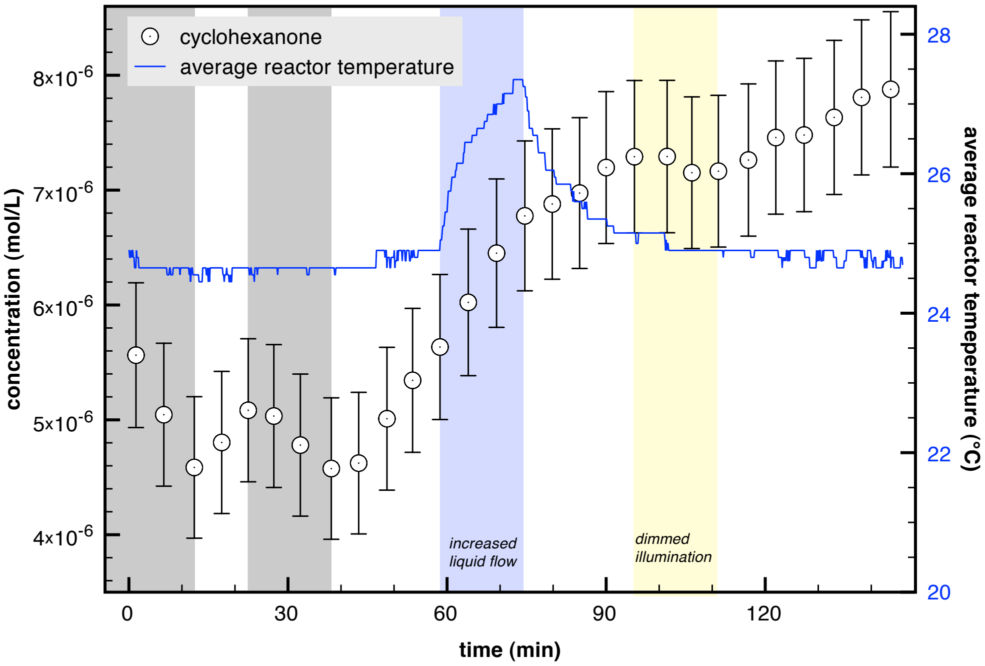

Figure H.0.2 — Reactor session 3: real liquid bulk concentrations of cyclohexanone and cyclohexanol (not corrected for evaporation) versus time. The reactor was illuminated during the whole experiment, except for the grey-coloured time intervals. The liquid flow was increased from 1.6 to 2.2 L min^{-1} during the blue-coloured time period, the illumination was dimmed for the yellow-coloured time interval. The blue line denotes average reactor temperature (right vertical axis).

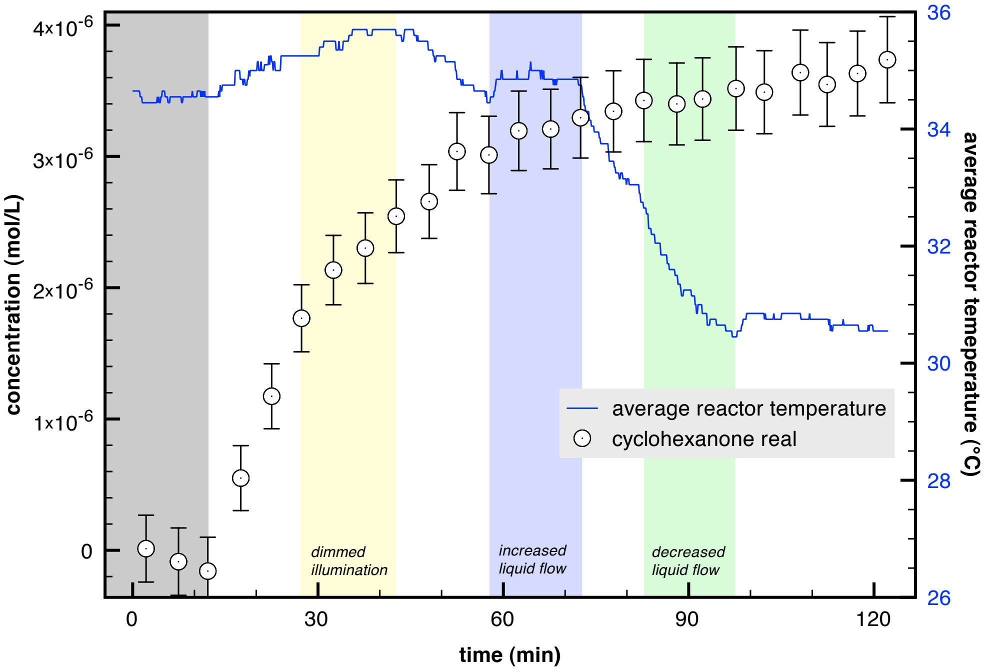

Figure H.0.3 — Reactor session 4: real liquid bulk concentrations of cyclohexanone and cyclohexanol (not corrected for evaporation) versus time.

APPENDIX I

Physical adsorption of cyclohexanone

I.1. Results: Monolith contained by IIMR

Five IIMR sessions were done without illumination and without gas flow to determine physical adsorption of cyclohexanone on the titania-coated monolith and the rest of the reactor system. The conditions of these five reactor sessions are listed in Table I.1.1. Liquid flow was 1.6 $\mathrm{L\,min^{-1}}$.

Table I.1.1 — Reactor conditions for physical adsorption experiments using IIMR. Numbers mentioned for “origin” denote the originating reactor session. The cyclohexanone solution contains $1.17 \cdot 10^{-3} \pm 5 \cdot 10^{-5}\,\mathrm{mol\,L^{-1}}$ cyclohexanone in cyclohexane (determined by GC).

Condition	Unit	Session 5	Session 6	Session 7	Session 8	Session 9
Liquid temperature	°C	24.4	24.3	24.1	24.9	24.9
Liquid volume and origin	mL	730 mL 4 and 145 mL fresh	5	740 mL 6	975 mL fresh	8
Monolith origin	n/a	4	5	6	regenerated	8
Volume cyclohexanone solution added	mL	none	none	1.6	1	1

Cyclohexanone liquid bulk concentrations determined in reactor session 5 are displayed in Figure I.1.1. Within 40 minutes cyclohexanone concentration decreased $0.9 \cdot 10^{-6}\,\mathrm{mol\,L^{-1}}$ (30%). From 40 minutes to the end of the session, cyclohexanone concentration was stable within uncertainty margins. Note that reactor session 5 was the only session of sessions 5–9 whose liquid was pre-saturated by air.

Reactor session 6 is a continuation of reactor session 5 the next day. See Figure I.1.2 for the resulting stable level of cyclohexanone bulk concentration.

We added cyclohexanone to the cyclohexane used in reactor session 6. Physical adsorption of this solution was determined in reactor session 7, see FigureI.1.3. Liquid bulk cyclohexanone concentration decreases $0.7 \cdot 10^{-6}\,\mathrm{mol\,L^{-1}}$ (15 %) within 110 minutes.

For reactor session 8 we regenerated the monolith and we used fresh cyclohexane. FigureI.1.4 shows the concentration of cyclohexanone was stable around zero, until we added cyclohexanone. Liquid bulk cyclohexanone concentration decreases $0.2 \cdot 10^{-6}\,\mathrm{mol\,L^{-1}}$ (17 %) within 15 minutes.

Reactor session 9 was conducted using the same liquid and monolith as session 8, with cyclohexanone added. See Figure I.1.5 for the stable course of cyclohexanone concentration.

I.2. Results: slice of monolith

A 1 cm slice of titania-coated monolith was immersed in a beaker filled with 200 mL cyclohexane. After 70 minutes, 1 mL of $1.17 \cdot 10^{-3} \pm 5 \cdot 10^{-5}\,\mathrm{mol\,L^{-1}}$ cyclohexanone in cyclohexane was added, see Figure I.2.1. Concentration of liquid bulk cyclohexanone does not decrease significantly.

I.3. Discussion

We tried to estimate the physical adsorption of cyclohexanone on a titania-coated monolith. We performed measurements on a monolith contained by the IIMR as well as on a slice of monolith contained by a beaker.

IIMR sessions 5 and 7 were done using a monolith that was used in illuminated photocatalytic experiments (IIMR session 4) and was not regenerated. These sessions show a significant decrease of cyclohexanone in the bulk. Session 5 shows more and faster decrease in bulk cyclohexanone than

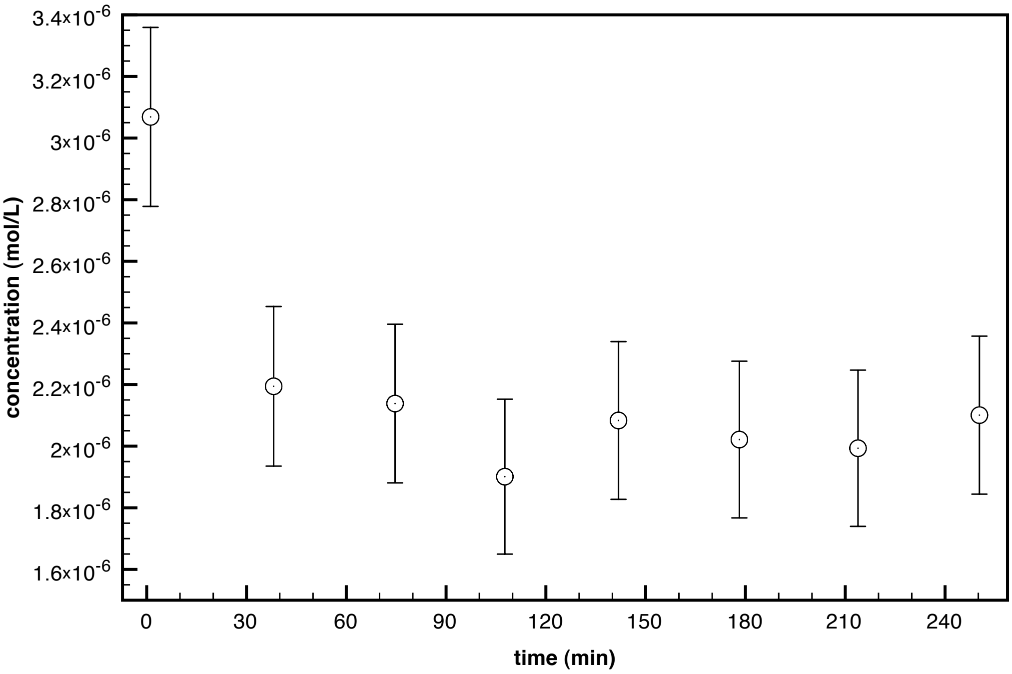

Figure I.1.1 — Reactor session 5: liquid bulk concentrations of cyclohexanone versus time. Pump was turned on around time 3 min.

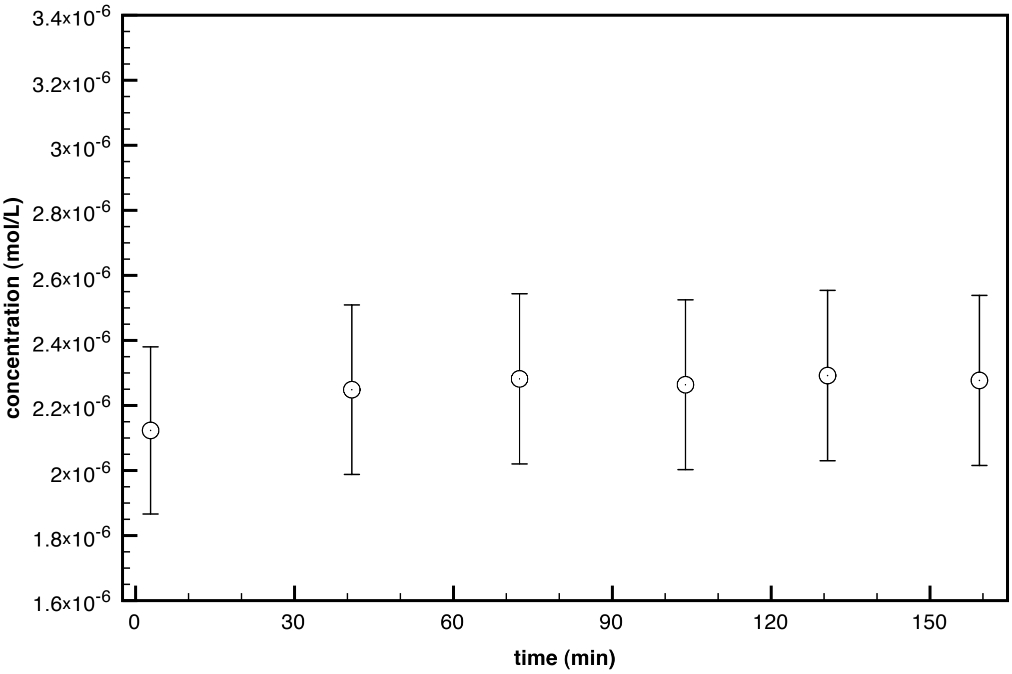

Figure I.1.2 — Reactor session 6: liquid bulk concentrations of cyclohexanone versus time.

session 7. Note that IIMR session 6 was only an extension of session 5 the following day, proving that equilibrium was established.

The cyclohexanone concentration decrease from the first to the second data point of IIMR session 7 could be partially due to mixing behaviour. More concentrated cyclohexanone in cyclohexane solution was added to the IIMR at the start of session 7. The dead spaces of the IIMR contained at that time less concentrated cyclohexanone from the previous reactor session. When the pump is switched on at time 0 min., mixing starts and cyclohexanone concentration determined

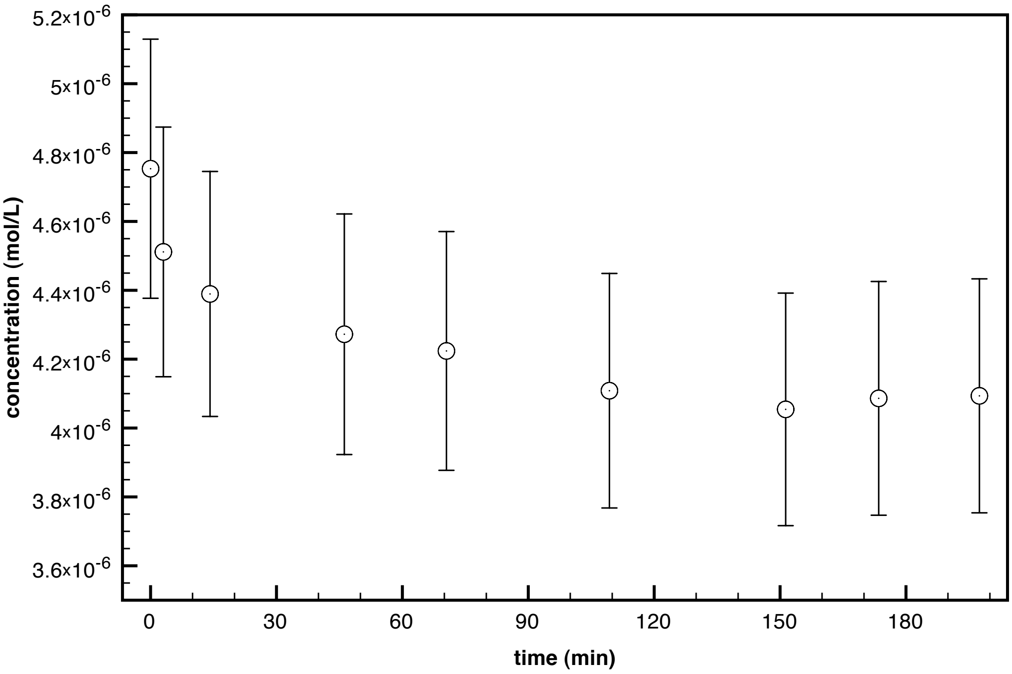

Figure I.1.3 — Reactor session 7: liquid bulk concentrations of cyclohexanone versus time. Cyclohexanone was added before time 0 min.

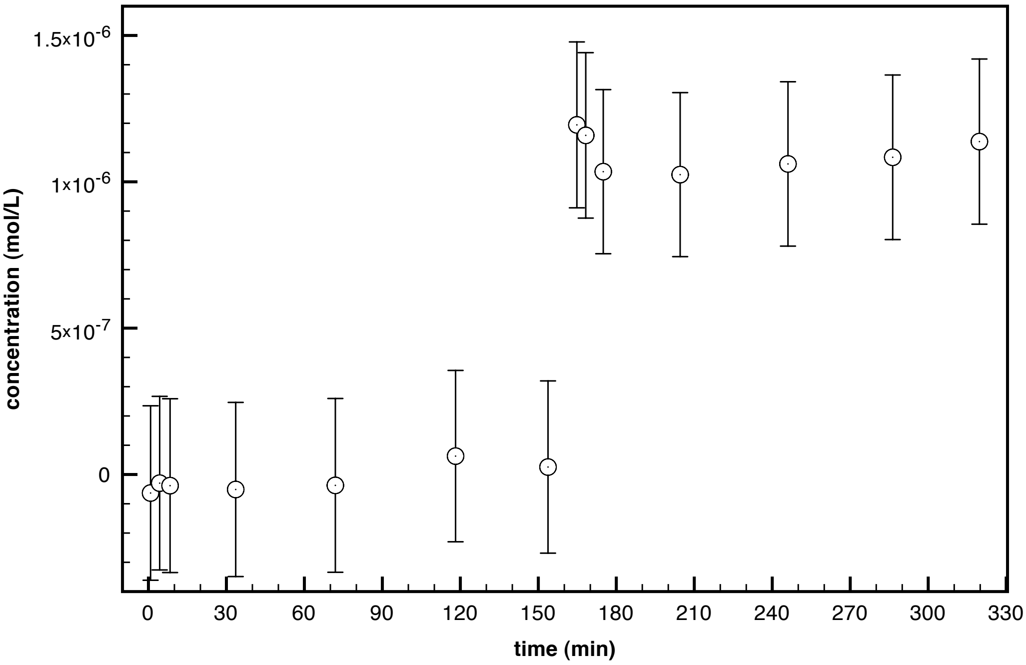

Figure I.1.4 — Reactor session 8: liquid bulk concentrations of cyclohexanone versus time. Around time 160 min. cyclohexanone was added.

can decrease due to mixing alone. A similar explanation could partially explain the concentration decrease in reactor session 8 after adding cyclohexanone.

Iimr sessions 8 and 9 were performed using a regenerated monolith and fresh cyclohexane. These sessions show less decrease in bulk cyclohexanone than session 5 and 7. Session 9 does not show significant decrease at all.

One experiment was done using a 1 cm slice of titania-coated monolith that was never used before under illumination. This beaker session 1 does not show any significant decrease in bulk

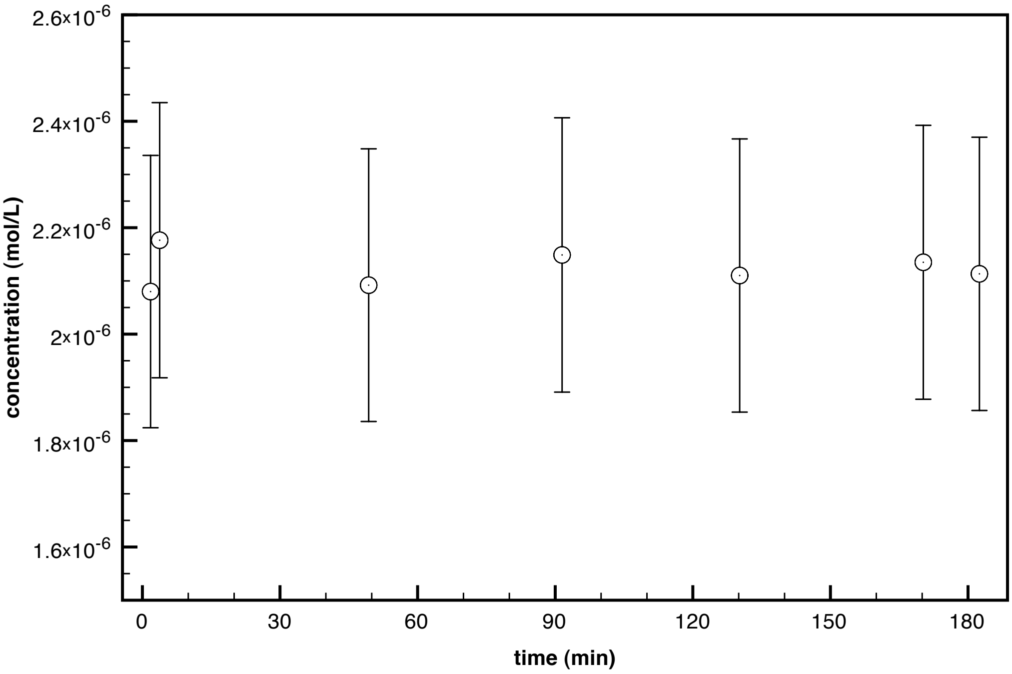

Figure I.1.5 — Reactor session 9: liquid bulk concentrations of cyclohexanone versus time. Cyclohexanone was added before time 0 min.

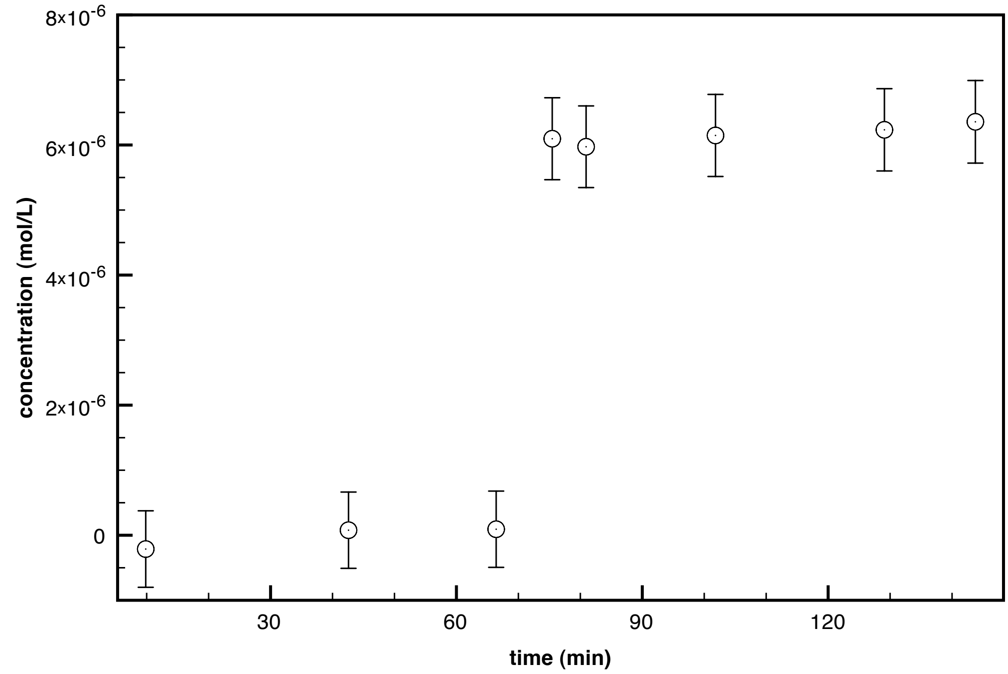

Figure I.2.1 — Beaker session 1: liquid bulk concentrations of cyclohexanone versus time, at 20 °C.

cyclohexanone. We attribute the minor increase in cyclohexanone (from 80 minutes) to evaporation of cyclohexane: the beaker was not completely closed from the environment by the watch glass on top of it.

Closed mode IIMR sessions 10 & 12

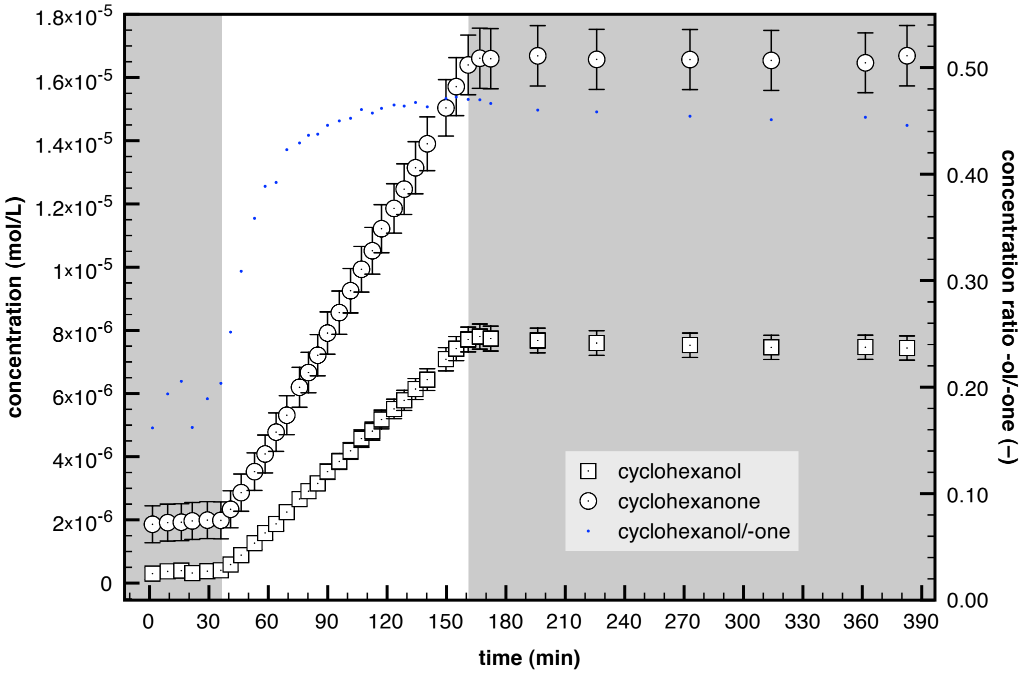

Figure J.0.1 — Reactor session 10 (closed mode): liquid bulk concentrations of cyclohexanone and cyclohexanol versus time. The closed reactor was illuminated during the whole experiment, except for the grey-coloured time intervals. The blue dots denote the liquid bulk concentration of cyclohexanol divided by cyclohexanone (right vertical axis).

See Figure 3.3.5 on page 28 for the concentration plot of reactor session 11.

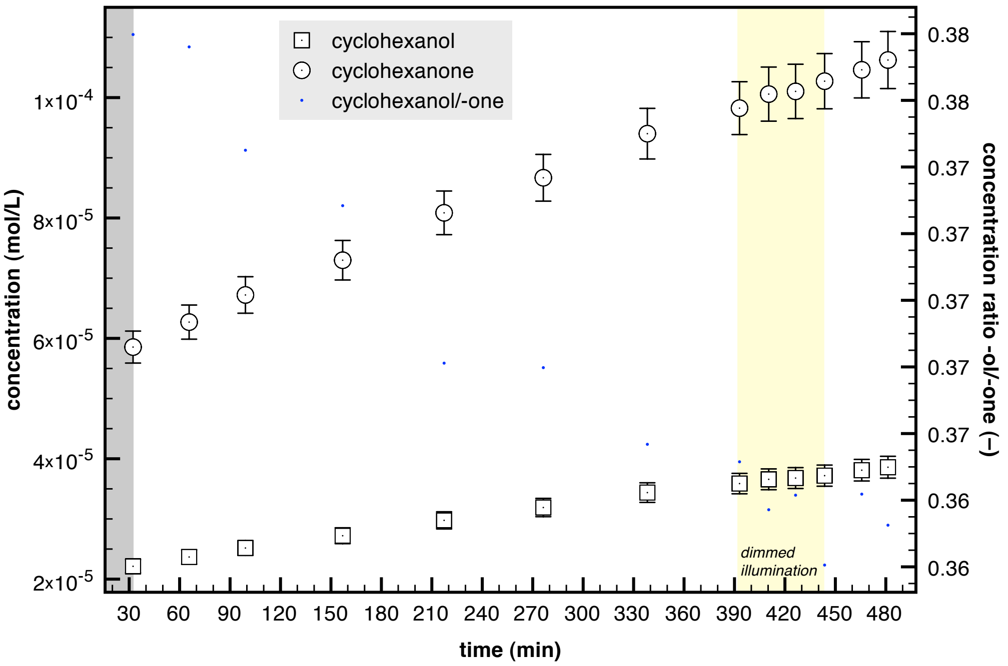

Figure J.0.2 — Reactor session 12 (closed mode): liquid bulk concentrations of cyclohexanone and cyclohexanol versus time. The closed reactor was illuminated during the whole experiment, except for the grey-coloured time interval. The blue dots denote the liquid bulk concentration of cyclohexanol divided by cyclohexanone (right vertical axis). During the yellow-coloured period illumination was dimmed.

APPENDIX K

Bulk production rates IIMR sessions

Table K.0.1 — The bulk production rates of cyclohexanone and cyclohexanone for IIMR sessions that are plotted in Figures 4.3.1 and 4.3.2.

IIMR session[a]	RH (%)	Bulk production rates $(10^{-6}\,\mathrm{mol\,h^{-1}})$		Rate ratio cyclohexanol/-one (−)	Classification	Liquid volume at start (mL) and originating session
		Cyclohexanone	Cyclohexanol			
1	0	2.46	0	0	after regeneration	910 mL fresh
3	0	3.24	0	0	after regeneration	750 mL 3 and 179 mL fresh
4	0	6.00	0	0	after regeneration	895 mL fresh
10	57.2	7.1	3.6	0.51	closed mode	850 mL 9 and 155 mL fresh
11	53.6	6.4	2.2	0.35	closed mode	925 mL 10
12	55.3	5.8	2	0.34	closed mode	860 mL 11
13	56.6	3.3	1.3	0.39	high $\theta_{\mathrm{H_2O}}$	810 mL 12 and 210 mL fresh
14d1	0.1	-13.1	-11.6	0.89	high $\theta_{\mathrm{H_2O}}$	942 mL 13
14d2	0.1	-7	-3.5	0.5	low $\theta_{\mathrm{H_2O}}$	
14w1	43.3	28	15	0.56	after dry illumination	
14w2	48.2	28	15	0.56	after dry illumination	
15d	0.1	2.1	0.35	0.17	after regeneration	995 mL fresh
15w	49.3	6.4	2.4	0.37	after dry illumination	
16d1	0	-0.8	-0.85	1.06	high $\theta_{\mathrm{H_2O}}$	
16w	9	1.2	0.22	0.18	after dry illumination	
16d2	0	-0.65	-0.5	0.77	high $\theta_{\mathrm{H_2O}}$	
17w1	93	4.3	3.7	0.88	high $\theta_{\mathrm{H_2O}}$	830 mL 16 and 205 mL fresh
17w2	66.6	1.9	0.96	0.5	high $\theta_{\mathrm{H_2O}}$	
17w3	27.7	-1.13	-2.6	2.33	high $\theta_{\mathrm{H_2O}}$	
18w1	26.9	3.5	1.3	0.37	low $\theta_{\mathrm{H_2O}}$	905 mL 17
18w2	6.2	-2.4	-1.9	0.8	high $\theta_{\mathrm{H_2O}}$	
18w3	48.6	11.8	5.6	0.48	low $\theta_{\mathrm{H_2O}}$	
19p1	52	13.4	8	0.6	low $\theta_{\mathrm{H_2O}}$	830 mL 18 and 200 mL fresh
19p2	52	3.4	2	0.6	high $\theta_{\mathrm{H_2O}}$	
30d	0	-6.1	-3.86	0.63	low $\theta_{\mathrm{H_2O}}$	889 mL 19
30w1	68.9	22	13.8	0.63	after dry illumination	
30w2	90.5	6.4	7.1	1.12	high $\theta_{\mathrm{H_2O}}$	

---

[a] "d" denotes a dry part, "w" a humidified part of the session. Numbers after "d" and "w" denote a part number.

APPENDIX L

Further discussion

L.1. Liquid-phase mass transfer

During reactor session 3 the liquid flow was increased to 2.2 L min^{-1}, to determine the existence of mass transfer limitations. Since cyclohexanone production rate did not change after increasing liquid flow, we think the IIMR is not mass transfer limited for liquid flow of 1.6 L min^{-1}. We think the decrease in cyclohexanone production rate right after the period of increased liquid flow (time = 75 min.) during reactor session 3 is due to deactivation of the monolith. Reactor session 1 and 4 show a decrease in cyclohexanone production rate after a comparable period of illumination (40–50 minutes).

Reactor session 4 proves that variation of liquid flow from 1.0 to 2.2 L min^{-1} does not influence cyclohexanone production rate.

L.2. Reactor temperature

Reactor temperature increase due to increased pump speed could in theory play a role in the observed increased cyclohexanone production rate. But, for reactor session 3 temperature is increasing during the whole time interval of increased liquid flow, and cyclohexanone production rate is stable during that period. Reactor session 4 suffers from even more variation in temperature, but does not show a consequence of temperature change for the cyclohexanone production rate.

From comparing the cyclohexanone production rates for dry sessions 1, 3, 4 and 15d (see Appendix K) we can learn that session 4 shows the highest rate, followed by session 3. Session 4 was done at the highest temperature (35 °C) and session 3 at the standard 25 °C mainly (session 3 contained a period of 27 °C).

Thus, we can conclude that an effect of temperature on bulk cyclohexanone production rate is difficult to determine for one experiment. But when comparing multiple experiments a trend can be seen: the higher the temperature, the higher the bulk production rate for regenerated monoliths under dry conditions.

L.3. Light transfer

Dimming the light during reactor session 3 leads to a decrease in cyclohexanone concentration. After undimming the light, cyclohexanone production rate returns to the rate before dimming the light. It seems that the cyclohexanone production rate in the IIMR is influenced by the amount of irradiance at employed conditions in reactor session 3. Observed changes in cyclohexanone concentration are within error margins, thus more experimental evidence is needed to support this conclusion thoroughly.

Reactor sessions 4 and 12 confirm the influence of irradiance on cyclohexanone production rate.

L.4. Increase between reactor sessions 1 and 2

The tenfold increase in concentrations of cyclohexanol and cyclohexanone between reactor sessions 1 and 2 leads to the thought that some parts of the monolith might have fallen dry during session 1, i.e. that no bulk liquid came past some parts of the monolith. Production of cyclohexanone and cyclohexanol might have continued inside the pores of the dry parts. These produced amounts might have dissolved in the bulk from reactor session 2, in which a much smaller gas flow was used than during reactor session 1. High gas flow could prevent liquid from entering some channels of the monolith.

Another possible cause for the concentration increase is desorption of adsorbed cyclohexanone during the temperature stabilisation period before the start of session 2. Due to the lack of illumination for some days between session 1 and 2, the adsorbed cyclohexanone can desorb.

APPENDIX M

Literature search

This chapter lists all search actions that were done to find necessary information in literature for this work.

M.1. Search for general info

M.1.1. 20110728 Scopus.

- “photocatalysis” –> 15979, too much

M.2. Search for reactor technology

M.2.1. 20100914 Scopus.

- photocatalysis AND reactor (all fields): 5230
- 20100916: photocatalysis AND reactor (title-abs-key fields): 1434, quite some relevant articles, gone through results 1-100, a lot of articles on air/water purification
- photocatalysis AND reactor AND cyclohexanone: 4 results. all relevant
- photocatalysis AND reactor AND cyclohexane: 12 results, all relevant
- photo catalysis AND reactor AND cyclohexane: 1 relevant result
- "photocatalysis" AND synthesis: 2450 results, too much
- "photocatalysis" AND synthesis AND system: 302, but not about reactor technology
- "photocatalysis" AND synthesis AND reactor: 70, of which some relevant
- "photocatalysis" AND industrial AND reactor: 123

M.2.2. 20100921 Scopus. Target: search for the economic/industrial challenges for application of photocatalytic systems, in special for monoliths.

- economics AND photocatalysis (title, abs, key): 17 results, not much relevant
- “Advanced oxidation proces” AND economics (title, abs, key): 0 results (AOP only 3 results)
- economics AND monolith (title, abs, key): 26 results, not relevant
- photocatalysis AND industrial (title, abs, key): 487 results, not relevant (first 20)

M.2.3. 20100924 Scopus. Target: search for the economic/industrial challenges for application of monoliths

- Author: Nijhuis, title etc.: monolith –> 14 results, some relevant
- Author: Kreutzer, title etc.: monolith –> 24 results, some relevant
- Affiliation: Delft, title etc.: monolith –> 122 results, some relevant [TODO 81-e.v.]
- TODO: search in encyclopaedia for monolith

20100927 Encyclopaedia monolith

- Kirk-Othmer: monolith: 20 not so relevant results
- Ullmann: monolith (titles): 2 results

M.3. Catalyst preparation methods

M.3.1. 20101110 Scopus.

- tio2 monolith preparation –> 33 results, not very relevant in terms of preparation
- tio2 monolith photo –> 13 results, not very relevant in terms of preparation
- tio2 photo preparation –> 544, too much
- tio2 photo preparation review –> 5, not relevant
- tio2 photo review –>

M.4. Light measurement methods

M.4.1. 20110107 Scopus.

- “actinometry photocatalysis tio2” –> 11 results, some interesting applications of actinometry”
- “ferrioxalate actinometry” –> 47 results, relevant

M.4.2. 20110221 Scopus photo-spectrometry side light emitting fibres.

- “photospectrometry fiber side” –> 0
- “photospectrometer fiber side” –> 0
- “side light fiber” –> 2445, too much
- “side emitting fiber” –> 227, seems good words, but too much
- “side emitting fiber intensity” –> 23, not relevant
- “side emitting fiber spectrum” –> 25, not relevant
- “side fiber intensity” –> 752, too much
- “side light fiber intensity” –> amongst first 160 not much useful hits
- “glowing light fiber intensity” –> 2, not relevant
- “side fiber flux” –> too much

M.5. GC

M.5.1. 20110125 Scopus.

- “gc cyclohexanone” –> 105 results, 1 relevant but not reachable
- “gas chromatography tailing” –> 236, some relevant

M.5.2. [TODO] Scopus.

- “gc cyclohexane cyclohexanone”

M.5.3. 20110519 Uncertainty analysis Scopus.

- "gas chromatography" uncertainty –> 636, 1 relevant
- "gas chromatography" error analysis –> 1736, 0 relevant
- "linear regression" uncertainty –> too much
- "linear regression" uncertainty squares –> 138, looked all through, quite some useful articles
- "linear regression" uncertainty gc –> 9, not interesting
- uncertainty gc –> 535, too much
- uncertainty gc regression –> 24, useful
- calibration "least squares" –> 7047, too much
- calibration "least squares" gc –> 111, 1st 2 pages studied, 1 relevant
- TODO: Journal of Chemometrics

M.6. Kinetics

M.6.1. 20110131 Scopus.

- “kinetics cyclohexane TiO2” –> 11 results, one relevant
- “rate cyclohexane TiO2” –> 39 results, some relevant
- “kinetic cyclohexane TiO2” –> 7 results, already known
- “catalytic combustion cyclohexane” –> 25, 1 or 2 interesting

M.6.2. 20110131 Sciencedirect (full text).

- FULL-TEXT(kinetics AND TiO2) and FULL-TEXT(cyclohexane AND cyclohexanone) –> 100 results,

M.6.3. 20110131 Google.

- “kinetics cyclohexane TiO2” –> al lot of results, none relevant

M.6.4. 20110202 Scopus general kinetics.

- “kinetics TiO2 oxidation” –> 1540 results, too much
- “kinetics TiO2 oxidation model” –> 396, doable, some kinetic models of comparable systems
- “photo cyclohexane” –> 214, too much
- “photo cyclohexane tio2” –> 35, many relevant but already in possession
- “kinetic model photo*” –> 7484, too much
- “kinetic model photocat*” –> 675, too much
- “kinetic model photocat* tio2” –> 440, too much
- TODO: cited by zoeken

M.6.5. 20110202 SciFinder kinetics.

- Substance Identifier "cyclohexane " > get references (13329) > Refine Answer set 4 by research topic: photo tio2 Answer set 7 created with 73 answers from CAPLUS refine "photo tio2" (73) –> many relevant, but already known

M.7. Adsorption

M.7.1. 20110620 Scopus adsorption.

- “cyclohexane photocat* TiO2 adsorption” in title etc. –> 9
- “cyclohexane photo* TiO2 isotherm” in title etc. –> 1, already known
- “cyclohexane photo* TiO2 Langmuir” in title etc. –> 2, 1 interesting
- “cyclohexane photo* TiO2 adsorption” in all fields –> 628, a lot but seems interesting, thus all were browsed, quite some useful articles were collected

M.7.2. 20110704 Scopus adsorption (cordierite).

- “cyclohexanone cordierite adsorption” –> 0
- “cyclohexanone cordierite adsorption” in all fields–> 5, not relevant
- “cyclohexane cordierite adsorption” in all fields–> 9, not relevant
- “cyclohexanone adsorption equilibrium” –> 27, not relevant
- “cyclohexanone adsorption isotherm” –> 26, not relevant

M.7.3. 20110704 Scifinder.

- substance “cyclohexanone” –> refs –> refine “adsorption” –> refine “isotherm” –> 56, not relevant
- TiO2, etc. TODO

M.8. Physical properties

M.8.1. 20110208 Diffusivity O2 N2 in cyclohexane, Scopus.

- “diffusivity o2 cyclohexane” –> 0
- “diffusivity oxygen cyclohexane” –> 2, irrelevant
- “diffusivity oxygen cyclohexane” in all fields –> 79, only one relevant

M.8.2. SciFinder.

- Substance Identifier "oxygen " > get references (333285) > refine "cyclohexane" (1288) > refine "diffusivity" (5) –> 5 results, two relevant

M.8.3. Sciencedirect full text.

- “diffusivity oxygen cyclohexane” –> 698, in first 100 some relevant ones.

M.8.4. Diffusion cyclohexanone in cyclohexane Scopus.

- “diffusion cyclohexanone cyclohexane” –> 14, 1 somewhat relevant

M.8.5. 20110829 Scopus, solubilities (and Henry) H2O, -ol & -one in cyclohexane.

- “henry, water, cyclohexane” in article title, abstract & keywords –> 19, relevant
- “solubility cyclohexanol cyclohexane” in article title, abstract & keywords –> 24, 1 relevant
- “solubility cyclohexanone cyclohexane” in article title, abstract & keywords –> 30, none relevant

M.9. Mass transfer

M.9.1. 20110322 kL film flow monolith, Scopus.

- “monolith film mass transfer” –> 44 results, very relevant

M.9.2. 20110421 Gas distribution monolith, Scopus.

- “gas distribution monolith” –> 201

M.10. Conventional cyclohexane oxidation

M.10.1. 20110408 Conventional cyclohexane oxidation, Scopus.

- “cyclohexane oxidation process review” –> 3294, too much
- “industrial cyclohexane oxidation process review” –> 1096, too much
- “industrial cyclohexane oxidation” in title –>2, not relevant
- “review cyclohexane oxidation” in title –> 0
- “review cyclohexanone production” in title –> 0

M.10.2. 20110408 Ullmann’s encyclopaedia of industrial chemistry.

- “cyclohexanone” in title –> 1 relevant article
- “cyclohexane” in title –> 1 relevant article

M.10.3. 20110408 Kirk-Othmer Encyclopedia of Chemical Technology.

- “cyclohexanone” in title –> 1 relevant article
- “cyclohexane” in title –> 0

M.10.4. 20110412 Conventional cyclohexane oxidation conversion and kinetics and thermodynamics, Scopus.

- “industrial cyclohexane oxidation process review kinetics conversion” –> 0
- “industrial cyclohexane oxidation review kinetics conversion” –> 1, not relevant
- “cyclohexane oxidation review kinetics conversion” –> 1, not relevant
- “cyclohexane oxidation kinetics conversion” –> 49, quite some relevant
- “cyclohexane oxidation kinetics” –> 398, too much